

2 MAY 1990



**FOREIGN  
BROADCAST  
INFORMATION  
SERVICE**

# ***JPRS Report***

**DECLASSIFICATION STATEMENT A**

Approved for public release  
Distribution Unlimited

# **Science & Technology**

***Japan***

PRECISION PROCESSING TECHNOLOGY FOR  
ENGINEERING CERAMICS

19980130 061

REPRODUCED BY  
U.S. DEPARTMENT OF COMMERCE  
NATIONAL TECHNICAL INFORMATION SERVICE  
SPRINGFIELD, VA. 22161

**DTIC QUALITY INSPECTED 3**

JPRS-JST-90-024  
2 MAY 1990

## SCIENCE & TECHNOLOGY JAPAN

### PRECISION PROCESSING TECHNOLOGY FOR ENGINEERING CERAMICS

43067178 Tokyo THE 91ST WORKSHOP ON PLASTIC WORKING in Japanese 16 Jun 89  
pp 1-60

#### CONTENTS

Injection Molding Technology, Its Applications [Toshiyuki Iwahashi].....	1
Selection, Characteristics of Binder for Injection Molding [Katsuyoshi Saito].....	19
Laser Processing Technology, Its Applications [Masaharu Moriyasu].....	32
Electrodischarge Machining Technology, Its Applications [Hiroshi Kubo, Masanobu Kuroda].....	40
Technology for Grinding Engineering Ceramics [Tetsutaro Uematsu, Kiyoshi Suzuki, et al.].....	52
Solid Phase Welding Technology, Its Applications [Shinichi Matsuoka].....	76

## Injection Molding Technology, Its Applications

43067178A Tokyo THE 91ST WORKSHOP ON PLASTIC WORKING in Japanese 16 Jun 89  
pp 1-11

[Article by Toshiyuki Iwahashi, Niigata Engineering Co., Ltd.,]

[Text] Injection molding technology has long been used for the molding and processing of engineering ceramics, but cases of the technology being employed in actual production are not as numerous. Among the reasons for this laggardness are probably the cost of dies and equipment, which is much higher than that for conventional technologies, as well as the longer time needed for the degreasing process which pushes up the overall production cost. However, with the increasing trends toward higher performance, higher functionality, and increased sophistication of products, as well as with the development of new products, the advantages of injection molding technology, i.e., the capacity to die-cast moldings with complex shapes accurately, uniformly, and in high yield, have come to be reviewed and the aforementioned disadvantages have been corrected. Therefore, the fields in which the features of injection molding technology can be put to good use are beginning to increase, and great expectations are being placed on the technology's future.

### 1. Features of Injection Molding Process

Table 1 gives the molding processes for some of the ceramic products that start from powder raw materials. Table 2 shows the features of these injection molding processes. From these tables, one may say that the injection molding process is best suited for use in fields with the following requirements: the product must be mass produced it is relatively small in size but demands rigorous dimensional accuracy, it is of a complex shape and its manufacture by a conventional technique would cost too much in after working, and it must be highly reliable and of high quality in terms of physical properties.

### 2. Outline of Injection Molding Process

Figure 1 shows the process for manufacturing ceramics by injection molding, from raw materials to products. Since raw materials for ceramics are powders, if their injection molding is to become feasible, they must be provided with fluidity, formability, and shape-retaining properties. To that end, organic binders have generally been added. Consequently, after a ceramic has been

Table 1. Powder Molding Processes

	Molding material	Molding method	Shape of mold	Features	Main products
Dry direct molding	Dry mode; small amounts of organic materials added	Die press	2-dimensional small complex shapes	Simple working, mass production	Electric insulators, condensers, IC devices
		Rubber press	Slightly complex shapes	Uniform mold density, cutting work available	Tools, ignition plugs, electric insulators, mechanism elements
		Hot press	Simple shapes	Simultaneous molding and sintering, high density	Structural materials, electric insulators
Plastic molding	Thermal plasticity or wet mode	Extrusion	Modified cross-section shape, bar shapes, pipe shapes	Ease of continuous manufacturing	Heat generators, resistors, optical fiber, connectors, catalytic honeycombs, pipes
		Injection	3-dimensional shapes	Good dimensional accuracy, uniform density	Cutters, medical instruments, hair clipper blades, thread guides, bolts and nuts, trays, bearings, turbochargers, valves
		Rolling	Sheets, film	Ease of continuous manufacturing	Thin substrates
Casting	Slurry	Slip cast	Complex shapes	No limitations on shape, ease of equipment installation	Insulating pipes, thread guides, turbocharger rotors
		Doctor braid method	Film, sheets	Ease of continuous manufacturing	Thin films, thin plates

Table 2. Features of fine Ceramic Injection Molding Technology

Item	Contents
•Molding of complex shapes	Any complex shape can be molded in a single process as long as the required dies are available.
•Dimensional precision •Microminiature parts	After binder has been removed, the sintered body shrinks to a great extent. However, since the shrinkage is isotropic, the dimensional distortion can be kept to below 1 percent. In small items, the shrinkage may be kept to below $\pm 0.3$ percent. Is superior in terms of its capacity to transcribe the die plane.
•High density •High strength	Since, when using high quality powders, the technology enables molding having a uniform density and less distortion to be generated, high density and high strength may be obtained.
•Productivity	Can produce green moldings faster than other methods can and is advantageous. Can be automated easily. However, the technology requires larger equipment for binder removal.

molded, the binder must be removed, and here the ease of binder removal comes into focus. The author believes that the preparation and addition of the binder is the most important step in the process involving the injection molding of ceramics. Other factors that affect the quality of ceramics are listed concurrently.

(1) Raw material powder, preparation of an organic binder, selection of the kneading and granulating machine and of the kneading conditions.

(2) Selection of an injection molding machine capable of coping with the factors associated with ceramic molding, such as abrasion resistance.

(3) Die designs, material properties, and proper injection molding conditions.

(4) Degreasing, selection of sintering equipment and of the proper conditions.

### 3. Raw Materials for Ceramics

Table 3 shows representative ceramics used in injection molding. The average grain diameters of the raw material pulverulent bodies are generally below  $1\text{ }\mu\text{m}$ , with the easy-to-sinter alumina having an average grain diameter of  $0.4\text{ }\mu\text{m}$ , while that of the  $\alpha$  crystal is  $0.3\text{ }\mu\text{m}$ . Since zirconia, silicon nitride, and silicon carbide are obtained by synthesis, they have much finer diameters. Zirconia products of from  $200\text{--}450\text{ }\text{\AA}$  in crystallite diameter and  $>0.2\text{ }\mu\text{m}$  in particle diameter have been placed on the market. As a result, some

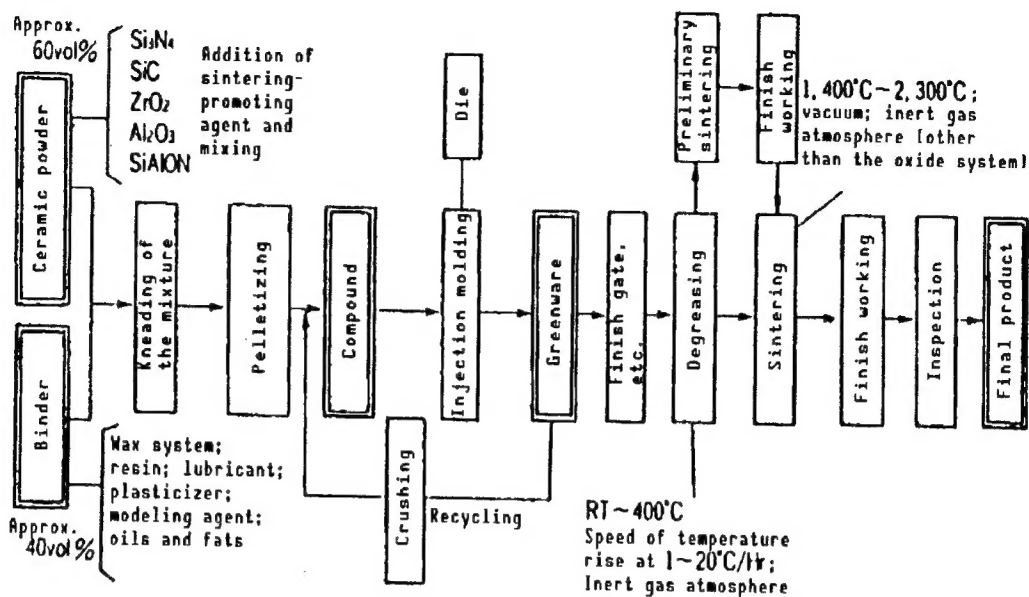


Figure 1. Process for Manufacturing Engineering Ceramics by Injection Molding

pulverulent bodies have relative surfaces of as large as  $20 \text{ m}^2/\text{g}$ , necessitating the addition of large amounts of binders. Sintering-promoting agents are sometimes needed in addition to the raw material itself.

#### 4. Organic Binders

The roles of binders can be broadly classified as follows:

- (1) Fluidity: waxes, resins, plasticizers
- (2) Bonding: waxes, resins, coupling agents such as surface treatment agents (partially replaced by elastomers to impart flexibility)
- (3) Degreasing: plasticizers, lubricants, sublimated materials
- (4) Detachment: waxes, lubricants
- (5) Others: dispersants (deflocculants), wetting agents

The decision as to what type of binder to select is determined after taking into account such factors as the formability, thermal stability, shape-retaining capability and degreasing capability, as well as the residual carbon, oxidation of the raw material elements and their denaturing.

#### 5. Preparation of Raw Materials and Their Mixing (Pelletizing)

In preparing a well-balanced composition of raw materials, consideration must be given to the roles of the binders described above and care also must be taken to minimize the amount of binder added. The binder, however, must be added in an amount sufficient to wet the specific surfaces of the raw material powder and fill up the cavities between particles. The amount of binder to be added is determined by the specific surface and the specific size distribution

Table 3. Characteristics and Properties of Major Ceramics

	Alumina ( $\text{Al}_2\text{O}_3$ )	Silicon nitride ( $\text{Si}_3\text{N}_4$ )	Silicon carbide ( $\text{SiC}$ )	Zirconia ( $\text{ZrO}_2$ )	Sialon ( $\text{SiAlON}$ )
Characteristics	Excellent mechanical strength; high abrasion resistance [AR]; high chemical stability	Highest strength, toughness of any existing ceramic; freedom from characteristic deterioration up to $1,000^\circ\text{C}$ ; excellent thermal shock resistance [TSR]	Slight deterioration in high temperature strength; heat resistance above $1,400^\circ\text{C}$ ; high hardness, high AR; utilization as material for heaters	High strength, high thermal characteristics; thermal expansion coefficient [TEC] values close to metals; effective as built-up member (filler)	High strength; small TEC; excellent TSR; hardness, abrasion resistance edge over zirconia; sliding AR superior to Al
Apparent specific gravity ( $\text{g}/\text{cm}^3$ )	3.95	3.15~3.35	3.15~3.20	5.7~6.08	3.23~3.26
Compressive strength ( $\text{kg}/\text{mm}^2$ )	330	—	—	—	350
Deflective strength ( $\text{kg}/\text{mm}^2$ )	40~55	65~102	51~66	120~180	95
Young's modulus ( $\text{kg}/\text{mm}^2$ )	$3.9 \times 10^4$	$3.4 \times 10^4$	$4.6 \times 10^4$	$2.0 \times 10^4$	$3.0 \times 10^4$
Hardness (Hv)	1800	1600	2500	1510	1580
Weibull coefficient (m)	—	10~16	11~14	13~20	11
TEC RT~ $800^\circ\text{C}$ ( $^\circ\text{C}$ )	$8.0 \times 10^{-6}$	$3.2 \times 10^{-6}$	$4.7 \times 10^{-6}$	$11.0 \times 10^{-6}$	$3.04 \times 10^{-6}$
Thermal conductivity ( $\text{cal}/\text{cm} \cdot \text{s} \cdot ^\circ\text{C}$ )	0.065	0.037	0.158	0.007~0.013	0.04
TSR ( $\Delta\text{Tc}$ )	210	700	330~370	320~400	>900
Inherent volume resistivity ( $\Omega \cdot \text{cm}$ )	$>10^{14}$	$>10^{14}$	$10^3 \sim 10^6$	$>10^{10}$	$>10^{11}$

of the raw material powder. This amount is about 40 vapor pressure volume percent in the case of alumina, and it increases to about 50 volume percent or more for zirconia. In the schematic diagrams shown in Figure 2, lesser amounts of the binder need to be added and, in addition, better fluidity can be obtained in the case of the grain size distribution shown in Figure 2(c)—the closer the grain diameter is to that of a sphere, the better—than in the case shown in Figure 2(a), where the grain sizes are uniform. When grain diameters are large and the grain size distribution width is narrow, under the shearing stress during kneading or forming, the mixture demonstrates a dilatancy state, as shown in Figure 2(b), and a drop in its fluidity is observed. In this situation, the mixture gives rise to dehydration, even under pressure, the binder alone is injected, and it is sometimes impossible for the molding operation to be realized.

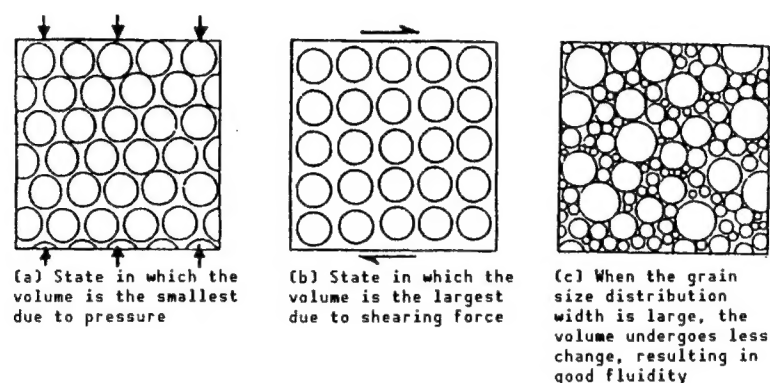


Figure 2. States of Pulverulent Body-Binder Mixtures

For kneading, a pressure kneader is usually used. The widely used mixing method applies the following procedure: the binder with a high melting point and large grain sizes is first kneaded and dissolved, followed by the addition of elements with lower melting points in a descending order; then, granules are added and finally, a liquid plasticizer is added for kneading exceeding 30 minutes. Pelletizing can be achieved by cooling the kneaded mass and pulverizing it, and the products produced this way can be offered as samples for experimental use. Subjecting the pulverized bodies to additional extrusion pelletizing enables ideal pellets with a uniform grain size to be obtained.

Direct mixed extrusion pelletizing equipment has also been placed on the market (Photo 1 [not reproduced]) shows alumina pellets).

## 6. Injection Molding Machine

Photo 2 [not reproduced] shows the external appearance of the injection molding machine. Broadly speaking, it consists of an injection unit, a clamping unit (die attachment section), an oil hydraulic unit, and an electric control unit.

The injection unit consists of a hopper that stores and feeds the raw materials, a heating cylinder made of abrasion resistant materials that is



heated and controlled by an external heater, and a screw. The rotation of the screw, injection, and forward and backward motion of the nozzle are controlled by hydraulic pressure. Ceramic compounds, in particular, sometimes demonstrate specific flow behaviors, so since the shape of the product to be molded varies, the injection molding machine must be provided with fine control functions.

### (1) Cylinder Material

The abrasion resistant cylinders currently being employed are mostly of a bimetallic-type of cylinder. The cylinder's inner surface has an abrasion- and corrosion resistant material, diffusion-bonded up to a depth of approximately 2 mm. Since the abrasion losses of the cylinder's inner surface are similar to those shown in Figure 3, coating the feed zone, in particular, with ceramics is quite effective. On an experimental basis, we coated the cylinder with a zirconia lining along its length, coated the feed zone with a sialon lining, and coated the other surfaces with an abrasion resistant alloy lining, and tests are currently underway.

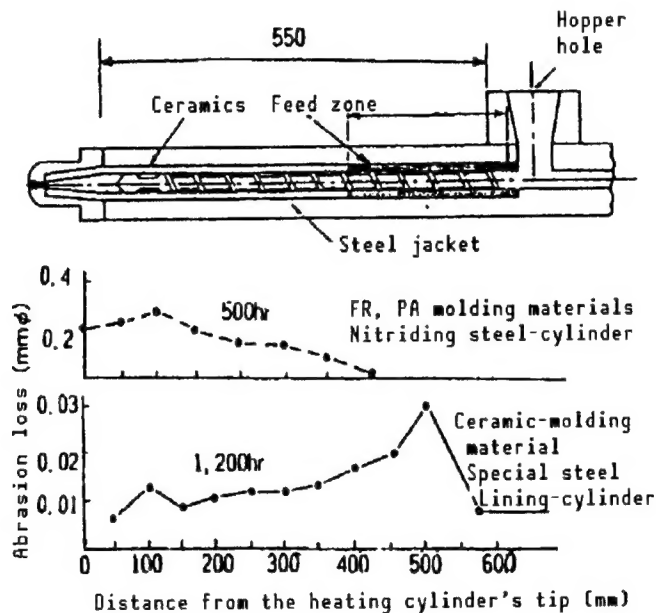


Figure 3. Cylinder Positions and Abrasion Losses  
(The upper diagram shows a cylinder with a ceramic sleeve being shrink fitted.)

### (2) Screw Material

As for the screw, abrasion was observed in the neighborhood of crests 5 through 8 in the feed zone, shown in Figure 4, in the case of the external diameter, while for the valley diameter, abrasion was observed in pitches 3 through 10 in the compression zone. The metalling zone was characterized by the presence of some pinholes, probably caused by corrosion, in addition to abrasion.

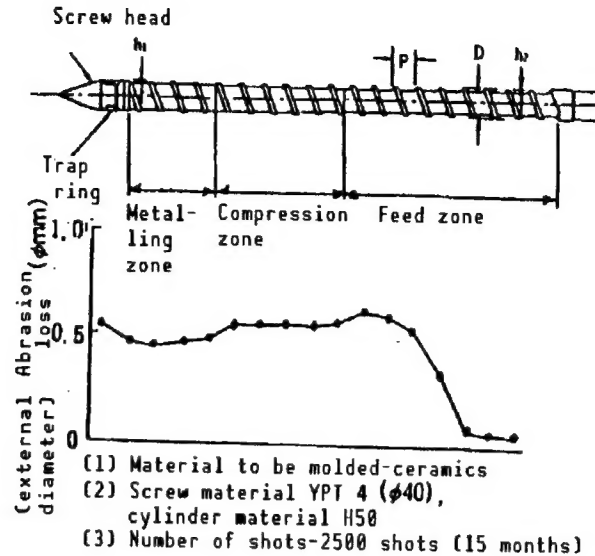


Figure 4. Positions of Abrasion in Abrasion Resistant Screw

As for the measures for increasing the hardness of the surface layer of the screw, a compound structure screw having SCM 440 as its core iron and a special product—a product manufactured by diffusion bonding and processing a layer of V50 (Tokyo Kohan Co. product) that is made by precipitating the superhard compound boride  $\text{Mo}_2\text{FeB}$  on a SUS matrix—as its surface material is effective, as shown in Figure 5, as are the methods of applying a coating of TiN, VC, or TiC by PVD or CVD up to a thickness of several microns. Consideration is also given to the screw design. The author, et al., manufactured an NED 15 (clamping 15T) screw with a  $\phi 18$  mm based on the former method, and a MIN7 (clamping force 7T) screw with a  $\phi 14$  mm based on the latter coating method, and the two are being subjected to tests.

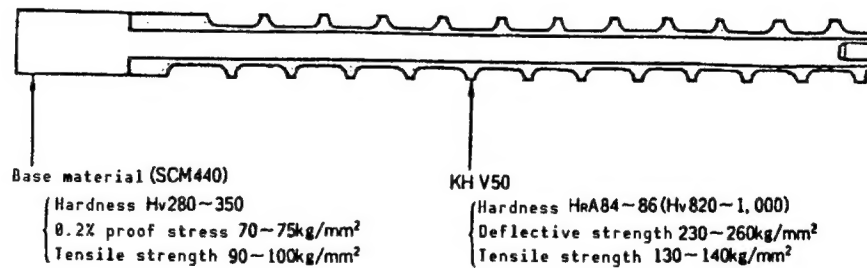


Figure 5. Structure of KH Screw and Its Mechanical Strength

In the injection molding machine in question, care is also being taken to prevent the abrasion of the three items, i.e., trap ring, screw head, and intermediate ring, with respect to material and design.

## 7. Points Requiring Careful Attention When Designing a Die

The flow behavior of ceramic molding materials during melting exhibits non-Newtonian fluid flow, as does that of ordinary polymer materials. Affecting the flow behavior are the grain diameter and the grain distribution of the ceramic raw material, as well as the melt viscosity of the binder and the amount of the binder added. Consequently, the author believes that the molding conditions, i.e., the setting temperature, speed and pressure, as well as the die design, and especially the gate position and shape, must be carefully examined, along with the molding material characteristics. Basically, since ceramic molding materials contain much smaller amounts of polymer materials than do ordinary molding materials, they have low compressibility, which is reflected in their almost zero recovery of elasticity. The result is that they have a small die swell when flowing from the gate into the cavity, which tends to give rise to jetting. The cooling speeds are generally fast, and solidification also takes place quickly.

A ceramic molding material shows a pressure drop in the mold that is larger than that for a plastic monomer, and this leads to inferior fusion in the weld section, possibly lowering its strength. Consequently, compared to plastic dies, in the dies for ceramic molding the gate design is critical, and an air vent and a slug well must be established.

### (1) Gate design

Ideally, the gate should be small. However, since a pin gate tends to give rise to jetting, it is to be avoided as much as possible. The slightly thick film gate and ring gate help maintain the proper flow and result in less distortion. A fan gate is desirable in a tub gate system, but the fan may have no effect at all if the angle of expansion of the fan is larger than  $60^\circ$  and if it is thin.

The side gate is effective for preventing the occurrence of jetting caused by the melt hitting the walls and expanding. However, it should be kept in mind that the differences in orientation and density, brought about by the difference in pressure transmission between the wall surface close to the gate and the opposite wall surface, may lead to its bending toward the gate side after sintering.

We produced moldings using experimental dies to examine the gate design and obtained optimal gate designs. With the exception of the film gate, they failed to prevent the occurrence of jetting, even when the injection speed was low. In the low speed region, raising the temperature (from  $120\text{--}160^\circ\text{C}$ ) helped the side gate to dissolve jetting.

### (2) Cavity design

There are two methods [for cavity design]: one is to etch a cavity directly into the die, and the other is the lining method. When the dimensions of a product are given, the dimensions of the die cavity and the core are determined from the total shrinkage rate  $S_{TL}$ .  $S_{TL}$  consists of  $S_G$ , the

shrinkage rate of the greenware, and  $S_L$ , the shrinkage rate that varies according to  $B$ , the component volume of the binder, and  $S_D$ , the relative density after sintering. In other words,

$$S_{TL} = S_G + S_L \quad (1)$$

Of these variables,  $B_V$  yields the greatest influence, and one needs to take into account the fact that although the binder leads to the generation of cavities after degreasing, the cavities almost disappear during sintering, thus enabling a high-density sintered body to be obtained, and that there remain some bores.

In the figure below, when the volume shrinkage rate during sintering is  $S_V$ , the volume of the sintered body is  $P_V$ , and the relative density ratio of the sintered body is  $S_D$ ,

$$S_V = 1 - P_V \quad (2)$$

$$P_V = \frac{1 - B_V}{S_D} \quad (3)$$

The sintering linear shrinkage rate  $S_L$  is expressed as follows:

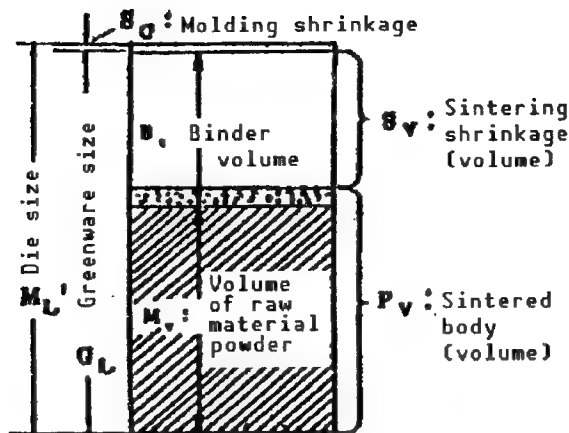
$$S_L = 1 - \sqrt[3]{1 - S_V} = \left( 1 - \sqrt[3]{\frac{1 - B_V}{S_D}} \right) (\times 100\%) \quad (4)$$

Although the linear shrinkage rate of the greenware  $S_{GL}$  is small, being in the 0.1~0.2 percent range, it varies depending on the kind of binder and the molding conditions, and is not necessarily uniform. The shrinkage rate arising from the binder is extremely large, but as long as the binder is dispersed uniformly,  $B_V$  is constant and variations are small. Consequently, with regard to variations, attention should be paid instead to the density ratio  $S_D$  of the sintered body. When the density of the sintered body is 100 percent, the sintering linear shrinkage rate can be given roughly by the following formula:

$$S_L = 1 - \sqrt[3]{1 - S_V} \approx \frac{1}{3} S_V + \frac{1}{9} S_V^2 + \frac{1}{16} S_V^3 \quad (5)$$

$B_V$  is usually 40 volume percent or so. The value is much higher than the shrinkage rate  $S_G$  of greenware. However, as long as the binder is dispersed uniformly, the shrinkage rate is the same, so one may assume that what determines the dimensional accuracy of a sintered body is the quality of the greenware. It has in fact been confirmed that there is little difference in dimensional scattering between greenware and the sintered body. Ceramic sintered bodies with a dimensional accuracy of below  $\pm 0.3$  percent have been

obtained, with some moldings having been found to have a dimensional accuracy of below  $\pm 0.1$  percent.



### (3) Draft, etc.

Molds for ceramic manufacturing are generally characterized by poor releasing properties, and the greenware also has low strength. Therefore, the draft must be about twice as large as that for plastics, attaining at least  $1/60(1^\circ)$  and above. The spool also must have a large draft of from  $5-10^\circ$ . In ceramic molding, not only cavities, but also these devices pose big problems, so they must be polished well. A split mold structure using a slide core, as in the case of turbocharger rotors, is advantageous for release from the mold.

Furthermore, bur-free air vents of less than 0.02 mm must be established to let the air escape during molding, and slug wells must also be established to lead the cold slug and weld section outside the cavities.

### (3) Die materials

Dies for ceramic manufacturing are required to be more abrasion resistant than those for plastics manufacturing. Both the trial manufacture type and production type of dies have come to be required to be produced in large varieties in small lots. In addition to having short life-cycles, such dies are expected to be delivered in a short delivery time. Consequently, some dies have come to be made of nonferrous materials featuring good cuttability at the expense of durability, while, in order to raise their surface hardness, the surfaces of some dies have been coated with TiN by PVD or CVD.

It is also advisable to place abrasion resistant inserts in the vicinity of gates where excessive wear and tear occurs.

As for the machining of dies, a method of implanting a hardening material directly into the die by an engraving electric discharge machine has come to be employed, and simple dies and unit dies have also come to be actively employed.

## 8. Forming Technology

In order to obtain defect-free, high precision moldings, the raw materials, dies, molding machines, molding conditions, and accessory machines must be in place, as in the case with the forming of plastics. With ceramics, the selection of the proper molding materials is of great importance.

Formability, especially, fluidity, can be examined by using a melt indexer, a flow tester, or a capillary rheometer. Each can examine formability using a small sample, but as for practical formability, the most precise technique for examining it is to measure the flow length.

As for practical viscosity, if the viscosity at the proper forming temperature within the shearing speed of from  $10^2$ – $10^3$   $\text{sec}^{-1}$  is below 10,000 poise, molding is available, but it is preferable that the viscosity be below 5,000 poise. At this time, the length of flow by a spiral flow type (a cross section measuring 10 mm across and 3 mm thick) is in the vicinity of 20 cm. Figure 7 shows the relationship between the injection pressure and temperature and the flow length.

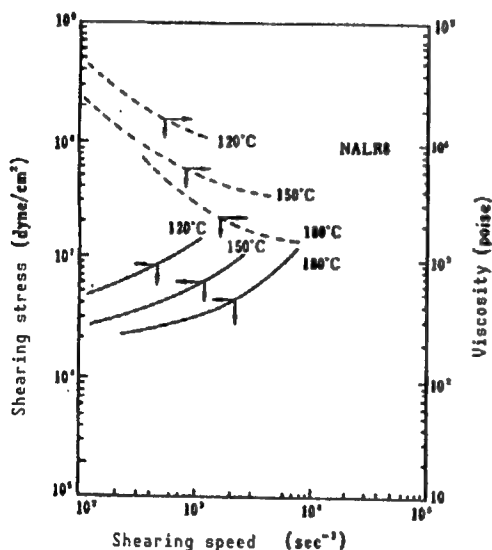


Figure 6. Flow Characteristics of Acryl-Base Ceramic Compound

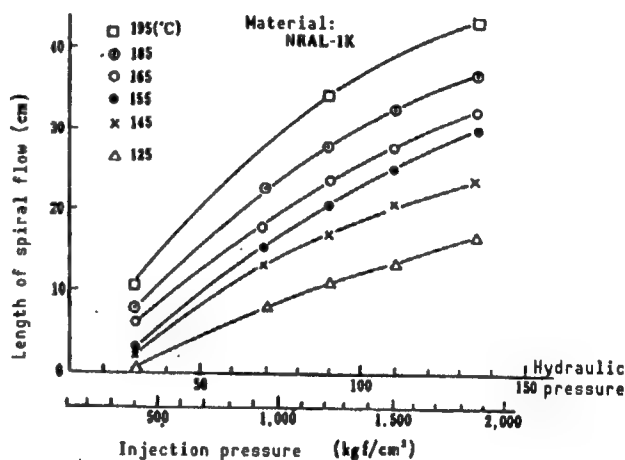


Figure 7. Relationship Between Injection Pressure and Spiral Flow Length

As for the relationship among the shearing speed, shearing stress and viscosity in wax- and acryl-based molding materials, in the wax-based materials, raising the temperature too much leads to a drop in the viscosity of the binder, which leads to the nonuniform transmission of pressure and gives rise to a peculiar viscosity curve. This is not desirable. Especially, a large particle diameter of the powder and small grain size distribution width tend to give rise to dilatancy, making it hard to mold the powder. In acryl-based materials having high viscosity, even the same pulverulent body exhibited normal flow behavior. Figure 6 shows the relationship.

The following are descriptions of examples of molding acryl-base alumina compounds into various products.

### (1) Example of molding using a test piece die

The dimensions of the die are shown in Figure 9. The testpieces used for bending strength and tensile strength testing had cross section to gate cross section ratios of  $4.0 \times 2.6 / 4.8 \times 3.6 = 10.4 / 17.28 = 0.6$  and  $14 \times 2.0 / 16 \times 2.5 = 28 / 40 = 0.7$ , and each exhibited good filling conditions.

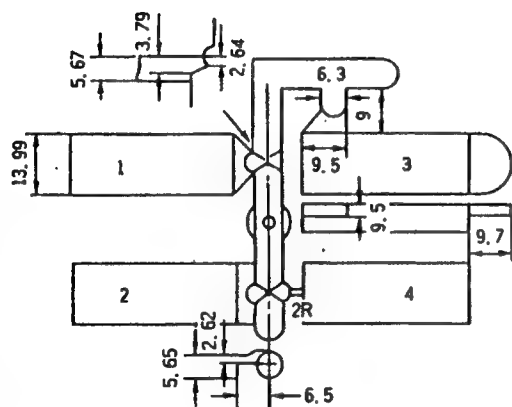


Figure 8. Die for Examining Gate Design

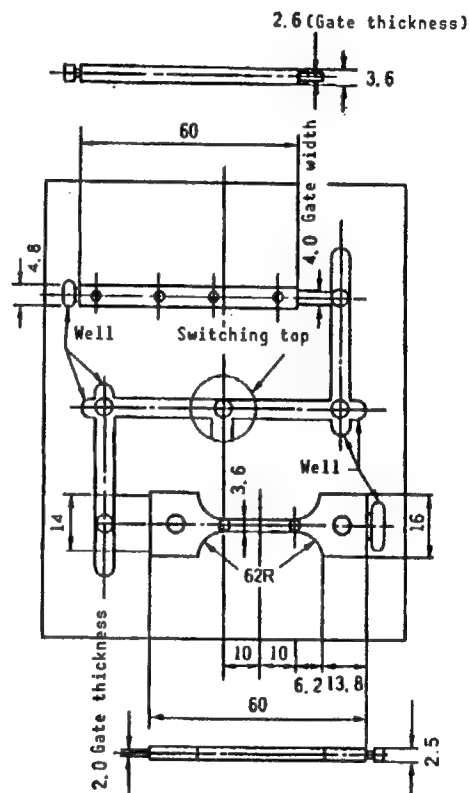


Figure 9. Dimensions of Die Cavities Used for Molding New Material Testpieces

### (2) Example of molding a turbocharger rotor

Table 4 gives the molding conditions that were used in molding a turbocharger rotor using a silicon nitride compound. Figure 10 shows the dimensions of the molded turbocharger rotor. Photo 3 [not reproduced] shows the die used.

Table 4. Turbocharger Rotor Injection Molding Conditions

Item		Setting conditions	Remarks
Raw material ceramics		Silicon nitride	Weight of molding 53.43 (g)
Injection molding machine		MN100H2000	
Cylinder temperature	Nozzle N	155 (°C)	
	H <sub>1</sub>	160 (°C)	
	H <sub>2</sub>	150 (°C)	
	H <sub>3</sub>	140 (°C)	
Die temperature	Fixed	42 (°C)	
	Movable	42 (°C)	
Screw rotation number		50 (rpm)	Screw diameter 40 (mm)
Injection pressure		570 (kgf/cm <sup>2</sup> )	
Pressure maintenance		170 (kgf/cm <sup>2</sup> )	0.68 sec
Injection speed		31.6 (mm/sec)	
Injection time		10 (sec)	
Cooling time		35 (sec)	
Dead time		3 (sec)	
Molding cycle time		60 (sec)	

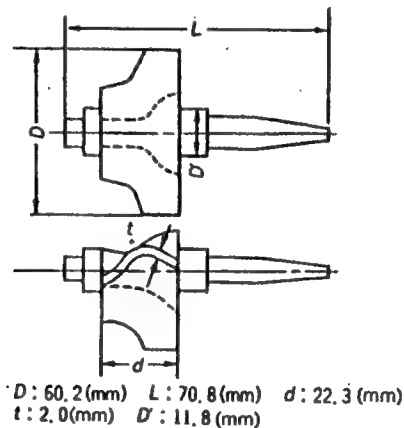


Figure 10. Dimensions of the Turbocharger Rotor Molded

### (3) Examples of molding cylindrical products

We compared the effects of various cylindrical moldings, such as "volute" gun nozzle, on the filling process of the gate design. We used zirconia for the molding material. Because excessive jetting was observed in each cross section, 2.5 x 2.0 (mm), of the four points in the spider gate and, furthermore, because a wide scattering in the strength of the sintered products was observed, we expanded the gate cross section to 6.8 x 2.0 (mm), which improved the jetting to a great extent. When using a molding material with good fluidity, jetting almost disappeared.



#### (4) Examples of molding optical fiber ferrules using model dies

Photo 4 [not reproduced] shows greenware and a sintered product made of zirconia compound by using model dies.

Types A and B of sintered ferrule products, each containing 50 pieces, were examined for staggerings in their weight and external dimensions in both greenware and sintered products, and the results are given in Table 5.

Table 5. Staggerings in Weight and Dimensions in Zirconia Ferrule Moldings and Sintered Products

Type		Weight (g)		Size (mm)	
		Greenware	Sintered product	Greenware	Sintered product
A	$\bar{x}$	0.3483	0.2972	2.4890	1.9565
	$\sigma$	0.00248	0.00363	0.0018	0.0013
	$3 \sigma/\bar{x}\%$	0.744	1.089	0.2169	0.1993
B	$\bar{x}$	0.3370	0.2931	2.4861	1.9088
	$\sigma$	0.00055	0.00048	0.0013	0.0005
	$3 \sigma/\bar{x}\%$	0.489	0.492	0.1569	0.0786

#### (9) Degreasing

The degreasing process removes the organic binder that has been added to help facilitate molding. When the binder element is discharged outside the system by the diffusion, evaporation or sublimation of the liquid or the melt system, there is little expansion in volume and the temperature can be raised at a fast tempo. With polymers, the volume expands rapidly due to decomposition and gasification. Consequently, rapid is in temperature must be avoided since they can generate cracks and swelling. The speed of the temperature increase is usually controlled within the scope of 1-20°C/hr, so a long time is required. As for the upper limit of the degassing temperature, since almost all organic binders decompose approaching 500°C, degassing is stopped below 400°C so that small amounts of the binder will remain in the degassed molding in order to retain its strength.

The atmosphere differs depending on the raw material powder—it is open air, N<sub>2</sub>, or Ar gas. In order to shorten the degreasing time, pressure degreasing, reduced pressure degreasing, supercritical gas degreasing, and solvent extraction have been used individually or in combination. Figure 11 shows the degreasing curves for ceramic moldings 3 mm thick and 5.9-7.6 g in weight. The degreasing rate differs depending on the kind of raw material powder, the grain diameter, the grains size distribution, and the binder processing used.

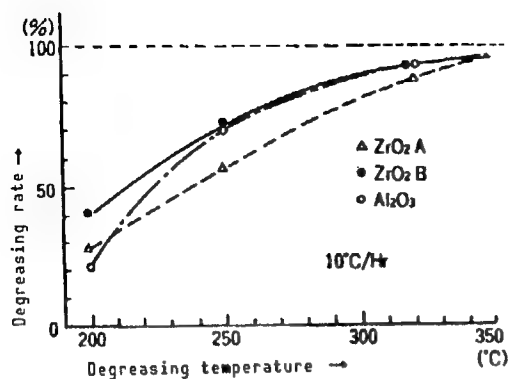


Figure 11. Comparison of Degreasing Rates for Various Powders

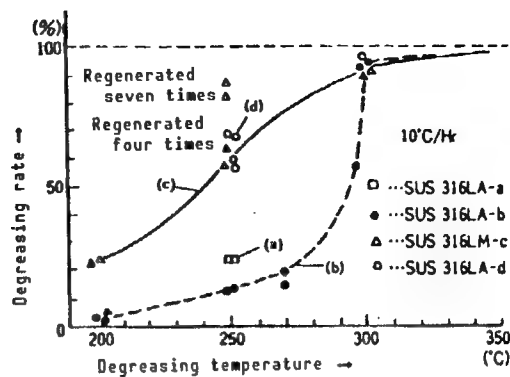


Figure 12. Effect of Plasticizer on Degreasing Rate

Figure 12 shows the degreasing processes for small moldings, 4 mm in maximum thickness, that have been manufactured using the SUS316 powder. Figure 12(b) shows a case in which wax has been used as the plasticizer, while Figure 12(a) shows a case in which a small amount of plasticizer has been retained and the rest has been replaced with wax. The mold-releasing properties have been improved, but the degreasing properties have deteriorated to a great extent, and this confirms the effect of the plasticizer on the degreasing properties. An increase in the amount of repeated use through regeneration improves the degreasing rate and the mold-releasing properties, probably due to a drop in the molecular weight of the binder.

## 10. Sintering

A molding that has been subjected to degreasing is almost identical in size to its greenware. In other words, it is a porous molding. It is then transferred to a sintering furnace for sintering, and if the molding is of alumina, the sintering follows the temperature curve shown in Figure 13.

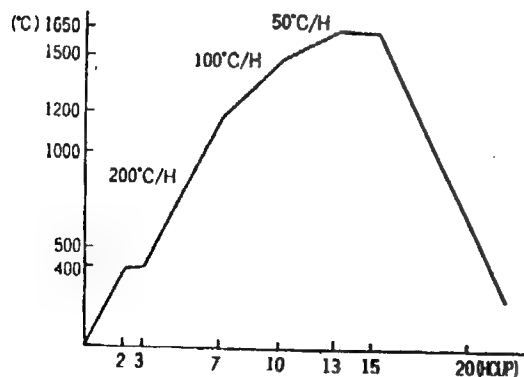


Figure 13. Sintering Curve for Alumina, 8 mm Thick

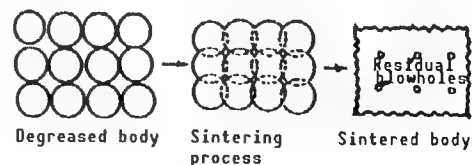


Figure 14. Schematic Diagram of Powder Particle Sintering Process

The speed with which the temperature rises follows a slow curve until the residual binder has been completely eliminated, and when the temperature reaches the 400~500°C range, it is retained in that state for 1~2 hours. According to Kuczynski, the sintering speed is determined by 1) viscous flow, 2) condensation, 3) volume expansion, and 4) surface expansion. The smaller the grain diameter, the lower the melt viscosity, and the larger the surface tension, the greater the sintering speed becomes. Figure 14 shows a schematic of a sintering process in progress. Photo 5 [not reproduced] shows samples of ceramic moldings.

Injection molding processes have slowly been finding increasing applications in the manufacturing of valves and bearings, as well as that of automotive parts, especially turbocharger rotors. The technique is also being used increasingly in fields in which products must have high heat resistance, corrosion resistance, and abrasion resistance, such as optoelectrical parts and tools, and cutting tools. The high quality and high performance of the products manufactured by the injection molding process have been acknowledged, but the technique still has far to go in terms of the raw material cost, the improvement of the degreasing process, the adoption of simple dies for lowering costs as well as for shortening the product delivery time, and the adoption of good die or mold materials featuring good processability if it is going to be able to compete with other techniques in the production of a variety of products in small lots.

#### References

1. Edited by Subcommittee, Editorial Committee of the Ceramics Industry Association.
2. Cookson, L., Sialon, Ltd., "Sialon 101—Typical Physical Property Data," No 4191, 1984.
3. Saito, K., "Molding of Fine Ceramics and Organic Materials," CMC, 1985, pp 77-78.
4. Yamaoka, K., "Proceedings of the Second Lecture Meeting on Injection Molding and Powder Metallurgy Technology and Application and Development," PURAKO GIKEN, 8-2, 1988, p 2.
5. Iwahashi, T., Ibid., 1-1-54, 1988, p 2.
6. Hitachi Metals, Ltd., "Technical Data on Abrasion-Resistant Screws."
7. Toyo Kohan Co., GIJUTSU SHIRYO.
8. Iwahashi, T., GOSEI JUSHI, Vol 34 No 2, 1988, pp 17-29.
9. Katagiri, T., "Proceedings of the Third Lecture Meeting on Injection Molding Technology of Engineering Ceramics and Application," 2-1, 1985.

10. Saito, K., "Molding of Fine Ceramics and Organic Materials," CMC, 1985, p 126.
11. Nakajima, N., CHEMICAL ENGINEERING, Vol 31 No 5, 1986, p 45.
12. Kikuchi, Y. and Muroi, A., GOSEI JUSHI, Vol 34 No 2, 1988, p 37.
13. Kuczynski, G.C., "Study of Sintering of Glass," J. APPL. PHYSICS, Vol 20, 1949, p 1160.

## Selection, Characteristics of Binder for Injection Molding

43067178B Tokyo THE 91ST WORKSHOP ON PLASTIC WORKING in Japanese 16 Jun 89  
pp 12-22

[Article by Katsuyoshi Saito, Kyoto City Industrial Laboratory]

### [Excerpt] 1. Foreword

The requirement for a binder is that it enable each particle of a powder to be coated efficiently in a short period of time with a minimum dosage. For molding, the problem at stake involves the fluidity of the kneaded compound. In general, since flow is treated as rheology, the behavior of the apparent viscosity in response to the shearing speed and die swelling becomes a key point.

Measurements of the shear rate of up to about  $10^4 \text{sec}^{-1}$  have represented the limit until now, but in high packing, the powder packing of materials inside a die is often done by jetting. When packing inside a die is to be done by high-speed flow, the variation in viscosity from cycle to cycle becomes important, and hence viscosity measurements in the ultrahigh shear rate region of about  $10^6$ – $10^7 \text{sec}^{-1}$  become necessary. The mode of flow is also important.

In degreasing, the key point is how to conduct the operation fast, in a short time, and yet defect-free. To that end, binder combination technology is necessary, but various methods have already been tried, such as degreasing, normal pressure, pressurization, ultracritical gases, and the extraction method. The issue becomes more complex when the speed for raising the temperature and ambients are taken into consideration.

Most cumbersome of all is the fact that no formula or theory exists that enables the binder selection to be performed by calculation, so the binder has been selected totally on a trial and error basis. The critical requirement associated with binder selection is that the binder not decompose and evaporate during the heating and kneading step of the injection molding process. This is also true with pelletizing and molding. From the viewpoint of degreasing, however, it is preferable that the binder start decomposing gradually from a relatively low temperature region. These two requirements are contradictory. Whether the binder is being used in a proper way or not has

great influence on the product yield, cost and performance. It is not an exaggeration to say that the quality of the product is determined by the binder added.

However, for the reason that the binder dissipates during degreasing and sintering, there has been a strong tendency to consider the binder as performing a strictly complementary role. It is a positive development that the importance of binders has come to be reviewed in recent years. Some papers have been published regarding the basic matters associated with binders, such as the state of a binder during uniform kneading, its behavior, the flow of the compound, and its association with the actual molding conditions, as well as the mechanism of degreasing, shedding some light on binder properties, but they have yet to be fully explained.

The author believes there is a need for basic and steady research into the basic nature of binders. To that end, a cooperative research structure involving the government, academia and industry will be needed.

In conclusion, I hope the binder, that has been delegated to a subservient role, will eventually come to play a leading role.

## 2. Selection of Binder and Actual State

### (1) Method of Selection

A binding agent helps retain the strength of the greenware. A lubricant helps improve moldability by improving the mold release properties and slip among grains. A plasticizer imparts rheology as well as plasticity and flexibility. A surface treatment agent improves the wettability of the powder, improving its moldability and degreasing properties. The binder for injection molding use comprises a binding agent, lubricant, and plasticizer, and, if needed, a surface treatment agent is added to it.

The key points in binder selection are the moldability and degreasing properties. The following describes the binder selection method that I have devised and that I am still using.

As shown in Figure 1, at the top of the coordinates is a binder with good heating fluidity. Plastic binders are indicated by the sign MI (MFI), and each polymer has a value. If available, a polymer with an MI value exceeding 20 g/10 min is desirable. Polyethylenes, polypropylenes, EVA resins, EEA resins, and polystyrenes belong to this category. Next, on the left side of the coordinates are binders with good degreasing properties, i.e., polymers that decompose during dissociation and polymerization, and this class includes polystyrene, atactic polypropylenes, methacrylic resins (butyl, isobutyl), and polymers with an ether linkage (polyacetals, celluloses). On the right side of the coordinates is a lubricant, which is paraffin wax, microcrystalline wax, stearic acid amide wax, or denatured wax. Phthalic acid esters (methyl, ethyl, butyl) are usually used as a plasticizer.

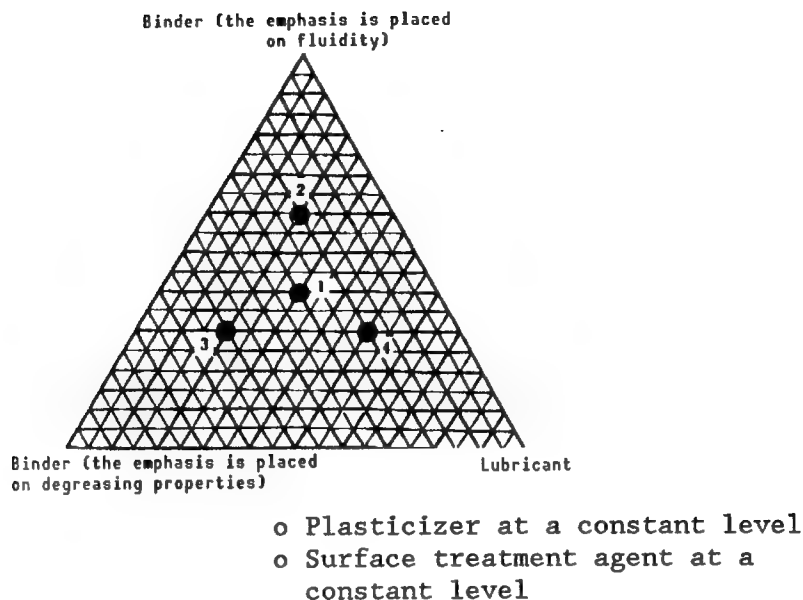


Figure 1. Triangular Coordinates for Binder Combinations

As an example, I used an EVA resin as the binder (top position), polybutyl methacrylate as the binder (bottom left), and dibutyl phthalate as the plasticizer.

A mixture for the central point of the triangular coordinates, 1, is prepared, and is then kneaded, molded, degreased, and sintered so that the results can be observed. If the results are good, the vicinity of central point 1 is studied further. If any defects are found, the left side point 3, the upper side point 2, and the right side point 4 are similarly examined. In the mixture in this case, point 2 shows good moldability but tends to give rise to defects during degreasing. Point 4 has extremely good moldability, but is so soft that it occasionally causes the molding to crumble. Point 4 has difficulty flowing unless the molding temperature and pressure are raised, but has good greasing properties. Point 1 is well balanced, enabling a good molding to be obtained.

If each of the points among the triangular coordinates fails to produce defect-free moldings, a combination of different kinds of binders and lubricants will have to be tested.

Next, is the amount of binders and lubricant to be added. It is advisable to calculate the amount based not on weight, but on volume, i.e., in the case of alumina, if the specific gravity of 4 is assumed to be 1 hypothetically (in reality, the calculations are conducted down to 2 decimal places), 100 g of alumina and 25 g of binder are heated and kneaded (1:1 in volume ratio). If the dough is as sticky as a Japanese rice cake, it is ideal. If the dough is crisp, additional amounts of binders are added. The compound is first pulverized into pellets and then into a powder, and is preheated in a high polymer type flow tester, "capillograph," or melt indexer in order to obtain fluidity.

With the high polymer flow tester, the volume of flow must exceed  $0.05 \text{ cm}^3/\text{sec}$  when forced through a nozzle with a diameter of  $1 \times 10 \text{ mm}$  under a pressure of  $30 \text{ kgf/cm}^2$  (random temperatures can be set). With the capillograph, the apparent viscosity must be below 1,000 poise in the shear rate range of  $100\text{--}1000 \text{ sec}^{-1}$  when forced through a nozzle  $1 \times 10 \text{ mm}$  in diameter (random temperatures). With the melt indexer, when the load is 6200 g, the volume of flow must exceed 30 g in 10 minutes at  $180^\circ\text{C}$ .

If the heating fluidity is found to be satisfactory, the compound is molded, degreased, and sintered into a product on a testpiece. When the ratio of powder to binder by volume is above 50:50, defects tend to appear during degreasing.

Therefore, tests should be conducted by changing the volume ratios of powder to binder.

Since the amount of binder to be added is influenced by the tap density and specific surface of the powder, a powder with an excessively large specific surface requires a large amount of binder and, therefore, is inappropriate. Powders for injection molding should have a specific surface smaller than  $10 \text{ m}^2/\text{g}$ .

As described above, binders should be examined from the perspectives of both quality and volume.

In alumina systems, the preferable volume ratio is 60 percent powder and 40 percent binder, while in the zirconia systems the ratio is 45 to 50 percent powder and 55 to 50 percent binder. In nonoxides ( $\text{SiC}$ ,  $\text{Si}_3\text{N}_4$ ), the ratio is 52 to 54 percent powder and 48 to 46 percent binder.

However, from the original objective of injection molding, the ideal powder to binder ratio is 60 percent to 40 percent, which will greatly facilitate the ease of degreasing. Consequently, various efforts, such as adjusting the grain size of the powder and using a surface treatment agent, have been made to that end. Requirements demanded of binders are stability in the kneading and molding processes and instability in the degreasing process. What this means is that the binder is expected to display two contradictory characteristics during a single process. Consequently, it may be said that binder selection is a process of compromise. This is an important point in selecting binders. No formula or theory currently exists that can be employed to calculate what binder to adopt, so the effort to find a suitable binder is being accomplished on a trial and error basis. Therefore, binder selection has much to do with expertise.

## (2) Actual Example

The  $\text{Si}_3\text{N}_4$  compounds for injection molding were prepared by the following method: The elements used were  $\text{Si}_3\text{N}_4$  powder (SN-9FW manufactured by Denki Kagaku Kogyo KK), EVA UE633 (Toyo Soda Manufacturing Co. product) as the fluidity-based binder, butyl methacrylate (CB-1, Sanyo Chemical Industries, Ltd., product) as the degreasing property-based binder, modified wax



("Celluna" D-793, manufactured by Chukyo Yushi Co.) as the lubricant, D.B.P. lubricant, and acryl oligomer ("Olicox" KD-140, manufactured by Kyoei-sha Yushi Kagaku Kogyo Co., Ltd.) since  $\text{Si}_3\text{N}_4$  has poor wettability with binders, and the combination shown in Figure 2 was examined.

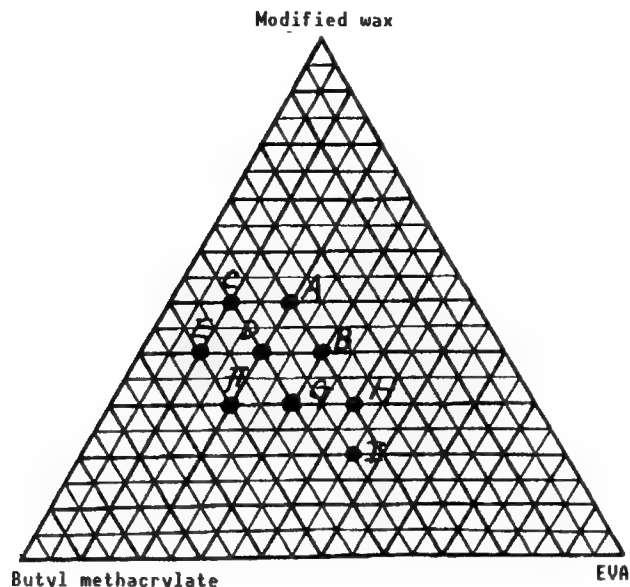


Figure 2. Coordinates of  $\text{Si}_3\text{N}_4$  Compounds

Details of the composition of the compounds are shown in Table 1. When the amount of the modified wax increases, the viscosity decreases, as does the molding temperature. With increasing binder amounts, the viscosity increases. The A through I compounds are molded, degreased, and sintered to determine which compositions are good and which are not.

### 3. Kneading and Fluidity

#### (1) Kneading

The objective of kneading is to coat each powder grain uniformly and effectively with the minimum amount of binder. For heat kneading a powder for use in testing and for heat kneading a small amount of powder, a lab plastomill as shown in Photo 1 [not reproduced] is used, the operating principle of which is shown in Figure 3.

For practical use, a scaled up version of the lab plastomill shown in Photo 1 [not reproduced] is used. A kneading operation has been conducted using this kneader.

Since this lab plastomill allows variations of the shearing torque ( $\text{kg}\cdot\text{cm}$ ) and internal temperature to be measured continuously, it enables various data to be obtained. An example is shown in Figure 4.

Table 1. Composition of  $\text{Si}_3\text{N}_4$  ( $\text{Si}_3\text{N}_4$  90 volume percent,  $\text{Y}_2\text{O}_3$  5 volume percent,  $\text{Al}_2\text{O}_3$  5 volume percent) Compounds (wt)

	Powder	"Celluna" D-793	CB-1	UE633	"Olicox" KD-140	D.B.P.	Equilibrium torque for plastograph
A	100	9.34	5.59	3.73	0.62	2.81	812
B	100	7.60	5.64	5.64	0.62	2.83	1,620
C	100	9.42	7.53	1.89	0.62	2.83	766
D	100	7.63	7.63	3.81	0.62	2.87	1,126
E	100	7.69	9.64	1.93	0.64	2.90	813
F	100	5.85	9.76	3.89	0.65	2.94	1,380
G	100	5.79	7.73	5.79	0.64	2.91	1,976
H	100	5.73	5.73	7.65	0.63	2.88	2,072
I	100	3.89	6.81	8.76	0.65	2.93	3,000

In all cases, the volume ratio of the powder and the binder total is 100:80.

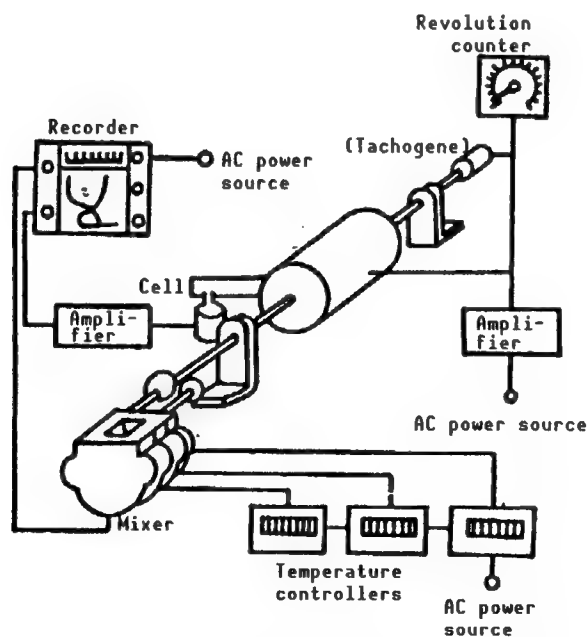


Figure 3. Principle of Lab Plastomill

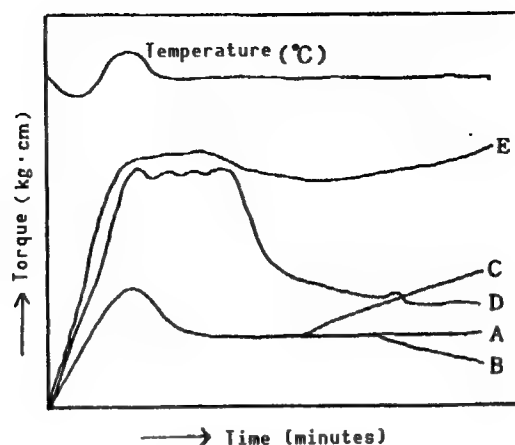


Figure 4. Kneading Behavior in Lab Plastomill

The most standard curve, Curve A, is typical of the kneading behavior of powders whose particles are well wetted by binders and are also close to spheres, as well as of powders that follow the ordinary closest-packed packing distribution. Curve B represents the kneading behavior in which the torque value decreases with time, and this phenomenon is seen when the binders used get decomposed by heat and their molecular weights decrease. Conversely, Curve C is seen either when the binders used have been subjected to chemical reactions by heat and have hardened, or when the binders and powder have reacted. Curve D represents the case in which the powder is made up of extremely finely pulverized particles, either square in shape or gourd-shaped, and when the powder particles have difficulty getting wetted by the binders, the kneading torque initially rises, but declines after some time. Curves A, B, C, and D all represent a phenomenon in which the powder particles are fully permeated with binders. In the case of Curve E, the torque value does not decrease even with time, but instead shows a tendency to increase. This behavior is observed when the amounts of binders are small. The mixture outwardly seems well kneaded, but the powder particles are not fully coated by the binders. As a result, frictions arise between the powder particles, the torque value fails to decrease, and the equilibrium state rises slightly. When the torque values are stable over a period of time it is assumed that the kneading process has followed its course. Although it may harbor problems on a microscopic level, it can be said that when the torque values have attained some empirical levels, the kneading operation has run its course.

## (2) Fluidity

Table 2 shows the compositions of compounds incorporating alumina with polybutyl methacrylate (PBMA), polystyrene (Pst), atactic polypropylene (App) and stearic acid (St). The compounds were kneaded in a lab plastomill for 40 minutes at 160°C. The flow characteristics of the compounds were measured from a capillograph.

Table 2. Compositions of Compounds (wt%)

	Al <sub>2</sub> O <sub>3</sub>	Pst	PBMA	APP	WAX	St	Total
A'	100	3.30	3.30	9.44	—	0.46	116.5
B'	100	3.30	3.30	4.72	4.72	0.46	116.5
C'	100	3.30	3.30	—	9.44	0.46	116.5

Figure 5 shows the apparent viscosities relative to shear rates for the compounds in a capillograph. It is generally assumed that when the viscosity is below  $10^4$  poise for the shear rate in the  $10^2$  to  $10^3 \text{sec}^{-1}$  range, molding is possible.

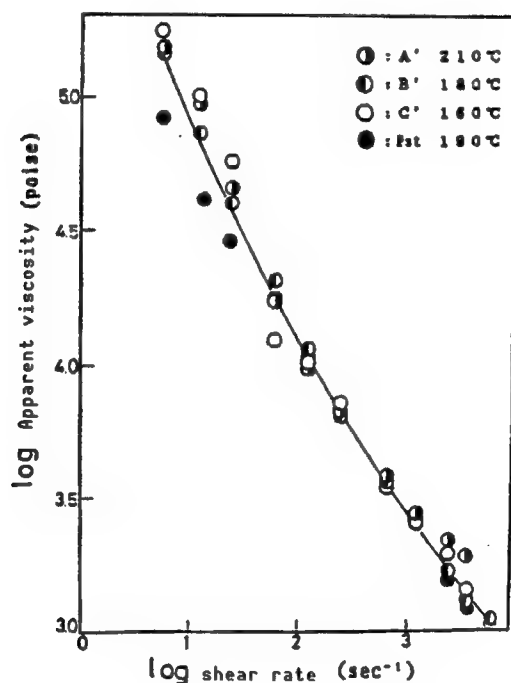


Figure 5. Variations in Apparent Viscosity Relative to Shear Rate

The bar flow test die is widely used as the yardstick in actual injection molding operations. When the flow length for the various compounds is measured, the moldable length exceeds 20 cm. The activation energies of flows at shear rates or  $1.2 \times 10^2$  to  $6 \times 10^2 \text{sec}^{-1}$  were in the 9~28 kcal/mol range in the capillograph.

Activation energy larger than 10 kcal/mol is required for molding.

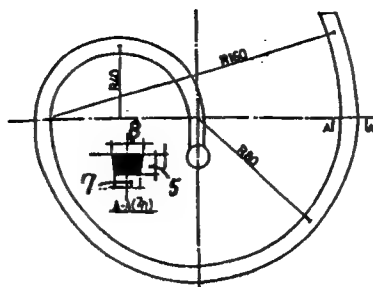


Figure 6. Bar Flow Test Die

#### 4. Degreasing Methods and Actualities

##### (1) Normal pressure

In determining what degreasing program to adopt, the pyrolysis curves for binders obtained by thermogram balance are of great help.

Figure 8 shows pyrolysis curves in air, while Figure 9 shows them in  $N_2$  gas, and Figure 10 in Ar gas.

By utilizing the information contained in the section entitled "Selection of Binders," two to four types of binders that follow a smooth curve have been selected in these diagrams.

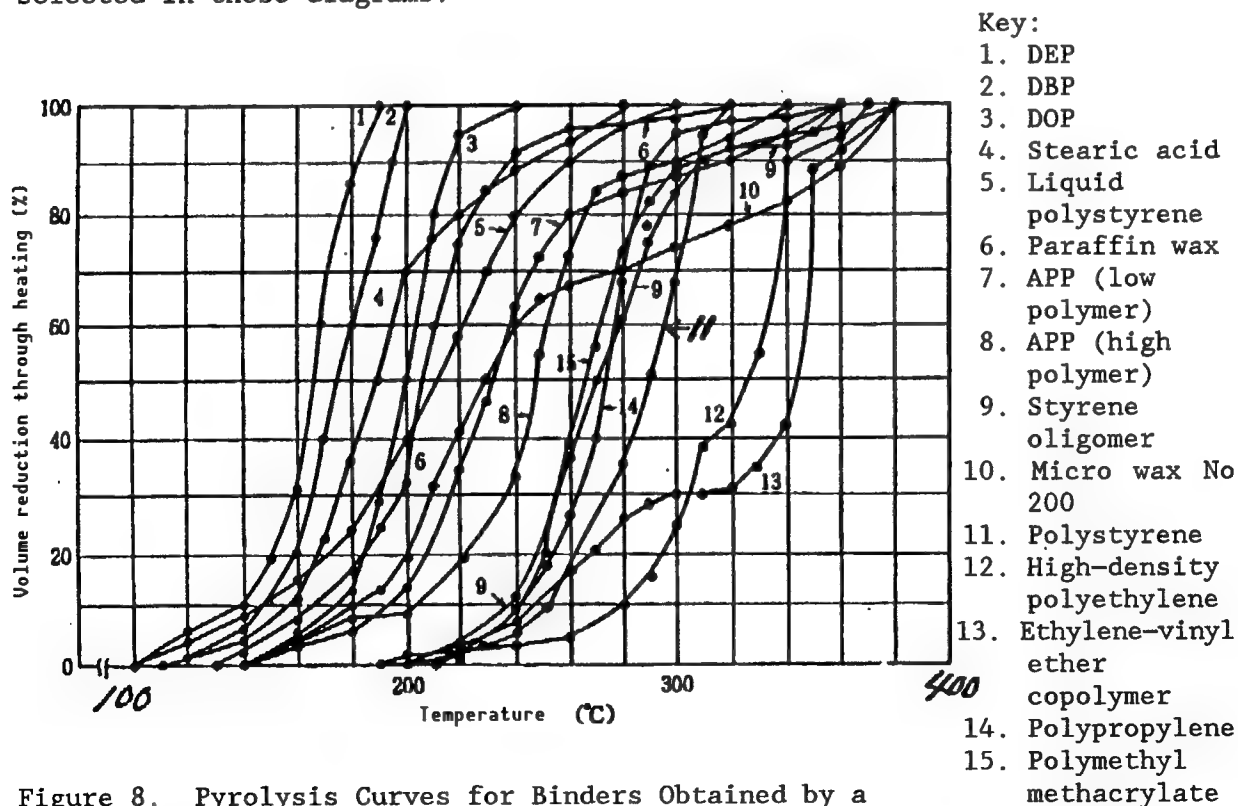


Figure 8. Pyrolysis Curves for Binders Obtained by a Thermogram Scale (In air, temperature rise speed  $2^{\circ}\text{C}/\text{min}$ )

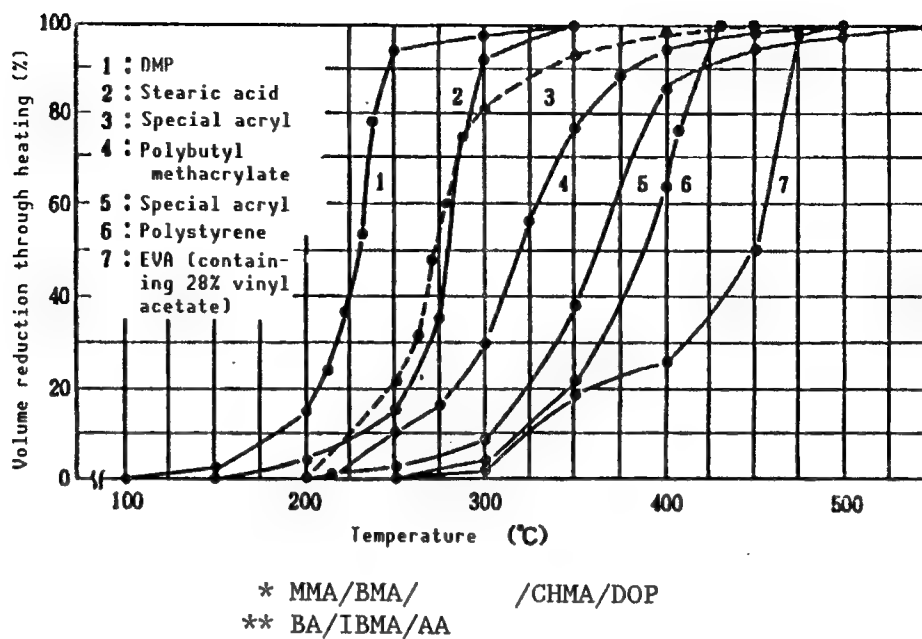


Figure 9. Pyrolysis Characteristics of Binders  
 (In  $N_2$  gas,  $3^\circ C/min$ )

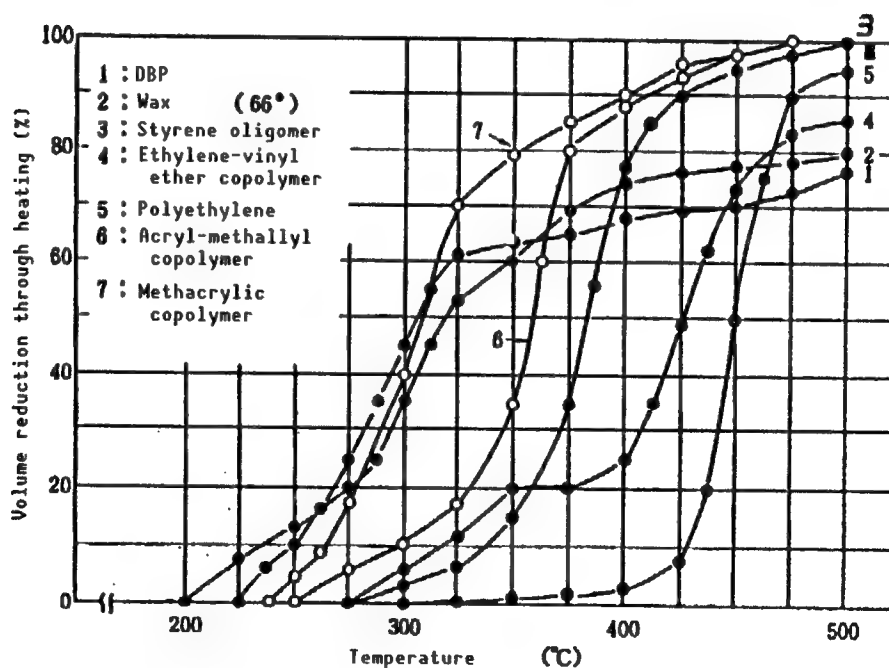


Figure 10. Pyrolysis Curves for Binders Obtained by Thermogram Scale  
 (In  $A_r$  gas ambient, temperature rise speed  $3^\circ C/min$ )

## (2) Pressurization

Applying pressure enables the volume of the pyrolysis gas to be reduced. Since the product of the volume of a gas generated at a certain temperature and its pressure  $PV$  is constant, when the pressure of the applied force is  $5 \text{ kg/cm}^2$ , the volume of gas generation can be reduced to one-fifth that for normal pressure. A good pattern was obtained with an  $\text{Si}_3\text{N}_4$  compact (cutter blade),  $12 \times 30 \times 85 \text{ mm}$  (35 g), containing 70.5 percent  $\text{Si}_3\text{N}_4$  (Denki Kagaku SN-9FW), 4.7 percent  $\text{Y}_2\text{O}_3$ , 3.2 percent  $\text{Al}_2\text{O}_3$ , 13.7 percent thermoplastic resin (PE.PP), 2.5 percent stearic acid, 4.9 percent wax, and 0.5 percent plasticizer, as shown in Figure 11. Of 62 cases tested, 34 were satisfactory (conducted at Tokai Konetsu Kogyo Co., Ltd.).

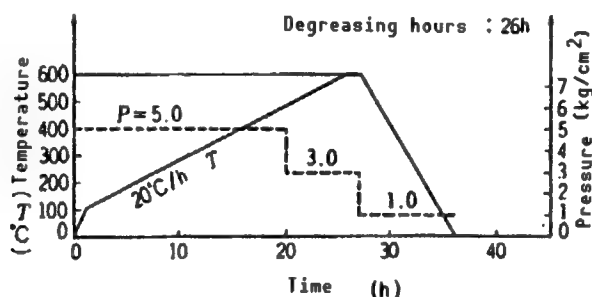


Figure 11. Example of a Degreasing Pattern Obtained With Pressurization

## (3) Decompression

Direct decompression tends to make the binders inflate like millet cakes. Therefore, a decompression method is effective when the volume of binders is reduced by 10~20 percent in volume percentage in advance by means of normal pressure extraction. When using a VS Lgr 10/18 furnace manufactured by Shimadzu Seisakusho, Ltd., a green body whose binders have been degreased in advance by 20~30 percent in volume under normal pressure can be degreased in 2~4 hours under reduced pressures down to  $500^\circ\text{C}$  (3~5 mm in thickness).

## (4) Extraction

According to U.S. Patent 4,197,118, 8 April 1980, binders can be extracted by using a polyolefin of a low molecular weight and a solvent of trichlene in the equipment, as shown in Figure 12.

According to a published patent, 1982-477741, subjecting a green body, molded using APP, stearic acid, and DBP binders, to a hot water treatment at  $100^\circ\text{C}$  to extract the stearic acid and DBP and then subjecting it to normal pressure degreasing enables good results to be obtained.

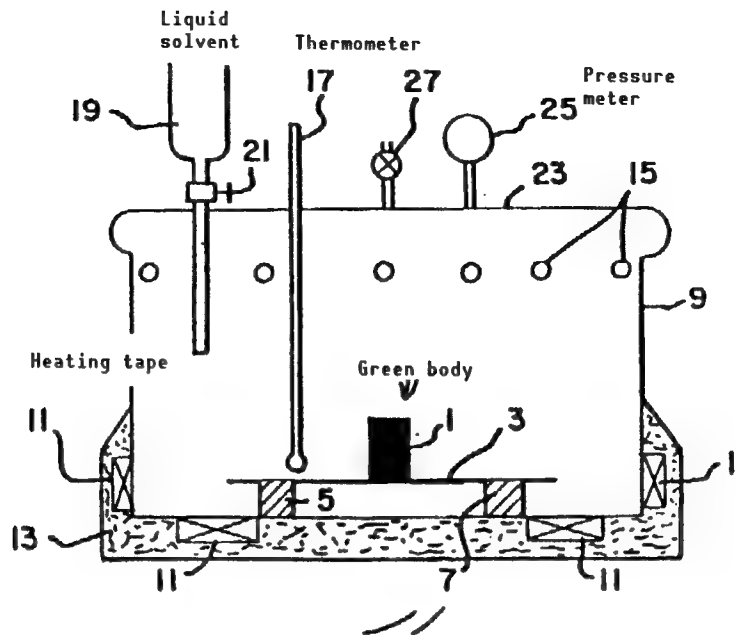


Figure 12. Extraction and Degreasing Equipment  
[Key to numbers not supplied]

#### (5) Supercritical Gases

The extraction technology using supercritical gas fluids has the following advantages: it can be done in a shorter time (2-3 hours); it is effective for thick green bodies; it features degreasing at low temperatures and small distortion; and it can be done in a nonoxide ambient. Among the technology's disadvantages are the high initial cost, batch process, and the application of the high pressure gases control law. Experiments have been conducted using compacts, 325 mm  $\phi$  x 15 mm, containing alumina and stearyl alcohol and stearic acid binders, and the results are shown in Table 3.

Table 3. Degreasing Test Results (From a Sumitomo Heavy Industries catalog)

Binder	Fluid	Temperature (°C)	Pressure kg/cm <sup>2</sup>	Degreasing rate (%)	Hours
Stearyl alcohol	CO <sub>2</sub>	45	200	70.2	2.2
" "	FREON 12	120	120	94.7	2.8
Stearic acid	CO <sub>2</sub>	45	200	85.0	2.5
" "	FREON 12	120	120	99.0	0.7

Much remains to be explained about the degreasing mechanisms of green bodies produced in ceramic injection molding. Maruya, et al., explained the mechanism in connection with the liquid phase behaviors of polymers in the



160~180°C temperature range on page 246 of the "Proceedings of the Japan Ceramics Industry Association Meeting 1988," and in the POLYMER PREPRINTS, Japanese, Vol 36 No 10, 1987, page 3473. Seno described the selection of binders for shortening the degreasing time in GOSEI JUSHI, Vol 34 No 6, 1988, page 17. Samukawa, et al., described the relationship between degreasing behavior and bending strength on page 65 of the "Proceedings of the Fourth Meeting of the Convention on Synthetic Resin Industry Technology" held in 1988.

#### References

1. Saito, K., "Molding of Fine Ceramics and Organic Materials," CMC Co., published on 26 August 1985.
2. Saito, K., Arkia, Y. and Inoue, M., "Injection Molding Technology of Fine Ceramics," published by Nikkan Kogyo Shimbunsha, 20 March 1987.
3. Saito, K., "Fine Ceramics: Basics of Binders for Molding of Metallic Powders and Technology for Their Application," IPC Publication, published 10 December 1988.

## **Laser Processing Technology, Its Applications**

43067178C Tokyo THE 91ST WORKSHOP ON PLASTIC WORKING in Japanese 16 Jun 89  
pp 23-30

[Article by Masaharu Moriyasu, Production Technology Research Laboratory,  
Mitsubishi Electric Corp.]

### **[Text] 1. Foreword**

Since Maiman's discovery 30 years ago of the laser (light amplification by stimulated emission of radiation), more than 1,000 kinds of lasers have been developed, and lasers have now come to be applied in various fields, including measurements, communications, data processing, materials processing, and medicine. In applying the laser to materials processing in which its heat rays are exploited, in particular, laser processing has come to be employed on a full-fledged basis in recent years, and the technology is expected to find increased application in the future.

For application to materials processing, the YAG laser (with a wavelength of  $1.06\text{ }\mu\text{m}$ ) and  $\text{CO}_2$  laser (wavelength  $10.6\text{ }\mu\text{m}$ ) have been widely used. The  $\text{CO}_2$  laser, in particular, emits far-infrared light of intense heat. Due to its relatively large oscillation efficiency and its capability to generate large output ( $\sim 20\text{ kw}$ ) on a stable basis, the  $\text{CO}_2$  laser has been used in various applications, such as the cutting, welding, and heat treating of various kinds of materials.

$\text{CO}_2$  laser processing technology has recently been drawing attention as a method for processing hard and brittle ceramics, for which secondary processing using the existing machining processes has been very difficult.

In the following, the author describes the characteristics of laser machining, the current status of  $\text{CO}_2$  lasers, and the characteristics of various laser processes for processing ceramics and their applications.

### **2. Characteristics of Laser Processing**

Laser processing is a thermal process in which the material is heated by irradiating a laser beam. Being a noncontact process, the technique enables

the processing of hard and brittle materials, such as ceramics, to be carried out with relative ease.

Being monochromatic, laser light features excellent focusing properties, so a laser beam can be focused, using optical devices like lenses, to a microscopic spot of approximately 0.1 mm  $\phi$ , thus enabling a high power density on the order of  $10^7 \text{ w/cm}^2$  to be obtained. With the laser, various types of processing can be executed by adjusting the power density and the length of the irradiation impinging on the workpiece, as shown in Figure 1.

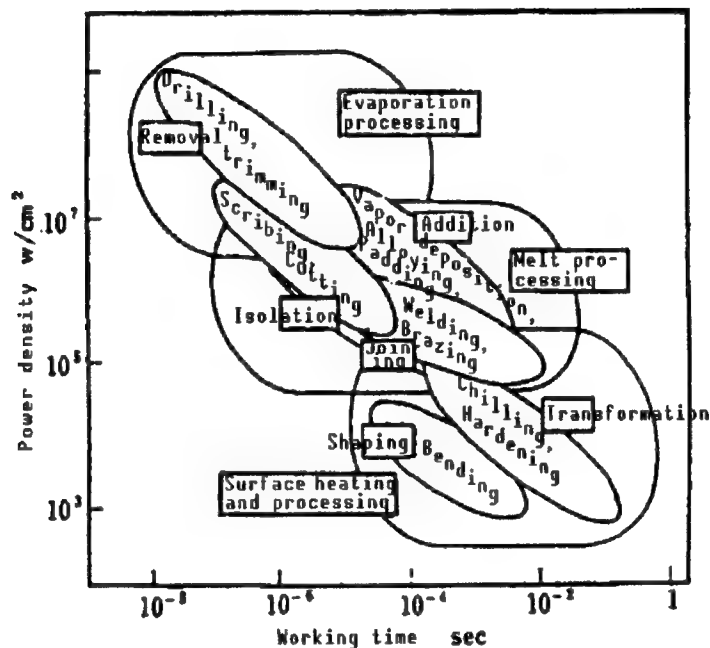


Figure 1. Classification of Laser Processing Methods

When the power density is relatively low and the working time is long, the surface temperature of the workpiece goes up. Although this does not lead to surface melting, it does cause the surface to undergo phase transformation or thermal distortion. When exploiting the characteristic of the laser, the technology enables surface heating and processing operations, such as transformation processing like hardening and shaping (bending) processing, utilizing distortion, to be performed.

A laser beam with a slightly higher power density will melt the workpiece, enabling bonding processing like welding, adding processing like padding, and separation processing like cutting to be performed.

A laser beam with a still higher power density will make the workpiece evaporate, enabling adding processing like vapor deposition, and elimination processing like trimming, cutting, and drilling to be performed.

As seen above, in laser processing various types of processing can be carried out by adjusting or controlling the power density and working time of the beam

and by controlling the laser output or the processing speed, as well as by using optics systems.

### 3. Current State of CO<sub>2</sub> Lasers

More than 70 percent of CO<sub>2</sub> laser processing can be accounted for by cutting and drilling operations. In this field, the needs are shifting away from the conventional cutting of simple shapes to such sophisticated operations as the processing of high-precision parts with higher added value, the processing of three-dimensional parts, and compound processing involving a combination of welding and heat treating. To cope with the trend, lasers have been becoming increasingly more sophisticated as evidenced by the development of pulse oscillators and mode-jumping oscillators with excellent output control characteristics, as well as high-speed and high-precision machines incorporating 32-bit CNCs capable of high-speed computation and multiple spindle-controlled machines capable of machining three-dimensional shapes.

Figure 2 shows the output pulse waveform of a three-axis orthogonal laser oscillator. Rectangular pulses can be obtained even during high peak pulse oscillation and, compared to triangular pulses, from an axial flow oscillator, they are very stable and are superior in terms of processibility. For cutting, single mode oscillation featuring excellent light focusing is generally used, while for welding and heat treating, the multimode and neuramode, capable of obtaining large outputs, are used. A mode-jumping oscillator will be versatile enough to carry out compound machining involving cutting, welding, and heat treating.

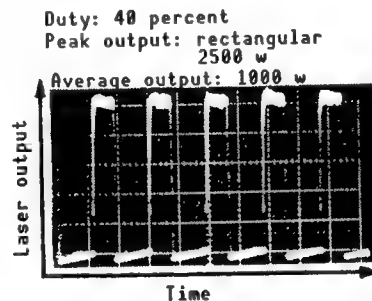


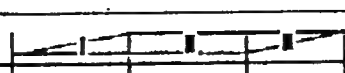
Figure 2. Output Pulse Waveforms of a Three-Axis Orthogonal CO<sub>2</sub> Laser Oscillator

Figure 3 [not reproduced] shows an example of a CO<sub>2</sub> laser for flat plates. A hybrid type incorporating the beam scan and table transfer functions, the machine features excellent working capabilities and saves space.

Table 1 shows the machine's cutting powers for cutting representative materials. Thanks to the development of the oscillator and processing system, as well as the machining technology incorporating it, it has become possible to obtain microscopic cuttings, as shown in Figure 4 [not reproduced].

The type of CO<sub>2</sub> laser used will depend on the application, such as the five-axis controlled three-dimensional processing machine and the multihead processing machine which enable multiple operations to be performed

Table 1. Power of CO<sub>2</sub> Laser To Cut Various Materials

Cutting power				
Soft steel	0.04 mm	0.1 mm	8 mm	21 mm
Stainless (SUS 304)	0.04 mm	0.1 mm	10 mm	12 mm
SK material	0.05 mm	0.1 mm	9 mm	12 mm
Aluminum	0.05 mm	0.1 mm	8 mm	9 mm
Steel	0.05 mm	0.1 mm	4 mm	(6 mm)
Acryl	—	0.5 mm	40 mm	60 mm
Quartz glass	—	0.5 mm	4 mm	6 mm
Ceramics Alumina	—	0.5 mm	2 mm	3 mm
Ceramics Silicon nitride	—	0.5 mm	4 mm	6 mm

- I: Attention should be paid to the method for fixing a plate.  
 II: Cutting can be obtained on a stable basis.  
 III: Cutting is unstable

simultaneously by using a beam splitter to split a laser beam from a single oscillator.

#### 4. Applications of CO<sub>2</sub> Laser for Processing Ceramics

The far-infrared light of a CO<sub>2</sub> laser with a wavelength of 10.6  $\mu$ m can be absorbed sufficiently by nonmetallic materials, so it is well suited to the processing of ceramics. However, problems with the application occur when ceramics, which are hard and brittle, yield to the crack generation caused by thermal distortion and thermal stress in the heated peripheries of the spot being processed.

Among the types of CO<sub>2</sub> laser processing of ceramics are elimination processing, such as cutting, drilling, and scribing, joining processing such as welding, and adding processing such as thermal spraying and vacuum deposition. The following describes the elimination processing methods for shape-forming, such as cutting and drilling, and a ceramic vacuum deposition method in which a ceramic coating is formed on the surface of a material that has already been shaped.

##### 4.1 Elimination Processing (Cutting, Drilling, Scribing)

The principle of elimination processing involves removing part of a mass from a material and/or splitting a material into two pieces by bombarding it with an irradiated beam to melt or evaporate it and by blasting the molten and

evaporated substance with a jet of gas. In addition to blasting away the molten and evaporated substance, the gas jet has such effects as increasing the cutting speed by taking advantage of the reaction heat and diminishing the area of the layer affected by heat through its cooling action.

### (1) Cutting

Laser cutting is expected to become a method that will enable ceramic boards to be processed into selected spaces. The cutting of ceramics differs from the cutting of metallic materials in that the reaction heat between the assist gas and material cannot be exploited and, furthermore, since ceramics have high melting points (high decomposition temperatures), cutting them requires a relatively large output.

As shown in Figure 5 [not reproduced], cracks are generated not only when thermal distortion is large due to excessive heat input, but also when output is too small or the cutting speed is too fast, making it impossible for a sufficient amount of energy to reach the back of the board, and, therefore, control of the cutting conditions is important.

Figure 6 [not reproduced] shows an example of the cutting of alumina ( $\text{Al}_2\text{O}_3$ ) and one of the cutting of silicon nitride ( $\text{Si}_3\text{N}_4$ ). When cutting  $\text{Al}_2\text{O}_3$  which melts easily, dross tends to adhere, but it can be removed with ease. When cutting easy-to-decompose  $\text{Si}_3\text{N}_4$  or silicon carbide ( $\text{SiC}$ ), on the other hand, the amount of dross is small, but removing the accumulated dross is very difficult. Shortening the pulse width of the pulse output as much as possible enables the dross adhesion to be inhibited to a great extent.

$\text{Si}_3\text{N}_4$  and  $\text{SiC}$  are expected to find applications as high-strength materials in the making of mechanical structural materials and die materials. The processed surface undergoes a qualitative change and gives rise to crack generation, which lowers its strength, but since the denatured layer is extremely shallow, grinding about 0.1 mm off the surface enables it to recover its strength.

### (2) Drilling

$\text{CO}_2$  laser drilling has already seen commercial application in the drilling of throughholes into substrates for hybrid IC circuits. Before the debut of the  $\text{CO}_2$  laser, throughholes were drilled using superhard tools, such as diamond drills, or holes were punched into the substrate using a punch before sintering. Both methods had problems: the former required a long working time and suffered from the excessive wear and tear of the tools, while the latter failed to attain high levels of accuracy due to shrinkage during sintering. Laser processing has solved all these problems simultaneously.

Figure 7 [not reproduced] shows an example of holes drilled into an  $\text{Al}_2\text{O}_3$  substrate and an SEM photograph of the cross section of a hole. Ceramics are hard and brittle materials, and  $\text{Al}_2\text{O}_3$  in particular is characterized by a large thermal expansion coefficient and not too great a strength. Therefore, although the photo shows that cracks have been generated on the processed plane, they pose no serious problems to the substrate performance. However,

much smaller spacings between holes cause cracking during processing, so there are limits to microprocessibility.

Figure 8 [not reproduced] shows an example of high-precision drilling of holes into a  $\text{ZnO-SiO}_2\text{-B}_2\text{O}_3$  (ZSB) system ceramic ("Mioceram") using the  $\text{CO}_2$  laser. Mioceram is a machinable ceramic, but it has been cited for its poor workability when drilling microscopic holes into it and, furthermore, the positional accuracy of the holes is not very good because of recesses on the drilling edge. The photo shows holes, 0.23 mm in diameter, drilled in a substrate 0.4 mm thick on an 0.64 mm pitch. High-accuracy control of the heat input by pulse means has resulted in drilling with accuracies of at least  $\pm 0.015$  mm in hole diameter accuracy (circularity) and  $\pm 0.01$  mm in positional (pitch) accuracy, and the drilling efficiency is several times higher.

Modulating the laser output into a higher pitch and shorter pulse mode (high peak value pulse) than the current norm, as shown in Figure 9, has enabled microscopic holes to be drilled at a high density, the level of which cannot be obtained with the conventional methods, as shown in Figure 10. The photograph shows 900 microscopic holes in a 10 x 10 mm area in an  $\text{Al}_2\text{O}_3$  plate, 0.64 mm thick. A 1000X SEM reveals no crack generation, proving that modulating the output mode into a high peak value pulse inhibits the generation of microcracks.

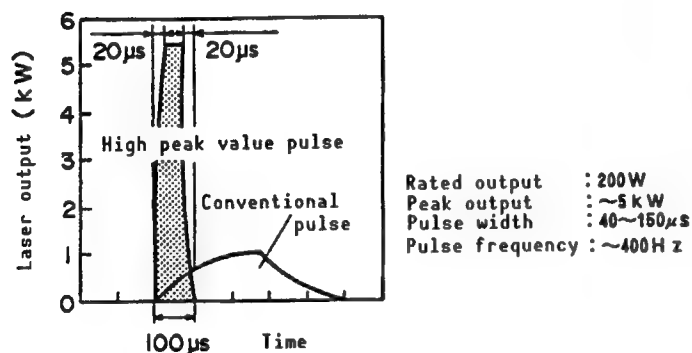


Figure 9. Pulse Waveform of Output of High Peak Value Pulse  $\text{CO}_2$  Laser

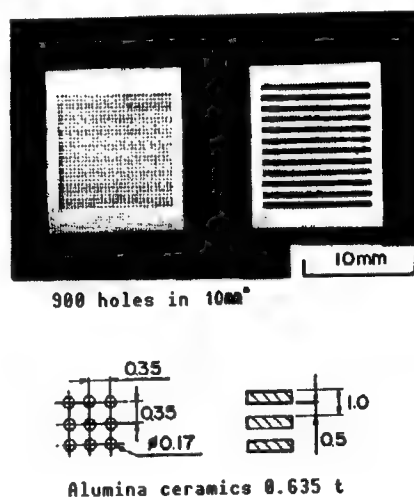


Figure 10. Drilling of Microscopic Holes by  $\text{CO}_2$  Laser of High Peak Value Pulse

### (3) Scribing

Scribing is a technique that has been put to practical use for a relatively long time. In scribing, a physical force is applied to a substrate requiring splitting into multiple chips, so grooves, cut in advance, are used as parting lines.

Such ceramics as  $\text{Al}_2\text{O}_3$ ,  $\text{SiC}$ ,  $\text{Si}_3\text{N}_4$ , and aluminum nitride ( $\text{AlN}$ ) have been used for fabricating substrates for use in circuits. Figure 11 [not reproduced]

shows an example of scribing  $\text{Al}_2\text{O}_3$  by  $\text{CO}_2$  laser. The laser output and the processing speed are selected so that the depth of scribing will reach about one-third the thickness of the substrate. When the substrate is an  $\text{Al}_2\text{O}_3$  substrate, 0.64 mm thick, for example, an output of 50 w will enable the scribing operation to be performed at a speed of 1.5 m/min.

As its principle demonstrates, scribing can be used only for breaking along a straight line. However, when the work requires shaping, the same laser can be switched over to a cutting mode, which will enable a desired shape to be cut.

#### 4.2 Vacuum Deposition Processing

Heat treating the surface of a material or its surface layer, or depositing a different material on the surface of a material or its surface layer is called surface reforming. A new technique called the laser vacuum deposition process has been developed, in which ceramics are evaporated by laser irradiation in a vacuum and the vapor is made to deposit on the opposing substrate. This technique is drawing attention as a surface reforming method, and studies are being promoted on its application to the coating of abrasion resistant or superconductive films.

Figure 12 shows the abrasion resistant characteristics of an  $\text{Al}_2\text{O}_3$  coating formed on an aluminum substrate. The amount of wear loss is about one-fourth that of an untreated material (aluminum alloy), and the coating is superior to spring steel, a steel widely used in sliding parts.

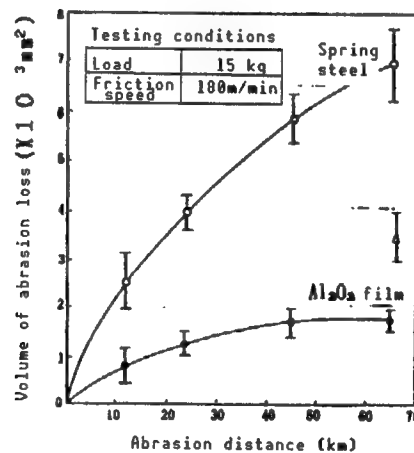


Figure 12. Abrasion Resistant Characteristics of  $\text{Al}_2\text{O}_3$  Film Formed on an Aluminum Substrate

Figure 13 [not reproduced] shows an SEM photograph of the cross section of an  $\text{Al}_2\text{O}_3$  film formed on an aluminum substrate.

Figure 14 [not reproduced] compares  $\text{Al}_2\text{O}_3$  film and the alumite treatment layer, an aluminum surface treatment method widely used in the past. Due to laser vacuum deposition, the  $\text{Al}_2\text{O}_3$  film, as opposed to the alumite treatment layer, has no holes and is densely packed. With a smooth surface, the  $\text{Al}_2\text{O}_3$  film features high hardness.



Compared to other deposition methods, the laser vacuum deposition method features a high deposition speed and the capability to form densely-packed and hard coatings of a variety of ceramics, and great expectations have been placed on its application research.

## 5. Conclusion

Helped by heightened stability and the increased reliability of laser oscillators and processing machines, and also by the development of new oscillators, CO<sub>2</sub> laser processing technology is expanding its processing limits. The technology has enabled conventionally hard-to-machine materials to be processed into products of a practical use level quality.

With the increasing demand for ceramic materials, the laser processing of ceramics is expected to gain an added importance in the future. Consequently, increased quality controls, such as protecting the plane being machined from thermal deterioration or inhibiting the generation of microcracks, are desired, and it is hoped that the technology will be established as a processing method in its own right, not as a mere substitute for the existing processing techniques.

## References

1. Maiman, T.H., PHYS. REV. LETTERS, Vol 4 No 11, 1960, p 564.
2. Omine, RESEARCH ON MACHINES, Vol 39 No 8, 1987, p 861.
3. Kaneoka, "International Lasers/Applications Fair," 1989 Seminar Text, (1989-1).
4. Hishii, et al., TECHNICAL BULLETIN OF MITSUBISHI ELECTRIC CORPORATION, Vol 61 No 6, 1987, p 460.
5. Yoshida, Yamamoto, Shibayama, Shirasu, Ibid., p 464.
6. Hiramoto and Moriyasu, "Text for the 99th General Symposium," (1988-2).
7. Omine and Moriyasu, AUTOMATION TECHNOLOGY, Vol 18 No 11, 1986, p 38.
8. Kitani, Hayashi, Kaneoka and Moriyasu, TECHNICAL BULLETIN OF MITSUBISHI ELECTRIC CORPORATION, Vol 63 No 4, 1989, p 281.
9. Maruo, Miyamoto, et al., JOURNAL OF THE JAPAN WELDING SOCIETY, Vol 51 No 2, 1982, p 182.
10. Omine and Moriyasu, PLASTICITY AND PROCESSING, Vol 27 No 307, August 1986, p 904.
11. Omine, KIKAI GIJUTSU, Vol 35 No 2, 1987, p 59.
12. Morita and Hiramoto, NEW WELTEC, No 10, 1988, p 41.

## Electrodischarge Machining Technology, Its Applications

43067178D Tokyo THE 91ST WORKSHOP ON PLASTIC WORKING in Japanese 16 Jun 89  
pp 31-41

[Article by Hiroshi Kubo and Masanobu Kuroda, Hitachi Metals, Ltd.]

### [Text] 1. Foreword

Although they are no longer treated as glamorously as they were a short time ago, engineering ceramics are still expanding their applications steadily.

Because of the nature of their applications, engineering ceramics have seldom been used as sintered bodies per se, but they have been used in most cases as processed products of high sophistication. A large part of the processing of engineering ceramics after sintering is accounted for by grinding using diamond grindstones. This grinding takes a long time and accounts for a large part of the total processing cost of a ceramic, raising its cost, and this has been the reason, in some cases, why engineering ceramics have had difficulty finding applications.

Recently, the complex profiling of engineering ceramics has come to be obtained thanks to NC grinding and processing, thereby greatly raising the processing efficiency, but the grinding techniques are in most cases finding themselves unable to cope with operations involving the drilling of narrow or deep holes, and especially holes with small dimensions. Among the techniques for processing such holes are supersonic and laser processing, but these techniques have yet to find wide application for the following reasons, i.e., although supersonic processing will make it possible for specific holes to be drilled in ceramics by the proper selection of tool shapes, processing speed will be slow and the tools will wear out rapidly. All this raises problems with the technology with respect to time and cost. Regarding laser processing technology, the use of a YAG (yttrium-aluminum-garnet) or CO<sub>2</sub> laser will enable drilling holes in ceramics or cutting them to be performed quickly. As a result, the technology has been used commercially in some fields, but it poses problems: only thin plates, about 5 mm in thickness at the most, can be processed with the technology and, furthermore, the hole drilled has a taper, and the processed surface is not in a good state because of the attached melt products.

## 2. Ceramics Suited for Electrodischarge Machining

Electrodischarge machining has come to be widely used in recent years in the high precision machining of complex shapes, such as dies for steel and super-hard alloys, and high-performance NC machines have been developed. If it becomes possible to employ electrodischarge machining technology in the processing of ceramics, it will become possible to machine complex shapes, including small holes, at relatively high efficiency. However, the major component elements of engineering ceramics, such as  $\text{Al}_2\text{O}_3$ ,  $\text{ZrO}_2$ ,  $\text{Si}_3\text{N}_4$ , sialons, and  $\text{SiC}$ , are not electrically conductive, with the exception of some types of  $\text{SiC}$ , so they are not applicable to electrodischarge machining as they are.

Studies have been made on methods for adding some conductive compounds to ceramics to make them conductive, thereby making them amenable to electrodischarge machining, and some ceramics are being put to practical use. At the time of publication, these include the  $\text{Al}_2\text{O}_3$ - $\text{TiC}$ ,  $\text{ZrO}_2$ - $\text{NbC}$ ,  $\text{Si}_3\text{N}_4$ - $\text{TiN}$ ,  $\text{Si}_3\text{N}_4$ - $\text{SiC}$ , Sialon- $\text{TiN}$ , and  $\text{SiC}$ - $\text{ZrB}_2$  systems of engineering ceramics. In addition, ceramics based on the conductive compounds of the  $\text{ZrB}_2$  and  $\text{TiB}_2$  systems have been developed, and studies are being advanced in their electrodischarge workability.

This paper describes a conductive sialon, a product that has been developed by adding  $\text{TiN}$  to a Hitachi Metals-developed sialon and which has already been placed on the market, with respect to material properties, electrodischarge processibility, and actual instances of processing.

## 3. Characteristics of Conductive Sialons

Among engineering ceramics, sialons have excellent characteristics in terms of normal and high temperature strength, as well as of corrosion, oxidation, and heat shock resistance, and efforts have been made for their practical applications to hot working tools, corrosion resistant tools, abrasion resistant parts, and automotive parts. The problems standing in the way of their practical application include the difficulties with processing them, so we have been conducting research on methods for making the electrodischarge machining of sialons feasible.

In order to impart conductivity to sialons, which are insulating materials, considerable amounts of conductive compounds (above 20 volume percent) must be added. In selecting a conductive compound, care needs to be taken that the sialon's characteristics, i.e., high temperature strength, resistance to oxidation, etc., are not degraded. Consideration also needs to be paid to the ease of sintering the sialon-conductive compound mixture and the conductivity of the sintered body. As for the sintering conditions, keeping the application of sintered bodies to large parts in mind, we considered the availability of sintering at normal pressure as the imperative condition.

We prepared sintered bodies containing various kinds of conductive materials, including carbides, nitrides, borides, and oxides of transition metals, and evaluated their characteristics. Partial results are shown in Table 1. From a study of various characteristics, it has been found that  $\text{TiN}$ , which is a

compound of a transition metal and which is a nitride as sialon is, is the conductive compound best suited for use as an additive to sialon. The following describes an inductive sialon containing TiN as an additive.

Table 1. Kinds of Conductive Compounds and Characteristics of Sintered Bodies

Matrix	Conductive compound	Conductivity	Sintering properties	Oxidation resistance
Sialon	HfC	$\Delta$	X	X
"	VC	$\Delta$	O	X
"	TiC	O	X	O
"	TiN	O	O	O

Figure 1 [not reproduced] shows a photograph of the tissue of a conductive sialon obtained by an SEM (scanning electron microscope). White particles in the tissue are TiN particles, and the rest is sialon (made of up of black sialon particles and streak-line grain boundary phases). Few bores are seen in the tissue, showing that a high density sintered body has been obtained under normal pressure sintering. The photo also shows that adding large amounts of TiN (in this case 40 volume percent) will only slightly degrade the sialon's degree of sintering, and that TiN has an extremely good affinity with sialon.

Figures 2 [not reproduced] and 3 [not reproduced] show the results of observation of the tissue using a higher magnification TEM (transmission electron microscope). In the TEM observation, the contrast is the opposite of that in the SEM observation, and black grains are TiN.

Figure 2 [not reproduced] shows the results of the observation of an area where a sialon grain, a grain boundary phase, and a TiN grain converge, were obtained using high magnification (about 500,000X) TEM. It shows that a grain phase boundary about 2~3 nm (20~30 Å) thick exists between the sialon grain and TiN grain, and that the grain boundary phase, which is a liquid phase, demonstrates a good wettability with the TiN grain during sintering.

Figure 3 [not reproduced] shows an area where TiN grains come into contact with one another contiguously. As was seen in Figure 1 [not reproduced] such areas are observed in various parts of the sintered body.

From this, one can learn that in conductive sialon, a three-dimensional network of the conductive compound TiN is formed, generating conductive paths, and that these paths give the sintered body conductivity.

Figure 4 shows the relationship between the amount of TiN and the electrical resistivity. The electrical resistivity fluctuates greatly depending on the amount of TiN. When the amount of TiN is 20 percent in volume, the resistivity

is above  $10^7 \Omega\text{cm}$ , but when TiN = 30 vol percent, the resistivity drops to the level of  $10^{-3} \Omega\text{cm}$ . The resistivity shows large variations in the 20-30 volume percent range of TiN. The large variations are believed to be caused by the rapid formation of a network of TiN grains in the high volume range of TiN. When TiN > 30 volume percent, the electrical resistivity begins to show smaller variations, and with increases in the volume of TiN, the electrical resistivities approach the electrical resistivity of TiN itself, which is  $4 \times 10^{-4} \Omega\text{cm}$ . In actual application, high-density sintered bodies can be obtained even when the volume of TiN is increased to about 60 volume percent, so the electrical resistivity goes down with the increasing volume of TiN. Electrodischarge machining characteristics of conductive sialon will be described in detail later, but the electrical resistivity and electrodischarge workability are closely related and, especially when trying to machine a thick sintered body by wire cutting, it is preferable that the electrical resistivity be lower than  $10^{-3} \Omega\text{cm}$ .

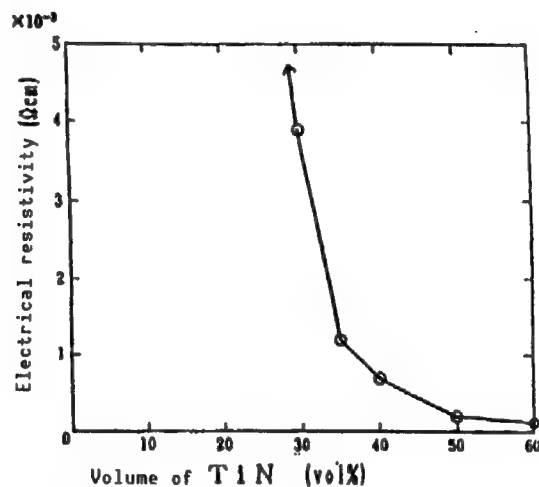


Figure 4. Relationship Between Volume of TiN and Electrical Resistivity

Figure 5 shows the relationship between the volume of TiN and the bending strength at normal temperature. From the figure, one can see that even when the volume of TiN is increased to 40-50 volume percent, the bending strength suffers only slight declines. This supports the assumption that adding TiN will not lead to a lower degree of sintering.

When the volume of TiN is increased, the level of hardness tends to decrease slightly, which is believed to come from the fact that TiN grains are slightly larger than sialon grains.

Figure 6 shows the temperature dependence of the bending strength, with the volume of TiN as a variable. From the figure, one can see that even if the TiN additions are increased up to 40 volume percent, the sialons containing TiN have roughly as much bending strength as the sialon containing no TiN until a temperature of  $1000^\circ\text{C}$  is reached. However, when the temperature

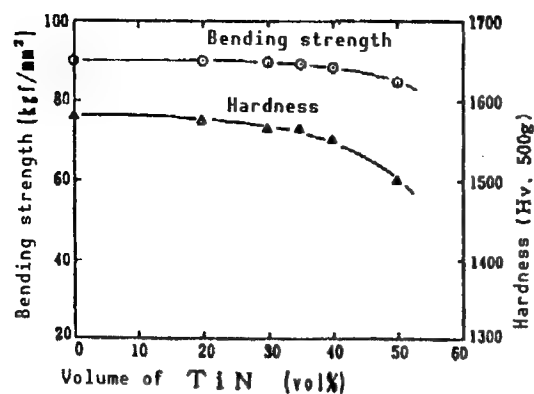


Figure 5. Relationships Between Volume of TiN and Bending Strength and Hardness

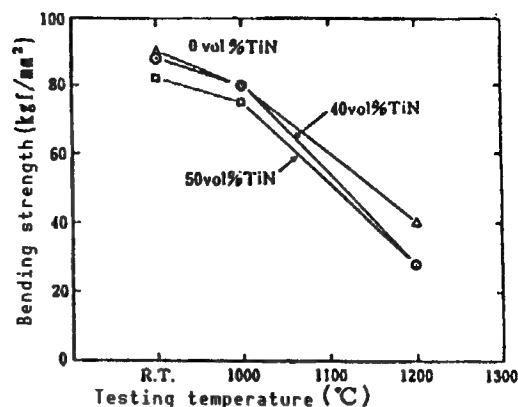


Figure 6. Bending Strength at High Temperature

reaches 1200°C, the sialons containing TiN have a bending strength about three-fourths that of the sialons with no TiN additions.

The foregoing has shown that adding TiN to sialon enables conductivity to be impacted to the ceramic and that the sialon suffers only a slight deterioration in its sintering properties, which in turn is reflected as a minor deterioration in its mechanical properties.

Table 2. Comparison of Characteristics of Conductive Sialon and Ordinary Sialon

Characteristics	Unit	Conductive sialon HCN-40	Sialon HCN-10
Density	g/cm <sup>3</sup>	4.00	326
Bending strength (3-point bending)	kgf/mm <sup>2</sup>	85	90
Fracture toughness	MPa m	5.0	6.0
Hardness	Load 500 g	1,550	1,580
Compressive strength	kgf/mm <sup>2</sup>	>330	>350
Young's modulus	kgf/mm <sup>2</sup>	33,600	30,000
Thermal shock resistance	ΔT°C	400	600
Thermal expansion coefficient	x 10 <sup>-6</sup> /°C, 20~800°C	5.1	3.0
Thermal conductivity	cal/cm·S·°C	0.06	0.04
Electrical resistivity	Ω·cm	7 x 10 <sup>-4</sup>	>10 <sup>11</sup>
Crystal grain diameter	μm	2	2

Table 2 compares the characteristics of a conductive sialon (HCN40, the standard material) with those of a sialon with no TiN addition (HCN10).

Adding TiN gives rise to changes in the density, the coefficient of thermal expansion, and the thermal conductivity, and these changes represent the intermediate values of the combined physical property values of the component elements of the TiN-sialon complex. Compared to HCN-10's thermal shock resistance of 600°C, HCN-40 has a thermal shock resistance of 400°C, a reduction of 200°C, which is believed to have been caused by its increased thermal expansion coefficient from  $3.0 \times 10^{-6}$  (1/deg) to  $5.1 \times 10^{-6}$  (1/deg), brought about by the addition of TiN. The thermal shock resistance value of HCN-40 is still larger than that of either  $\text{Al}_2\text{O}_3$  (200°C) or  $\text{ZrO}_2$  (350°C), and this value can be raised to 500°C by the selection of appropriate manufacturing conditions.

#### 4. Electrodischarge Machining of Profiles

The following describes the electrodischarge machining of conductive sialon. In order to determine the machining conditions for profile electrodischarge machining of the electrically conductive sialon, we bored throughholes in a workpiece, 11 mm thick, using a small-diameter pipe electrode, and examined the electrode polarity, the electrical conditions permitting machining on a stable basis, the machining time, and the electrode loss. The results revealed that, in the case of the conductive sialon, the use of a negative electrode (straight polarity) enabled the machining time to be reduced to one-half and the electrode loss to be reduced to about one-third, so we conducted the following test using the straight polarity of a negative (-) electrode.

##### 4.1 Machining Characteristics of Profile Electrodischarge Machining

Figure 7 shows the dependence of the machining speed and electrode loss on the pulse width. The larger the machining current and the smaller the pulse width, the faster the machining speed becomes. The electrode loss rate tends to decrease with the increasing pulse width. From the above, it can be said that in the smaller pulse width range, the machining speed becomes faster but the electrode loss rate becomes large, while in the larger pulse width range, the machining speed becomes slower but the electrode loss rate becomes small.

As for the taper of the flank being machined, the smaller the pulse width, the larger the amount of taper becomes. This is believed to be caused by the fact that a smaller pulse width leads to a larger electrode loss. As for clearance, a larger pulse width tends to lead to a larger clearance.

Figure 8 shows the relationship between the pulse width and the coarseness of the machined bottom surface. The set values for the maximum current value were divided into the four stages of  $I_{p1}$  through  $I_{p4}$ , and tests were conducted. The average current values on the meter are given in the figure. The results reveal that the surface coarseness is affected by the pulse width, but is only slightly affected by the maximum current value.

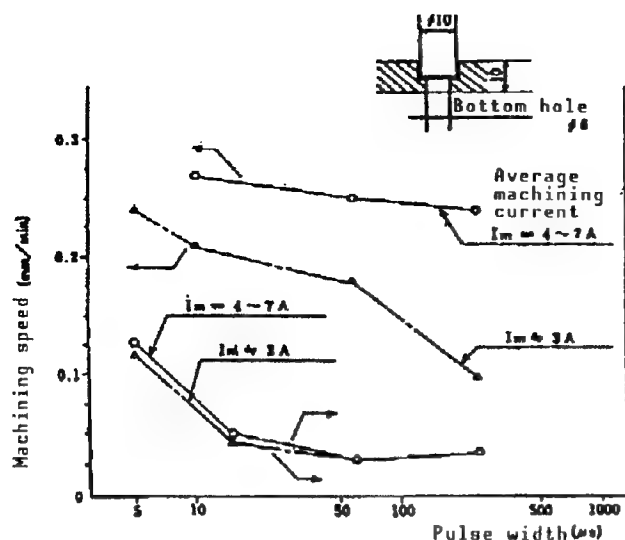


Figure 7. Dependence of Machining Speed and Electrode Loss Rate on Pulse Width

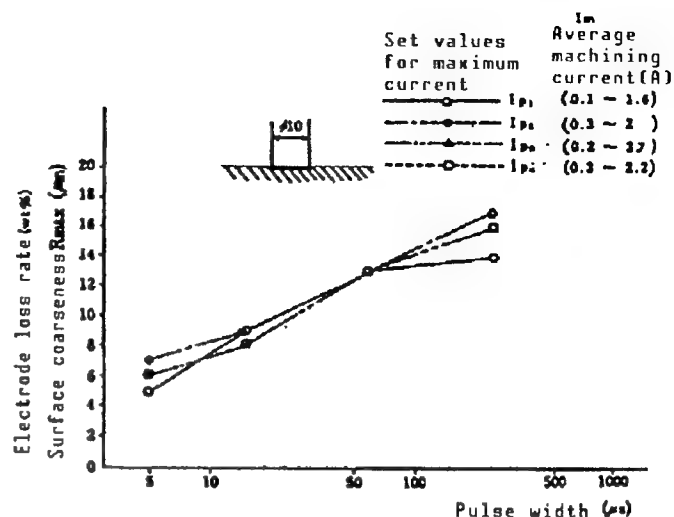


Figure 8. Relationship Between Pulse Width and Coarseness of the Machined Bottom Surface

Tests were conducted using a copper and a graphite electrode. With the graphite electrode, arcs were generated in 2~3 minutes, making it impossible to continue machining on a stable basis. When machining the conductive sialon, a graphite electrode is not appropriate, but a copper electrode can guarantee stable machining.

Figure 9 [not reproduced] shows photographs of the surface and cross section of the machined bottom faces, imaged from the same field of view. The machining conditions and the surface roughnesses are given on the right. In (a), crack generation is observed in the pits on the machined surface, and extend about 30  $\mu\text{m}$  from the surface. No cracks are observed on the cross section in (b). An observation of various machined specimens revealed that the greater the level of roughness of the machined surface, the higher the chance of cracks being generated and the deeper the extent of those cracks. This shows that the larger the pulse width, the rougher the surface becomes and the greater the damage caused by machining becomes.

#### 4.2 Comparison of Conductive Sialon, Steel, and Superhard Alloy for Machining Properties

Table 2 compares the machining properties of conductive sialon, steel, and superhard alloy. If smooth surfaces are not required, the machining speeds of the steel and superhard alloy can be raised to a great extent. When  $R_{\text{max}} = 20\sim 35 \mu\text{m}$ , the machining speed of the steel can be raised to 30~40  $\text{mm}^3/\text{min}$ , while when  $R_{\text{max}} = 200 \mu\text{m}$ , it can be raised to 380  $\text{mm}^3/\text{min}$ . In the case of conductive sialon, even when the surface roughness was raised to  $R_{\text{max}} = 10\sim 22 \mu\text{m}$ , the machining speed could be raised only to the 5~13  $\text{mm}^3/\text{min}$  range. However, when the surface roughness is on the order of  $R_{\text{max}} = 5 \mu\text{m}$ , the machining speeds of the steel and superhard alloy are about 2  $\text{mm}^3/\text{min}$ , while that of the conductive sialon is the largest, being in the range of 11~14  $\text{mm}^3/\text{min}$ , and the electrode loss rate is the smallest.



Table 2. Profile Electrodisharge Machining

Material	Conductive Sialon HCN-40		Steel SKD-11			Superhard alloy WC-Co		
Electrode material	Cu		Cu			Cu-W or Ag-W		
Electrode polarity	(-)		(+)			(-)		
Pulse width $\mu s$	60~250	5~15	1000	60~250	2~3	2~3	2~3	2~3
Quiescent time $\mu s$	250~1000	15~60	1000	60~250	2~3	8~12	4~7	2~5
Surface roughness $\mu m$	10~22	4~7	200	20~35	5	24	10	4~6
Machining speed $mm^3/min$	5~13	11~14	380	30~40	2	170	15~16	1.5~5
Electrode loss rate in volume percent	2.5~3.5	4~11	Less than 1	1~9	13~14	50	40	35~40

Consequently, for profile electrodisharge machining, it can be said that steels and superhard alloys have a better machining efficiency than conductive sialons when their surfaces are rough, but conductive sialons can be machined at much higher speeds than steels and superhard alloys can when the surface roughness must be kept to within a smaller range.

## 5. Wire-Cut Electrodisharge Machining

In the wire-cut electrodisharge machining of workpieces, i.e., of three types of boards varying in thickness (10 mm, 40 mm, and 70 mm), using a brass wire 0.2 mm in diameter, we determined the electrical conditions that permit stable machining at their maximum machining speed. Using those conditions, we conducted tests by varying the pulse width.

### 5.1 Machining Characteristics of Wire-Cut

Figure 10 shows the machining speed versus plate thickness. The cutting speeds are 16 mm/min for a plate thickness of 10 mm, 5 mm/min for 40 mm, and 3 mm/min for 70 mm. These speeds are in the 160~200  $mm^2/min$  range when expressed in cross sectional terms, and the cutting speed of 200  $mm^2/min$  is about the same as that for steel.

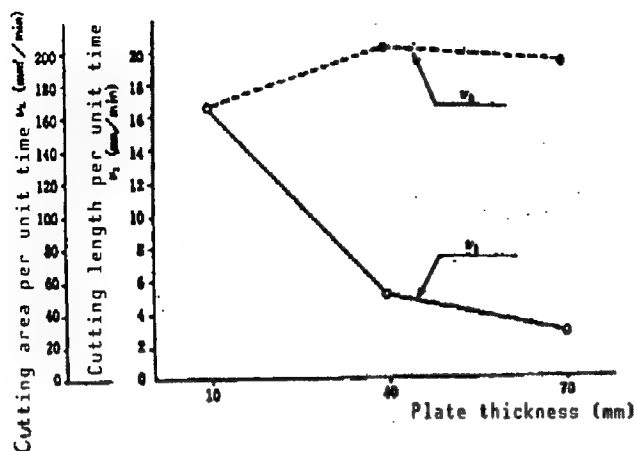


Figure 10. Relationship Between Machining Speed and Plate Thickness

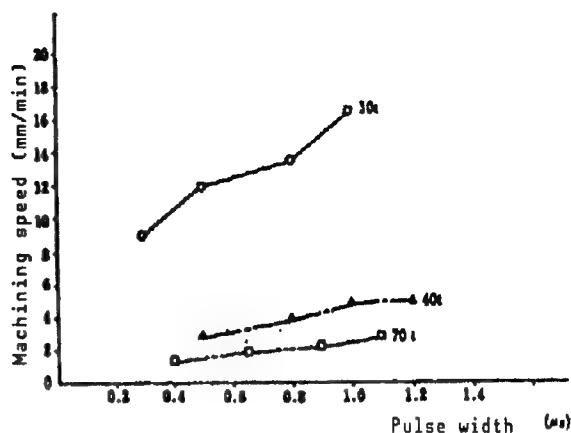


Figure 11. Machining Speed Versus Pulse Width

Figure 11 shows the relationship between the machining speed and pulse width. The larger the pulse width, the higher the machining speed. With pulse widths below  $0.2 \mu s$ , a stable discharge could not be obtained, while on the other hand, when the pulse width was above  $1.2 \mu s$ , the wire snapped and machining could not be conducted on a stable basis either. We examined DF (duty factor = pulse width/(pulse width + quiescent time)). The machining speed tended to increase slightly as the DF increased, but variations in the pulse width have a larger influence on the machining speed than the DF does.

Figure 12 shows the relationship between surface roughness and the pulse width. It shows that the greater the board thickness the coarser the machined surface becomes. This is believed to be caused by the following fact: in our experiments, the electrical conditions were set by placing the utmost priority on machining speed, and this inevitably led to the application of higher voltages for greater board thicknesses, which in turn led to high discharge energies, causing larger amounts of the machined surfaces to be destroyed.

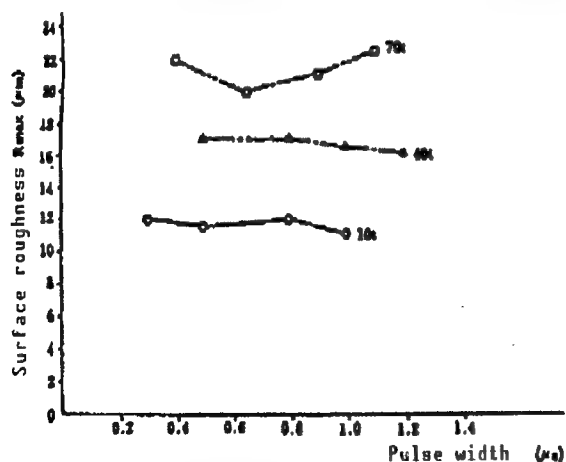


Figure 12. Surface Roughness Versus Pulse Width

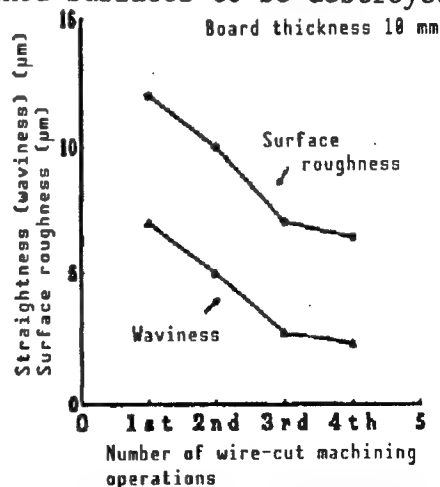


Figure 13. Waviness and Surface Roughness Versus Number of Cutting Operations

Figure 13 shows the relationship between the number of wire-cut operations and the straightness and surface roughness. For raising the surface accuracy of the wire-cut surface, increasing the number of machining operations has been employed widely. Workpieces, 10 mm thick, were subjected to cutting up to the fourth cut in order to examine their surface roughness and straightness (waviness) levels. The surface roughness shows an improvement from  $R_{max}$  12  $\mu m$  for the first cut to 6  $\mu m$  for the fourth cut. The waviness also exhibits improvement, from 7  $\mu m$  to 2.7  $\mu m$  for a thickness of 10 mm, showing the effect of increased cutting operations.

Microscopic observation of the machine surfaces by wire-cut electrodischarge machining has revealed the generation of porous defects, about 15  $\mu m$  deep from the machined surface, in the interiors of the workpieces with machined surface roughness levels in the  $R_{max}$  16~17  $\mu m$  range. Consequently, in order to obtain a normal machined surface, the surface accuracy will have to be set at about two times the  $R_{max}$ . In other words, we believe it necessary to apply a finish machining to a depth equivalent to another  $R_{max}$  after the machined surface has been planarized.

## 5.2 Comparison of Conductive Sialon, Steel, and Superhard Alloy for Machining Characteristics

Table 3 compares the machining characteristics of conductive sialon, steel, and a superhard alloy in wire-cut electrodischarge machining. When machining electrically conductive sialon, the same electrical conditions as those for steel and the superhard alloy cannot generally be employed. A stable machining operation can be obtained when the quiescent time is long and DF is in a smaller range.

Table 3. Comparing Various Materials With Respect to Machining Characteristics

Board thickness	10 mm			40 mm			70 mm		
Material	Sialon	SKD-11	Superhard alloy	Sialon	SKD-11	Superhard alloy	Sialon	SKD-11	Superhard alloy
Wire material	B S - P			B S - P			B S - P		
Wire diameter	$\phi 0.2$ mm			$\phi 0.2$ mm			$\phi 0.2$ mm		
Wire polarity	(-)			(-)			(-)		
Conductivity of machining liquid(mA)	2	12	2	2	12	2	2	12	2
Machining voltage (V)	32	40~45	45~50	65	40~45	45~50	70	40~45	45~50
Pulse width ( $\mu s$ )	0.3~1	0.6~0.7	0.6~0.7	0.5~1.2	1~1.2	0.6~0.7	0.4~1.1	1~1.2	0.6~0.7
Quiescent time ( $\mu s$ )	10~30	Below 10	Below 10	10~30	Below 10	Below 10	10~30	Below 10	Below 10
Machining speed (mm/min)	9~16.5	8~10	4~5	3~5	3~3.5	1.2~1.3	1.5~3	1.6~1.8	0.8~0.9
Surface roughness $R_{max}$ ( $\mu m$ )	10~12	19~20	12~13	16~17	19~20	12~13	20~24	19~20	12~13
Clearance ( $\mu m$ )	30~40	30~40	30	40~60	30~40	40	40~60	40~50	40~45

As for the machining speed, the conductive sialon could be machined at a speed similar to or faster than that of steel, and two to three times faster than that of the superhard alloy. As for surface roughness, the conductive sialon sustained surface roughness levels equal to or superior to those for the other materials up to thicknesses of 40 mm, but it had surface roughness levels slightly higher than those for the other materials when the board thickness was 70 mm.

## 6. Examples of Application of Conductive Sialons

Conductive sialons are beginning to find applications in various fields. Hot extrusion dies (Figure 14 [not reproduced]) represent an example of this. When drilling holes that are not round, such as square or special-shaped holes, in conventional ceramics, ultrasonic machining techniques have been employed, and these techniques have the disadvantages of long machining time and high machining costs. The use of electrodischarge machining has enabled conductive sialons to be machined into dies with ease, and the conventional problems associated with die steel or ultrahard alloy based dies, such as seizures and abrasion, are beginning to disappear.

Figure 15 [not reproduced] shows rotary atomizers used in high-temperature environments. The top photograph shows an assembly and the bottom shows a part made of a conductive sialon. Since these atomizers spin at a rate of 10,000-30,000 rotations per minute, they must be provided with high heat and abrasion resistance properties in addition to a high withholding strength to the centrifugal force. Metals were conventionally used for fabricating such rotary atomizers, but an atomizer incorporating a Ti alloy on its outside and a sialon ceramic on its inner side has been proven to have longer durability. As for the machining method of the atomizer, the external and internal peripheries were cut out by wire cut, which was followed by the polishing and profile electrodischarge drilling of holes on the external periphery.

Figure 16 [not reproduced] shows an example of small-diameter holes drilled by means of electrodischarge machining. The 0.3-mm diameter holes were drilled in a plate about 1 mm thick using an NC profile electrodischarge drilling machine, and they feature extremely high circularity. Such small holes can be drilled using lasers. The problems with laser machining, however, are that as the hole diameters become increasingly smaller, burrs tend to generate and the holes tend to take an elliptical shape due to the adhesion of melt deposits, and that cracks appear depending on the type of ceramic being machined. With conductive sialons, ideal holes can be obtained by means of electrodischarge drilling.

In the foregoing, the authors have described the electrodischarge machining of electrically conductive sialons. By setting the proper conditions, this technique makes it possible to realize machining speeds as fast as those for the machining of steels. As the accumulation of machining data increases and as machining conditions continue to improve, further improvements are expected in the technique's machining efficiency and machining precision, as well as in the surface roughness obtainable with the technique, and the technique is

expected to play a large role in the machining of complex-shaped products, among others, and to expand the scope of its applications.

This paper has described the electrodischarge machining of electrically conductive sialons, but other ceramics with conductivity include  $\text{Si}_3\text{N}_4$ ,  $\text{ZrB}_2$ ,  $\text{SiC}$ , etc. Since the machining characteristics differ from one material to another, when trying to machine any of these materials, one must first determine the machining conditions best suited to the material of interest.

#### References

1. Kubo, et al., "Proceedings of the 1985 Spring Symposium," the Industrial Association of Powder, Pulverulent Body, and Metallurgy of Japan, 1985, p 80.
2. Ibid., Japan Ceramic Industry Association, 1987.
3. Kubo and Hara, "Sintering: 87," Tokyo, Abstract, 1987, p 54.
4. Kubo, et al., "Preprint of First Autumn Symposium by Japan Ceramics Industry Association," 1988, p 115.
5. Kubo, INDUSTRIAL MATERIALS, Vol 37 No 2, 1989, p 57.
6. Tanaka, et al., "Materials for the 15th PS Seminar by the Japan Precision Engineering Society," 1986.
7. Kobayashi, et al., NIKKEI MECHANICAL, Separate Volume Supplement, 1987.

## Technology for Grinding Engineering Ceramics

43067178E Tokyo THE 91ST WORKSHOP ON PLASTIC WORKING in Japanese 16 Jun 89  
pp 42-52

[Article by Tetsutaro Uematsu of Toyama Prefecture Junior College of Technology; Kiyoshi Suzuki of Nippon Institute of Technology; Takeo Nakagawa of the Research Institute for Industrial Technology, the University of Tokyo]

### [Text] 1. Foreword

Ceramics are generally said to be the hardest of the hardest materials to grind or cut. This saying comes partly from the fact that ceramics are extremely hard, and partly from the fact that since ceramics are usually not conductive, they must be machined by an inefficient method, i.e., grinding using diamond grinding stones. Until a short time ago, in fact, more than half of the manufacturing costs of ceramic parts were said to be consumed by the cost of grinding and processing them. Therefore, for ceramics to find widespread application in machine parts or components, bringing down their machining cost is an essential condition.

The tasks currently facing ceramic machining are: 1) machining at an elevated level of efficiency; 2) improved dimensional accuracy and surface properties; and 3) the profiling of complex shapes.

Toward these goals, the various approaches listed in Table 1 are being attempted. From the aspect of hardware, for example, these include improvements of the grinding machines and grinding stones, while from the software side, these include efforts toward obtaining an understanding of the optimal grinding conditions or combining the grinding technology with some other machining technology.

In order to realize the most critical tasks of them all, i.e, the realization of a high-efficiency grinding technique, this paper describes a new grinding technology that combines a machining center (MC) featuring high rigidity and excellent control capabilities with metal bond diamond grinding wheels.

Table 1. Tasks Associated With Ceramic Grinding and Purposes

Task	Objective	Purposes
1. Enhanced grinding efficiency	Increased amount of removal	Grasp the optimal machining conditions, improve the grindstones, devise complex grinding methods
2. Improved ground surface properties	Surface roughness, properties, accuracy	Improvements of grindstones and grinders
3. Coping with complex shapes	Three-dimensional profile grinding	NC control of tool trajectories

## 2. Conditions for High-Efficiency and High-Performance Grinding

### 2.1 Grinding Machines

In order to grind ceramic parts of various shapes efficiently, we believe that a grinder with a control function, such as MC in cutting work, is needed. Ordinary grinders are not necessarily suited to what we are aiming at here, i.e., high-efficiency grinding, partly because they are built with the utmost priority placed on accuracy. Grinding centers (GC), as counterparts of the MCs which are proving to be extremely valuable in the field of cutting work, are needed in the field of grinding work. GCs developed in the past were exclusive machines designed to be used for a specific purpose, and unlike MCs, they do not have general-purpose utility capabilities. Therefore, we attempted to employ cutting-use MCs for GC machines.

The MC differs greatly from the ordinary grinder in both structure and function, but the two also share many features. Using an MC as a GC is expected to bring about many advantages (Table 2). Among the anticipated advantages are the automatic exchange of grindstones or workpieces, the generation of three-dimensional shapes, and easier truing and dressing of grindstones by exploiting the NC function. Since, compared to grinding machines, MCs have larger motor outputs and higher mechanical rigidity, we believe they will enable ceramic grinding to be performed efficiently. Furthermore, the MC's capabilities to widely alter the number of rotations of the main shaft and the feed speed are of great convenience when determining the optimal grinding conditions.

### 2.2 Diamond Grindstones

In order to solve the three tasks associated with the grinding of ceramics described at the beginning of this paper, diamond grindstones satisfying the following conditions are needed: 1) the grindstone must have sufficient

Table 2. Advantages and Disadvantages of Grinding by Machining Center

Advantages/disadvantages	MC function
o Profile grinding	NC function + backlash-less feed
o Heavy grinding	High mechanical rigidity, high motor output
o Creep feed grinding	High mechanical rigidity, variable feed speed
o Automatic grinding, long-term grinding	Automatic grindstone/workpiece change function (ATC/APC)
o High accuracy on-machine truing/dressing	NC function + various types of dressers (electric discharge removal method)
o Highly efficient grinding by special processing	As a replacement for exclusive grinders
Δ Economy	As a replacement for exclusive grinders
Δ Mechanical accuracy	Increased accuracy of the main spindle, scale feedback
• Countermeasures against cutting debris	Measures for preventing attachment of scraps to the sliding surfaces and rotation axes

strength; 2) the grindstone should be very resistant to abrasion; and 3) the grindstone should cut well and remain in that state for a long time.

Finding a grindstone that meets all the above conditions is very difficult. Resin bond and vitrified bond grindstones meet the requirements in item 3), i.e., good cutting quality and retention of the quality for a long time, but have problems with respect to the grindstone strength and abrasion resistance described in items 1) and 2), respectively. Metal bond grindstones are reportedly inferior in terms of the cutting quality in item 3), but satisfy all the conditions in items 1) and 2). Therefore, if the optimal cutting conditions that meet the requirements in item 3) and an effective in-process dressing technique are to be discovered, metal bond grindstones are expected to lead to the realization of a high-efficiency grinding operation.

### 2.3 Grinding Conditions

For realizing high-efficiency grinding, two methods are being considered: one method is to increase the amount of removal per unit time, while the other is to reduce the amount of nongrinding time due to table overruns. This paper addresses the former, i.e., methods for increasing the amounts of removal.



Increasing the revolution speed of a grindstone will enable a larger amount to be removed without increasing the load working on its grains. However, the peripheral speeds realized in practice are limited. Therefore, in order to increase the removal amounts, one of the following three conditions must be met: 1) increase the depth of cut  $Z$ ; 2) increase the feed speed  $Z$ ; and 3) increase both the  $Z$  and  $f$  simultaneously. It is important that the above conditions be used in determining the grinding conditions that will satisfy the requirements of a grindstone, i.e., maintaining a good cutting quality for a long time.

### 3. High-Efficiency Grinding Methods on MC

#### 3.1 Understanding the Optimal Cutting Conditions

##### (a) Alumina ceramics

Although they are extremely hard, alumina ceramics are lacking in toughness. Therefore, with the selection of the proper machining conditions, a large-scale reduction in the grinding resistance and inhibition of the grindstone abrasion become feasible.

Figure 1 shows the grinding resistance values in the normal direction obtained when drilling a 10-mm wide groove in an alumina block. In it, the grinding removal efficiency rate, which is the product of the depth of cut  $Z$ , feed  $f$ , and width  $W$ , is maintained at a constant value of  $Q = 12,000 \text{ mm}^3/\text{min}$ . The experimental results show that the grinding resistance decreases in the region where  $f/Z$  is large, but that it increases sharply when  $f/Z$  is small, the so-called creep feed grinding conditions. Consequently, assuming that the grinding resistance is to be as small as possible, if the same removal efficiency is to be obtained, grinding should be performed when  $f/Z$  is set at as large a value as possible.

Similar trends were observed with other ceramics.

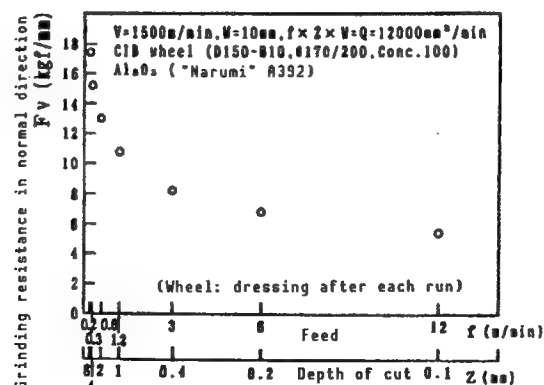


Figure 1. Relationship Between Grinding Conditions and Grinding Resistance When the Amount of Removal Is Kept Constant

### (b) Silicon nitride ceramics

High grinding efficiencies can be obtained when grinding relatively soft ceramics, such as alumina. In an experiment involving the drilling of a groove similar to the one described above, which was carried out by altering the conditions, the high removal rate of  $Q = 42,000 \text{ mm}^3/\text{min}$  was attained. In the grinding of hard ceramics, such as silicon nitride, the conventional wisdom has been that metal bond wheels whose cutting edges have no regeneration capability become clogged or blunted easily, leading to a rapid increase in the grinding resistance. Therefore, in the grinding of these materials, resin bond diamond wheels have been used by ignoring their low grinding ratio.

In our experiment involving the grinding of silicon nitride using a metal bond wheel under conditions close to those of normal grinding ( $V = 1,500 \text{ m/min}$ ,  $f = 15 \text{ m/min}$ ,  $Z = 20 \text{ }\mu\text{m}$ ), the increases in the grinding resistance were slight and the cutting quality of the wheel stayed intact, even after many hours of grinding, as shown in Figure 2. Even when the depth of cut was expanded to  $200 \text{ }\mu\text{m}$ , a value 20 times the norm for ordinary grinding operations, no breakage of the wheel or abnormal falling-offs of the grindstone grains were observed, and the good cutting quality found during the initial stages sustained itself throughout the operation. Even more advantageous was the fact that the grinding ratio attained the extremely high value of  $GR = 1000$  ( $Z = 200 \text{ }\mu\text{m}$ ,  $f = 6 \text{ m/min}$ ). This will not always be the case with ordinary grinders. We believe the use of a highly rigid grinding machine, such as the MC we used, was instrumental in ensuring that the grindstone grains penetrated the material to be ground, leading to our good results.

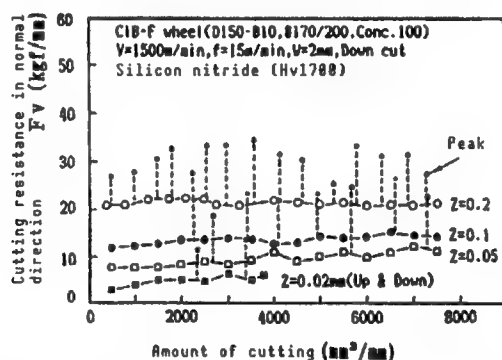


Figure 2. Retention of the Cutting Quality of a Wheel at Medium Depth of Cut and High Feed Speed Grinding and the Phenomenon of Regeneration of the Wheel's Cutting Edge

### 3.2 Rapid Feed Deep Grinding

Figure 3 shows changes in the grinding resistance when silicon nitride was ground to a depth of cut of  $Z = 0.5 \text{ mm}$ , about as deep as that for a cutting operation, under various feed conditions. When the feed speeds are relatively slow, at  $f = 2$  or  $6 \text{ m/min}$ , although the grinding resistance values in the normal direction  $F_v$  increase steadily during the initial stages, they then stabilize, except for occasional increases or decreases, permitting grinding to be conducted on an extremely stable basis.

When the feed speeds were raised to  $f = 10$  or  $15$  m/min, the resistance values declined steadily as the grinding progressed during the initial stages, and then stabilized. For a comparison, Figure 3 includes changes in the resistance when the peripheral speed of the wheel was increased to  $V = 2500$  m/min. The grinding resistance shows a great reduction to  $F_v = 32$  kgf/mm, and the cutting quality is maintained well. Even after being subjected to such a heavy grinding, the workpiece displayed no evidence of defect formation, such as chipping, and putting our conditions to practical use will pose no problem at all. The amount of removal per unit width of the wheel reaches  $q = 7500$  mm<sup>3</sup>/mm/min when  $f = 15$  m/min, which is the highest value yet achieved.

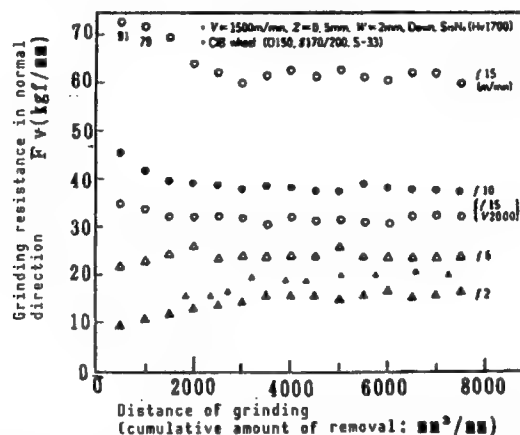


Figure 3. Feed Speeds and Changes in Grinding Resistance in Medium Depth Grinding ( $Z = 500$   $\mu$ m)

When the amounts of removal were  $q = 1000$  mm<sup>3</sup>/mm/min, the generation of intense sparks was observed, and these sparks are believed to be the factor contributing to the extended cutting quality of the grinding wheel. We have assigned the term "spark dressing" the phenomenon, which has been confirmed as having no adverse effects on the surface being ground.

The foregoing results confirm that this grinding technique for medium depth of cut and rapid feed, which differs from the conventional grinding technique for shallow depth of cut and rapid feed (for example,  $\sim 0.01$  mm for depth of cut, and 10~15 m/min for feed speed), as well as from the creep feed grinding which involves deep depth of cut and low feed speed, can greatly raise the grinding efficiency. We have termed the technique of grinding under intermediate depth of cut and fast feed conditions "rapid feed deep grinding."

### 3.3 Rapid Grinding

A grinding wheel with good cutting is synonymous with a grinding wheel with small grinding resistance. However, raising the grinding speed also makes it possible to reduce the grinding resistance or to raise the grinding efficiency (amount of removal).

Figure 4 shows the effect of rapid feed deep grinding on the grinding speed. Although the grinding speed and grinding resistance are not always in an

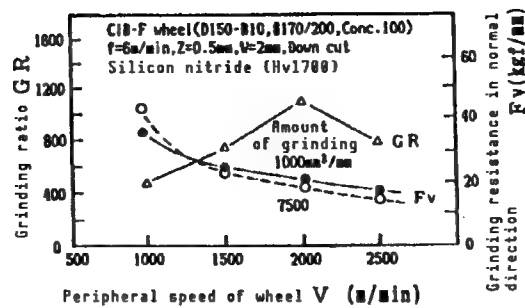


Figure 4. Relationship Between Grinding Speed and Grinding Ratio in Rapid Feed Deep Grinding

inverse proportion, raising the grinding speed, twofold enables the resistance to be reduced by about one-half.

Since an increased grinding speed leads to a reduced load working on the grindstone grains, increasing the grinding speed is desirable from the view-point of inhibiting grinding wheel abrasion. In our experiment, increasing the grinding speed from  $V = 1000$  m/min to  $V = 2000$  m/min enabled the grinding ratio to be increased greatly, from  $GR = 460$  to  $GR = 1100$ . However, raising the grinding speed further conversely resulted in a diminished grinding ratio. This is believed to have been caused by the elongation of the cumulative friction distance between the grindstone grains and workpiece. The results show that there is an optimal grinding speed.

### 3.4 High Efficiency Finish Grinding (Helical Scan Grinding)

The surface roughness of a ground plane can be improved by adopting one of the following measures or a combination of them. These are 1) to use a grinding wheel of a higher count; 2) to reduce the depth of cut; and 3) to reduce the feed speed (especially so in the case of a cup grinding wheel). However, these measures inevitably lead to reduced grinding efficiency. Therefore, we have developed a helical scan grinding method, which enables the surface roughness to be improved while retaining a high rate of removal.

In the helical scan grinding technique, the same effect as that obtained by feeding the grinding wheel with its axis tilted, as shown in Figure 5(b), can be realized by tilting the workpiece and by feeding the grinding wheel in an oblique direction, as shown in Figure 5(b), in an effort to improve the surface roughness.

Figure 6 shows a roughness curve of the surface of a cermet ("Cera" chip N, manufactured by Kyoto Ceramic Co.) ground by using a relatively coarse axial grinding wheel (No 100/120),  $\phi 30$  mm. When the inclination  $\alpha = 0^\circ$ , i.e., normal grinding, the surface roughness  $R_{max}$  is at the level of only  $4\sim 5 \mu\text{m}$ , but with increases in  $\alpha$ , the surface roughness levels improve rapidly, improving to about  $0.6 \mu\text{m}$  at  $\alpha = 45^\circ$ .

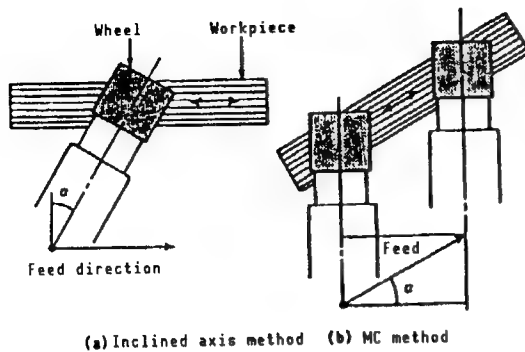


Figure 5. Helical Scan Grinding on MC

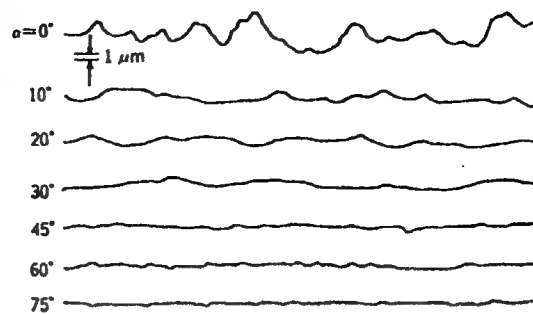


Figure 6. Improving the Surface Roughness by Helical Scan Grinding (Cermet)

#### 4. Complex Grinding Methods

##### 4.1 Development of Ultrasonic Grinding Attachment

Applying an ultrasonic vibration to the diamond grinding wheel in operation has been known to increase the grinding efficiency, and exclusive ultrasonic grinders have already been placed on the market. However, exclusive machines are not only expensive, but also lack general-purpose utilities, so the development of a much less expensive and simpler method or piece of equipment has been awaited.

In order to meet this demand, the authors have developed an ultrasonic grinding attachment that can be mounted on machining centers (Figure 7 [not reproduced]).

Thanks to the optimization of the shape and dimensions of its ultrasonic oscillator, this attachment features a small size, high output, and high rigidity (Figure 8). When used as an exchange tool on an MC, the attachment will greatly facilitate ultrasonic grinding, enabling the operation to be readily carried out as needed.

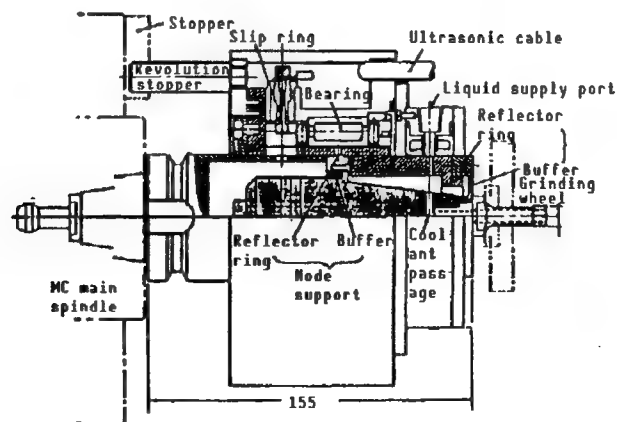


Figure 8. Internal Structure of Ultrasonic Grinding Attachment

## 4.2 Ultrasonic Grinding

The following describes surface grinding and coring performed using a metal bond diamond grinding wheel coupled with ultrasonic vibration.

Figure 9 shows the results of a test involving the grinding of a 20-mm wide strip of an alumina surface ( $V = 94 \text{ m/min}$ ,  $f = 500 \text{ mm/min}$ ,  $Z = 0.04 \text{ mm}$ ) using a  $\phi 30\text{-mm}$  cup wheel (bore: 20 mm, No 100/120). When ultrasonic vibration was not used, the grinding resistance in the axial direction  $F_z$  increased with the grinding, increasing from  $F_z = 9 \text{ kgf}$  during the initial stage to  $F_z = 11 \text{ kgf}$  at the grinding length  $L$  of 80 mm. The application of an ultrasonic vibration caused the values of  $F_z$  to drop sharply, and at  $F_z = 4 \text{ kgf}$ , stable cutting quality was obtained. Suspending ultrasonic oscillations after grinding to the distance of  $L = 320 \text{ mm}$  or its vicinity led to more increases in  $F_z$ . From the figure, one can see that the application of an attachment-derived ultrasonic vibration leads to a large-scale reduction in grinding resistance and to long-lasting cutting quality.

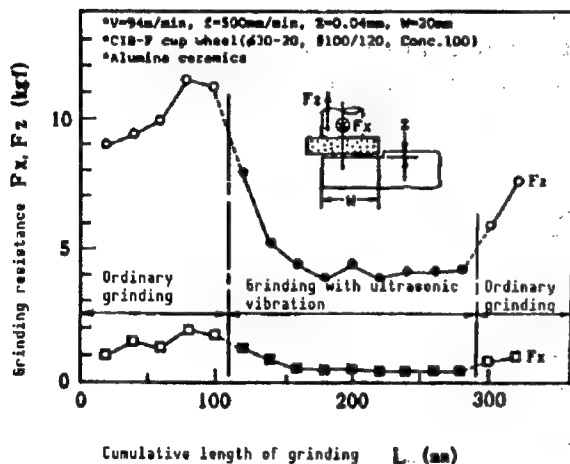


Figure 9. Effects of Ultrasonic Vibration on Grinding Resistance Reductions

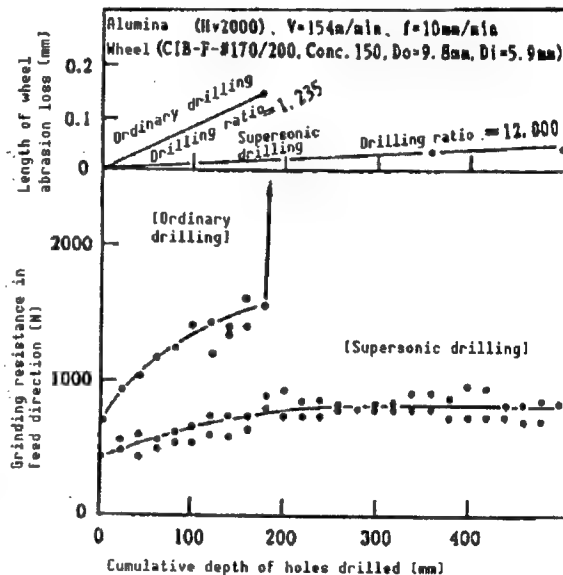


Figure 10. Improved Drilling Characteristics by Application of Ultrasonic Vibration (by Ishiwatari, et al.)

Figure 10 shows the results of a test involving the drilling of holes  $\phi 10 \text{ mm}$  in an alumina material. The figure also shows that applying ultrasonic vibration leads to reduction in the grinding resistance and an extension of the good cutting quality of the wheel. The grinding ratio is extremely large, at  $GR = 12,000$ , when the grinding process is coupled with the application of an ultrasonic vibration, confirming that the ultrasonic coring method is a grinding method with excellent characteristics.

#### 4.3 Ultrasonic Vibration and Electrodischarge Machining

The disadvantages of fine ceramics have been their low toughness. In recent years, however, thanks to various improvements of ceramics, new ceramics featuring high hardness and high toughness have been developed and placed on the market. However, from one way of looking at it, the debut of these high-strength and high-toughness ceramics has further aggravated the difficulty of machining them. Consequently, if no new grinding techniques appropriate for machining these hardest of the hardest materials to process had been developed, the outstanding characteristics of the new materials would have been wasted.

To cope with these ultrahard-to-machine materials, the authors have developed a completely new complex grinding method. Being a technique involving the simultaneous use of ultrasonic vibration and electrodischarge machining during a grinding operation, we have termed it "an ultrasonic electrodischarge grinding method."

Figure 11 shows a conceptual diagram of the ultrasonic electrodischarge grinding method. The mechanism of applying an ultrasonic vibration to the grinding wheel is done by taking advantage of the ultrasonic grinding attachment for MC that we proposed and developed earlier, and electrodischarge is obtained by supplying the base of the ultrasonic grinding attachment and a workpiece that is insulated from the table by means of electricity.

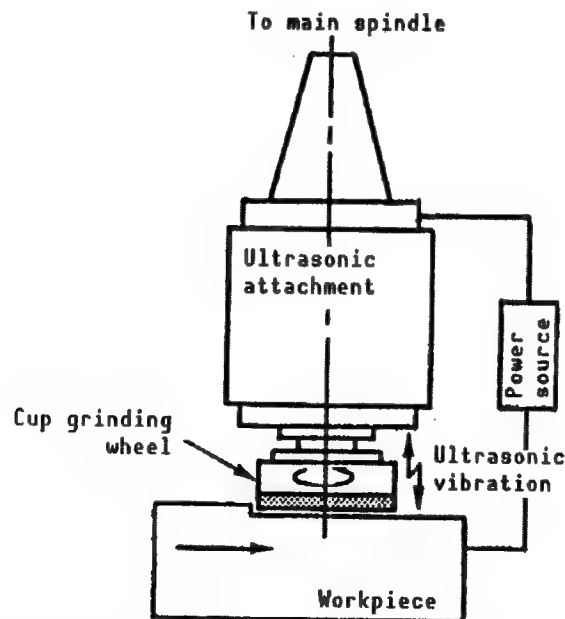


Figure 11. Conceptual Diagram of Ultrasonic Electrodischarge Grinding Method

The following experiments were conducted using a cup wheel, but the technique is apparently applicable to straight and axial wheels.

For our experiments, we selected titanium boride ( $TiB_2$ ), a material considered to be representative of the hard-to-machine materials. This material is hardly machinable, even with the rapid feed deep grinding method that has proved to be highly effective for other materials.

Titanium boride material was ground using various grinding methods, and the transitions in grinding resistance for these methods are given in Figure 12. In the case of ordinary grinding (G), the grinding resistance increases sharply from the initial grinding stage, apparently making it impossible to continue. With electrodischarge grinding (ED-G) and ultrasonic grinding (US-G), although the grinding resistance values are not as large as those for ordinary grinding, they are not so small as to be termed "inhibitory to sharp rises in grinding resistance." On the other hand, in the case of ultrasonic electrodischarge grinding (US-ED-G) in which grinding is assisted by an ultrasonic vibration and electrodischarge, great reductions in the grinding resistance are seen and the cutting quality of the wheel is kept intact for a long time.

The ultrasonic electrodischarge grinding method has been proven to be highly effective not only for titanium boride materials, but also for other conductive hard-to-process materials (conductive sialons, conductive silicon nitride, ultrahard alloys).

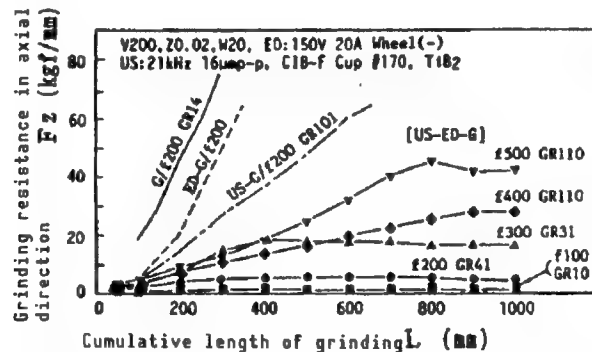


Figure 12. Effects of Ultrasonic Electrodischarge Grinding in Grinding Hard-To-Process Materials

#### 4.4 Vibration Electrodischarge Grinding by Vibration Table

As described above, the ultrasonic electrodischarge grinding method is an extremely effective method for machining hard-to-process materials, but it has limitations with respect to the types of grinding wheels that can be used since the technique uses vibrating ultrasonic waves. Therefore, we have attempted to utilize a workpiece vibration mode of the vibration electrodischarge grinding method which is free of limitations on the shape or dimensions of the grinding wheel. For vibrating the workpiece, we used a tri-force vibration table (Figure 13(a) [not reproduced], (b), and (c)) incorporating layered piezoelectric devices. The grinding wheel used was a straight wheel,  $\phi 150$  mm.



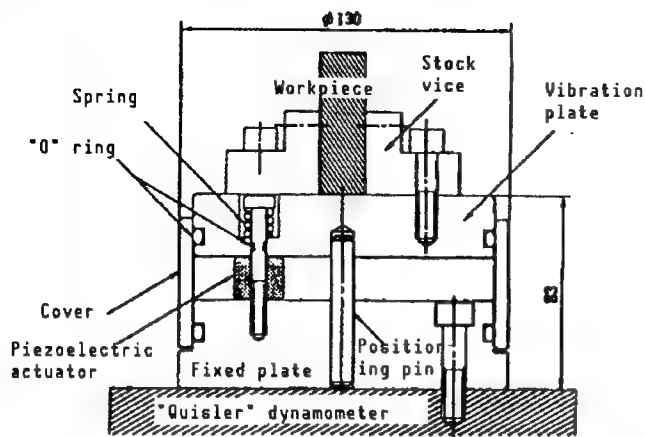


Figure 13(b). Internal Structure of Vibration Table (Omori)

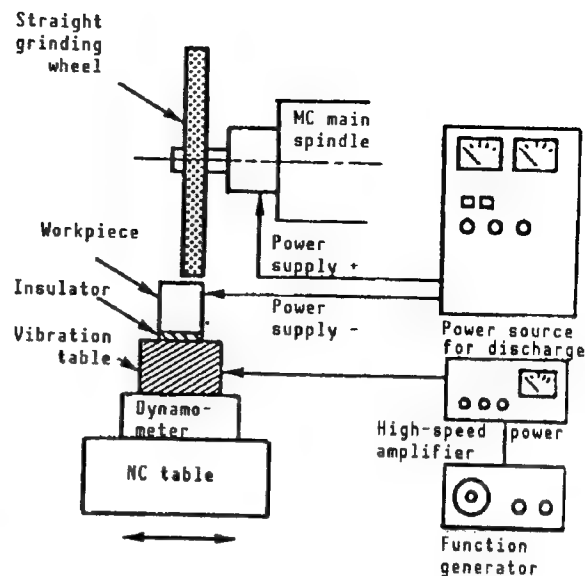


Figure 13(c). Configuration of Systems for Vibration Electro-discharge Grinding

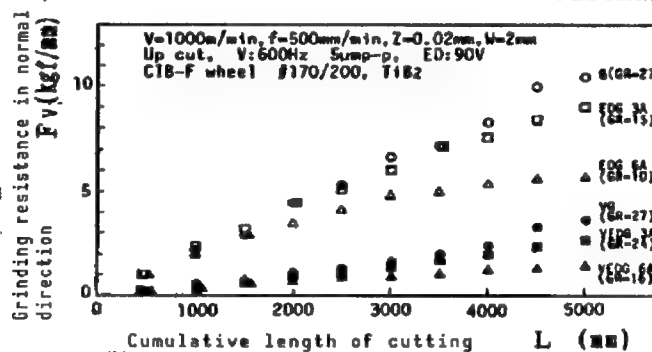


Figure 14. Results of Vibration Electrodischarge Grinding of Titanium Boride

Figure 14 shows the results of vibration electrodischarge grinding of titanium boride. When using a cup grinding wheel, the effects of the ultrasonic vibration and the electrodischarge applied are not very conspicuous, but when a straight wheel is used, these effects are conspicuous. In vibration electrodischarge grinding in which an ultrasonic vibration and an electrodischarge are applied simultaneously, reductions in the grinding resistance were much more conspicuous. The fact that such a large effect was obtained despite the small amount of vibration imparted by the vibration table, i.e., 600 Hz, warrants attention.

## 5. Development of High-Accuracy On-Machine Truing Method

### 5.1 The Need for On-Machine Truing/Dressing

Because of their high grain-retention power metal bond wheels are best suited for the high-efficiency grinding of ceramics, but problems are found with truing and forming.

When the objective is to keep the flat-type wheel from vibrating, truing is difficult to achieve with a single-stone diamond and is generally conducted on the grinding machine using a rotary-type grinding wheel (C, GC, WA). This method is simple and easy, but has the following disadvantages: 1) a long time is needed for truing; 2) the wear and tear of the truing wheel while in use leads to reduced dimensional and shape accuracies of the diamond wheel; 3) its application to a form wheel involves much difficulty; and 4) it is not appropriate for automation.

The forming of a form wheel or restoration of a deformed wheel are beyond the capability of the user, and such jobs have always been undertaken by wheel manufacturers. These manufacturers have been using metal electrodischarge machining for the forming of metal bond wheels, but we have developed a method that enables the job to be done easily on a grinding machine.

## 5.2 Proposal for an On-Machine Electrodischarge Truing Method

Aimed mainly at increasing the ease of truing and at eliminating the wheel attachment errors, in the method we have devised the truing of a metal bond wheel is performed on a grinding machine, as shown in Figure 15. This "on-machine electrodischarge truing method" enables forming and high-accuracy truing to be performed by taking advantage of the NC drive mechanism being incorporated in the table attached to the grinding machine, and it also enables in-process dressing to be performed.

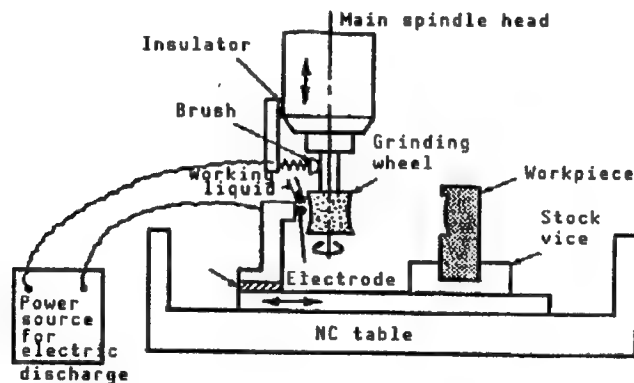


Figure 15. Schematic Diagram Showing the Principles of On-Machine Electrodischarge Truing

The following is a list of characteristics of the on-machine electrodischarge truing method:

- (1) It is applicable to metal bond wheels and conductive wheels.
- (2) It enables truing to be performed while the wheel is attached to the spindle of the grinding machine, thus facilitating high-accuracy truing.
- (3) Merely by altering the electrodischarge conditions, the method can be applied to the truing and dressing of wheels of various grain sizes.

(4) Thanks to its small machining pressure, the method enables high-accuracy truing/dressing of small-diameter axial wheels and thin cutting wheels to be performed.

(5) It enables forming truing of various shapes to be performed on a grinding machine by exploiting the NC drive mechanism of a machining center or grinding center.

(6) Since it exploits the NC drive mechanism of a grinding machine (such as an MC), there is no need for installing an electrode servo drive mechanism, thus enabling, as a whole, highly functional truing to be achieved at a small cost.

The following three methods are being considered for application to truing by means of electrodischarge: 1) a method based on profile electrodischarge machining using a block electrode; 2) a method using a pair of electrodes; and 3) a method using a wire electrode. Table 3 outlines these methods, comparing them with the conventional electrodischarge truing method.

Table 3. Comparison of Methods for Truing of Metal Bond Wheels by Electrodischarge Machining

	Conventional method	On-machine electrodischarge truing	
Place of forming	Manufacturer (off-machine)	User (on-machine)	
Shape of electrode	Block electrode	Wire electrode	Block electrode
Forming of electrode	Off-machine (cutting)	Unnecessary	On-machine (cutting)
Wear of electrode	x	o	x
Measures against wear	x	Unnecessary	• (on-machine adjustment)
Removal efficiency	o	Δ	•
Method of forming forming wheel	Forming electrode	NC table	Forming electrode
Limitations on forming profile	None	Wire diameter	None
Attachment error	Δ	•	•
Grinding accuracy	Δ	•	•

### 5.3 On-Machine Electrodishcharge Truing by Wire Electrode

As shown in Figure 16(a), in the on-machine wire electrodischarge truing/dressing method, truing/dressing is performed on the grinding machine by using a wire electrode running along a guide groove. Its features include the following: 1) there is no deterioration in accuracy that would be caused by the loss of the electrode through wear and tear; and 2) the forming wheel can be formed without a forming electrode by exploiting the NC drive mechanism for the table feed. The double end guide method shown in Figure 16(b) is for the forming of a groove.

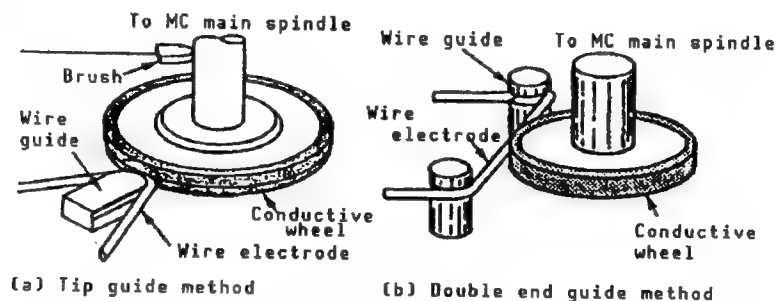


Figure 16. Principle of Electrodishcharge Truing by Wire Electrode

Figure 17 [not reproduced] shows an experiment involving on-machine electrodischarge truing/dressing, with wire electrodischarge truing equipment mounted on the vertical machining center. A brass wire electrode runs along an alumina ceramic wire guide, and a discharge is generated between it and the wheel's external periphery for removal. In order to raise the machining efficiency, the electrode brush side that is in contact with the wheel's surface or the wheel's axis is used as the positive electrode, and the wire side is used as the negative electrode. We used a grinding liquid (Johnson's JC-707 x 50) for the electrodischarge machining liquid due to its ease of use in actual application, and no problems of any specific importance were observed.

The experiment also had as its objective on-machine electrodischarge forming of the forming wheels, so the wire electrode was made to run horizontally as shown in Figure 16(a). If this operation is to become applicable to various shapes of grinding wheels, some ingenuity is needed in the placement of the electrode running equipment, such as giving it a tilt.

Electrodischarge truing of a vibrating wheel was conducted while supplying the required feed amount  $\Delta Z_d$  for each pass, and we examined the vibration connection effect. Figure 18 shows the results of a test when the peripheral velocity of the wheel  $V_d$  was 100 m/min. Under any current conditions, the amount of eccentricity  $E_g$  diminishes with the number of wire passes  $N$ . Diminishing the current value gradually enables the amount of eccentricity  $E_g$  to be improved, ultimately approaching 3  $\mu\text{m}$ .

### 5.4 On-Machine Electrodishcharge Truing by Block Electrode

The use of a wire electrode has such disadvantages as the discharge being limited to a localized area, the average current value not being permitted to

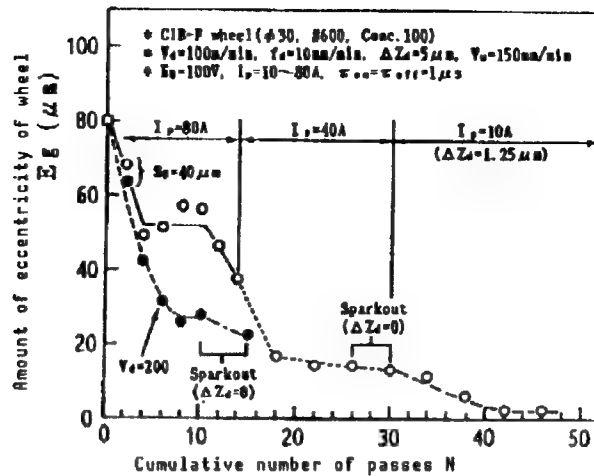


Figure 18. Effect of Wire Electrodischarge Truing on Vibration Correction

be large in magnitude, and the air cut state increasing during forming truing, and all this leads to the following problems: the truing efficiency is not necessarily high; and since the levels to which the wire electrode diameter can be reduced are limited, the shapes that can be generated are also restricted.

The use of a block electrode, on the other hand, has a problem of reduced truing accuracy arising from the wear and tear of the electrode, but when observed strictly from the viewpoint of truing efficiency, the method is advantageous in that large currents can be introduced.

Major problems with on-machine electrodischarge truing using a block electrode are the wear and tear of the electrode and its attachment errors, all of which lead to inferior shapes. These problems have been solved by the adoption of a rotary forming electrode and by the creation and adjustment of a forming block electrode on the machine.

Figure 19 shows the principles of the on-machine electrodischarge truing method by on-machine creation/adjustment of the electrode. This method follows the following procedures: 1) a cylindrical electrode material fastened to the axis of the rotary truing equipment mounted on the NC table is cut on-machine to the intended shape using a cutting tool mounted on the main spindle, creating a forming electrode; 2) a metal bond wheel is attached to the main spindle using an ATC, and electrodischarge truing (rough machining) is conducted between it and the formed electrode; 3) a cutting tool is again mounted on the main spindle to make corrections for the loss of the electrode; and, finally, 4) electrodischarge truing is obtained between the adjusted electrode and the wheel for the finish.

Due to the weak electrodischarge conditions at this time, dressing of the wheel is performed simultaneously.

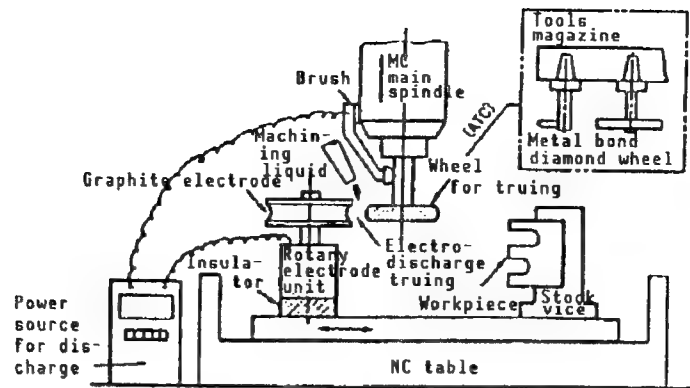


Figure 19(a). Configuration of Machines and Instruments for On-Machine Electrodischarge Truing Using a Block Electrode

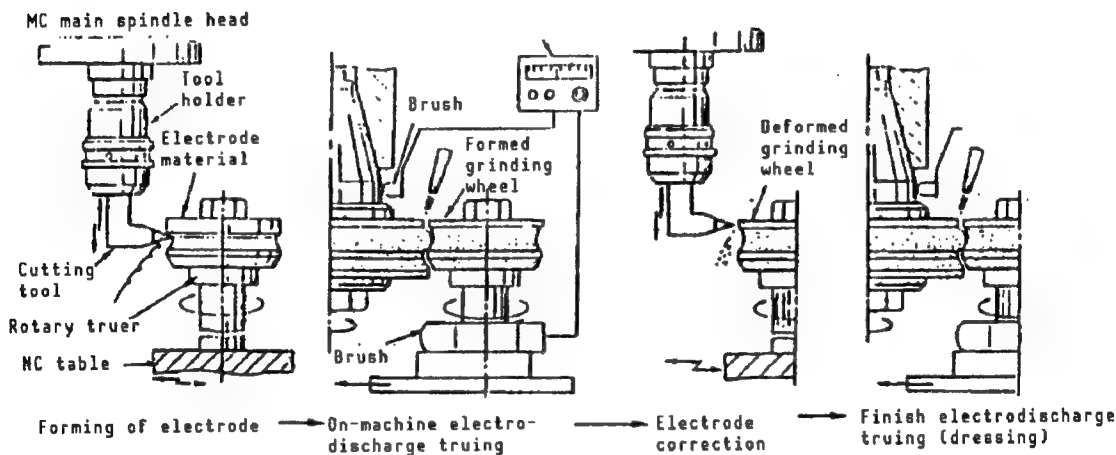


Figure 19(b). Steps of On-Machine Electrodischarge Truing Process by On-Machine Creation/Correction of Electrodes

Characteristics of this method are that, in addition to there being no need to retain a forming electrode in place beforehand, electrodischarge truing can be obtained while the electrode is kept in rotation and that corrections of the electrode can be made on the machine, all of which prevents the truing accuracy from dropping as a result of wear and tear on the electrode. Figure 20 [not reproduced] shows a scene in which a graphite electrode is being shaped on an MC. Figure 21 [not reproduced] shows a scene in which forming truing is being performed using a cylindrical forming electrode on the machine. Figure 22 [not reproduced] shows grinding wheels thus formed. As these grinding wheels show, with this method, sharply concave shapes can be created.

### 5.5 Automation of On-Machine Electrodischarge Truing

Regardless of whether it involves the wire electrode method or the block electrode method, the on-machine electrodischarge truing enables truing to be

performed without an electrodischarge servo mechanism, but selecting the optimal feed speed entails much difficulty. Therefore, in order to improve the efficiency of the on-machine electrodischarge truing method, as well as to automate the process, we conducted studies on methods of driving the electrode based on a servomechanism.

In order to realize electric discharges based on a servomechanism, one idea is to have truing equipment that is itself incorporated with a servo-drive mechanism, but this method has disadvantages in that the equipment increases in complexity and grasping the relative position from the grinding wheel axis becomes difficult. Therefore, we adopted a method for controlling the table feed drive system by directly sending, as feedback, the anode-cathode voltage information during electrodischarge truing to the overdrive function in the NC control section of the grinding machine being used (in this case an MC). Figure 23 shows a diagram of the circuits for the servo system.

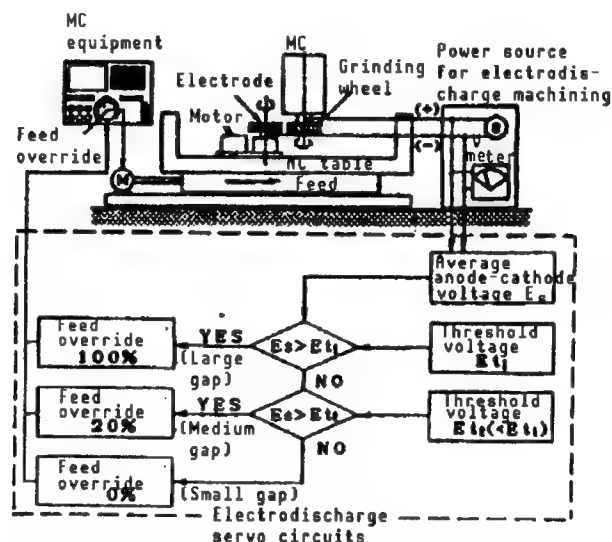


Figure 23. Diagram of Circuits for Electrodischarge Servo for On-Machine Electrodischarge Truing

In this servo system, the table (=electrode) feed speed takes one of the three override stages of 100, 20, or 0 percent, according to the measured anode-cathode voltage (corresponding to the anode-cathode distance). This way, when the grinding wheel and the electrode are placed too far away, the electrode can be moved at high speeds in an override 100 percent mode, while following the start of an electric discharge the feed speed can be decelerated so that the proper distance between electrodes will be maintained. When the distance between the electrodes is narrower than the target value, the override is automatically reduced to zero percent, that is, feeding is stopped, in order to restore the distance between the electrodes. The feed speed for a 100 percent override can be set at random on the NC program.

## 5.6 Grinding Capabilities of Grinding Wheels Subjected to On-Machine Electrodischarge Truing

Using a bronze grinding wheel (No 170/200), we conducted a grinding test of silicon nitride to study the grinding capabilities of grinding wheels that have been subjected to electrodischarge truing. For comparison, two methods of truing/dressing were adopted. One was electrodischarge truing using the rotary block electrode method, and truing/dressing was obtained under certain electrodischarge conditions ( $E_0 = 150$  V,  $I_p = 20$  A,  $\tau_{off} = 5$   $\mu$ s,  $Z_d = 0.1$  mm) to examine the effect of  $\tau_{on}$  on the grinding performance. In the other, the surface of the grinding wheel was made smooth using a brake truer (C grinding wheel), and was then subjected to dressing using a WA stick grinding wheel (No 400).

Figure 24 shows changes in the grinding resistance when silicon nitride was ground using the above two grinding wheels under the grinding conditions of  $V = 1500$  m/min,  $f = 15$  m/min,  $Z = 0.05$  mm,  $W = 4$  mm, and down cut. The grinding resistance values for the grinding wheel subjected to electrodischarge truing are scarcely affected by the amounts of  $\tau_{on}$  (8~100  $\mu$ s), and are 25~30 percent smaller than those for the WA stick grinding wheel. The trends change little with increases in the amount of grinding. The grinding ratios GR are smaller than those for the WA stick grinding wheel in the large  $\tau_{on}$  region (20~100  $\mu$ s), but they improve greatly in the small  $\tau_{on}$  region (8~12  $\mu$ s), with GR attaining 429, a value larger than that attainable with the WA stick grinding wheel. The roughness levels of the ground surfaces are in the 7~8  $\mu$ m range, regardless of  $\tau_{on}$ , and these values are slightly inferior to those of the WA stick grinding wheel ( $R_t = 5.4$ ).

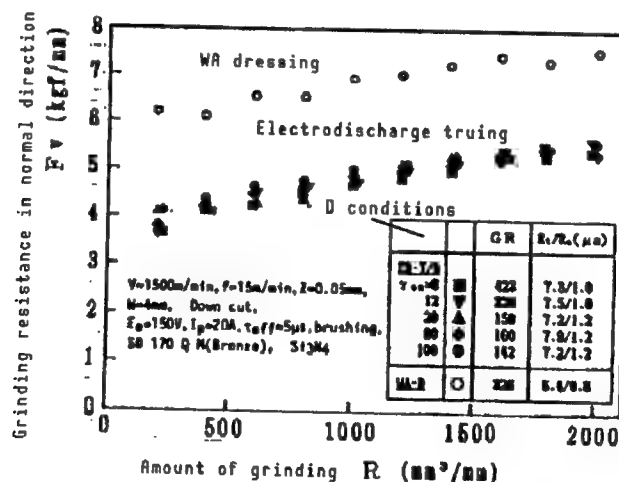


Figure 24. Cutting Performance of a Grinding Wheel Treated With Electrodischarge Truing (Bronze bond grinding wheel, silicon nitride)

Figure 25 [not reproduced] shows the surface properties of diamond and CBN grinding wheels treated with electrodischarge truing. They show no cavities around the peripheries of the grindstone grains and have ample projections,



and these are believed to have contributed to the aforementioned improvements in the grinding performance.

A survey of the on-machine electrodischarge truing conditions has confirmed that the method has a truing efficiency and effects sufficient for grinding wheels of any grain size, and that it is applicable not only to metal bond grinding wheels, but also to electrically conductive resin bond grinding wheels.

### 5.7 Development of On-Machine Electrodischarge Truing Equipment

In order to promote the practical use and diffusion of the on-machine electrodischarge truing method, we studied the specifications for the electrodischarge truing unit and the power source equipment and manufactured the equipment on a trial basis.

Since the on-machine electrodischarge truing unit is installed on the table of a grinding machine, the system will preferably be as compact as possible as long as the small size does not interfere with its performance. The unit must also be capable of coping with various shapes of grinding wheels and various objectives of truing/dressing. Figure 26 [not reproduced] shows an example of a truing unit capable of meeting the requirements for both the wire electrode and the block electrode process.

The power source for electric discharges should be able to output electrical conditions corresponding to the wire and the block electrode. After taking into account the preliminary experimental results, the experimentally manufactured power source had specifications that enabled it to output the following electrical conditions: no load voltage  $E_0 = 60\sim 150$  V, peak current  $I_p = 2\sim 75$  A (155 A for the wire electrode alone), electrodischarge pulse width  $\tau_{on} = 1\sim 200$   $\mu s$ , and quiescent time  $\tau_{off} = 3\sim 100$   $\mu s$ .

For setting the electrodischarge truing conditions, the following three methods are available: 1) the conditions can be set manually each time electrodischarge truing is to be employed; 2) the pre-set conditions can be called out from the memory by a selective switch; and 3) the conditions can be called out from the MC's program by designating a memory. As a safety precaution, a system is employed in which when the grinding machine being used comes to a halt because of an emergency, the power source for electric discharge also stops.

It is not necessary to equip the power source with a built-in NC control system, but the aforementioned circuit for controlling the anode-cathode distance is incorporated as a built-in system. Figure 27 [diagram not reproduced] shows the external appearance of the power source equipment SUE-87 manufactured on a trial basis.

We installed the experimentally manufactured electrodischarge truing unit on the table of a vertical machining center, and conducted truing tests of bronze bond diamond grinding wheels (grain size = No 600). Figure 28(a) [not reproduced] shows a forming grinding wheel formed by means of a wire electrode

point guide method, and Figure 28(b) [not reproduced] shows an example in which the grinding wheel has been etched with deep grooves by a both-end guide method. With the use of the latter method, a wide-width grinding wheel can be easily shaped into a multiblade grinding wheel. Figure 28(c) [not reproduced] also shows a forming grinding wheel formed by a rotary block electrode.

Type	SUE-87 ("Sodek" product)
External dimensions	600 x 600 x 800 mm
Monitors	(1) voltmeter, (2) ammeter, (3) machining condition display, (4) override level display, and (5) off-extension display
Voltage	$E_o = 60\sim 150$ V
Current	$I_p = 2\sim 75$ A (155 A-wire electrode)
Pulse width	$\tau_{on}/\tau_{off} = 1\sim 200 \mu s/3\sim 100 \mu s$
Condition setting	(1) manual, (2) preset method, (3) external call-out method
Safety device	Automatic power source cut-off system (in linkage with NC)

Figure 27. External Appearance [Diagram] and Specifications of Power Source (SUE-87)

In the truing tests conducted using the trial manufactured equipment, we adopted the electrode methods believed to be most appropriate for each of the various grinding wheel shapes, and the experimental truing equipment showed stable operation in each case. Regarding the forming time, in the case of Figure 28(c) [not reproduced] it took only 20 minutes, realizing high efficiency.

The combination of a forming grinding wheel formed by an on-machine electrodischarge truing method and the NC function of an MC makes it easy to machine complex shapes, such as the one shown in Figure 29 [not reproduced].

## 6. Conditions for Grinding Centers

The authors have been conducting studies on methods of realizing high efficiency and high accuracy grinding of ceramics on a high rigidity and multifunctional machining center by using metal bond diamond grinding wheels featuring high grain-retaining capacity. However, if existing MCs are to be able to fully function as grinding centers (GC), they must be improved in several respects. Table 4 lists these problems and measures to cope with them.

The scrap from ceramic grinding is made up of fine particles, so the ordinary grinding machine designed for grinding metals must be provided with some anti-dust measures. It is generally believed that protecting the sliding surface with anti-dust measures will serve the objective perfectly. In our machining method, however, large amounts of grinding liquids are used, so extra precautionary measures must be implemented to prevent dust and water from reaching the bearing section of the main spindle. Therefore, the sliding surface has been doubly protected with a bellows cover inside a slide cover to

Table 4. Problems of MC Associated With Use of MC as MG, and Measures To Cope With Them

Problems	Countermeasures
1. Incomplete measures for preventing dust from sticking to the layer being ground, which gives rise to a shorter machine life and inferior mechanical accuracy	Sliding surface: a double-layer dust cover Main spindle: air seal, labyrinth
2. Insufficient number of rotations of the main spindle, giving rise to low grinding speed in small-diameter grinding wheels	Increasing the rotation speed of the main spindle High-speed grinding material attachment
3. Insufficient main spindle rotation accuracy and positioning accuracy, giving rise to chattermarks and poor dimensional accuracy	Adoption of high accuracy bearings Scale feedback
4. Short supplies of grinding liquid (pressure, amount, position) leading to wheel clogging and heat generation	Large-capacity pump, high pressurization Spindle/tool through
5. Insufficient measures for grinding liquid filtration	Paper filter + centrifugal separation + sedimentation
6. Vibrations of grinding wheel accompanying tool change, leading to chattermarks and poor surface properties	On-machine truing (NC drive mechanism + electrodischarge machining)
7. Lack of efficient dressing method, leading to dressing-caused deformation	On-machine dressing (NC drive mechanism + electrodischarge machining)
8. Movements as a grinder	Preparation of NC software for grinding operation, and adoption of appropriate control

prevent grinding dust from penetrating, and the main spindle's bearings section has incorporated ingenuities, such as letting the air gush out from the inside, or building the labyrinth into a complex shape.

The finish grinding surface may be disrupted by the grinding liquid containing large amounts of grinding scrap, so the grinding liquid must be fully filtered. In a recently-developed GC, filtration is conducted in the following three stages of paper filter, centrifugal separation, and sedimentation tank.

The automatic tool change (ATC) function not only makes it possible to automatically exchange a worn-out grinding wheel, but also enables a grinding wheel with the shape, size, and grain size best suited for grinding the

intended area to be selected so quickly, this capability is regarded as an inevitable function for long-term automatic operation or for the grinding of complex and high value-added shapes. There was a time in the past when the accuracy of exchanging a tool by ATC posed a problem, but some GCs currently have accuracies of about  $0.6 \mu\text{m}$ .

The ATC function is also inevitable for inclusion in compound machines in which a grinder is employed as the base. For example, a GC equipped with a tool holder with a built-in ultrasonic oscillator will metamorphose itself into an ultrasonic machine, proving itself to be highly effective in the drilling of small holes or in profile grinding by small-diameter grinding wheels. Under a similar concept, when a GC is joined by a grinding unit incorporating a high frequency motor, the machine will be transformed into a jig grinder for use in the high-accuracy grinding of holes. Adding some improvements to the grinding wheel or the tool holder will easily enable the machine to perform electrodischarge grinding operations.

Since its effects have increasingly come to be appreciated, the on-machine electrodischarge truing/dressing method for metal bond grinding wheels that has been developed to make high-accuracy grinding feasible is beginning to show signs of widespread diffusion. Combining an NC grinder or a GC with the aforementioned electrodischarge truing equipment or the ultrasonic grinding attachment turns the combination into a so-called hybrid grinding center. Due to the advantages that accrue from the use of such a compound machine, such as the availability of adopting the grinding method and conditions most suited to the workpiece to be machined, we believe compound machines warrant full consideration in the future. Figure 30 shows a conceptual diagram of the hybrid grinding center being studied by the authors.

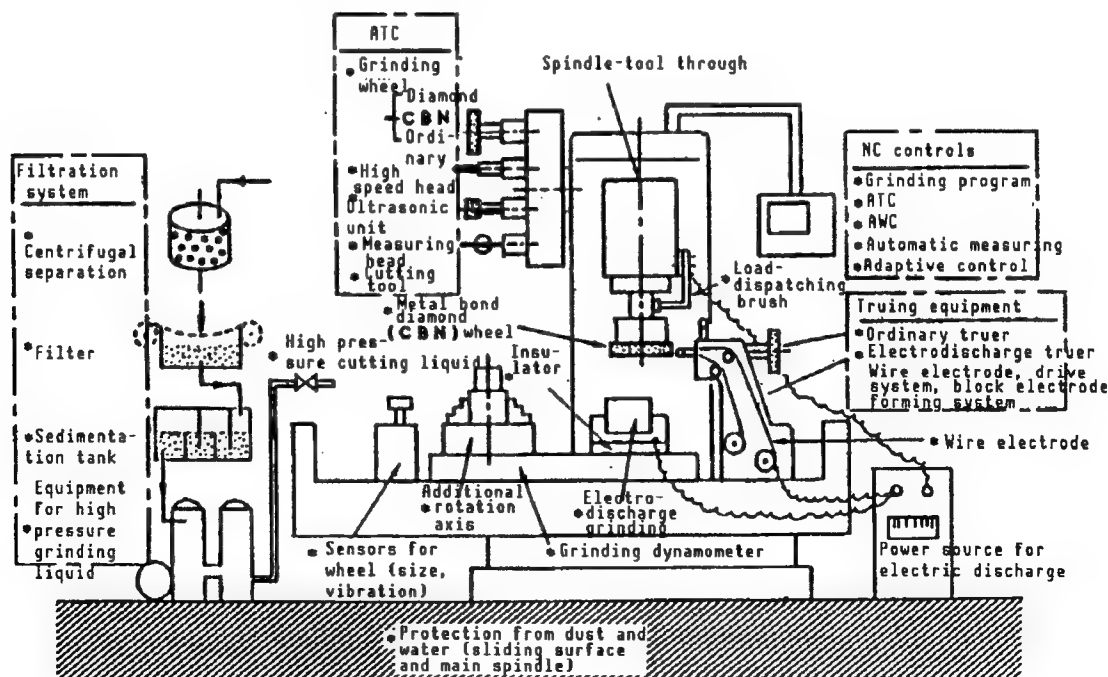


Figure 30. Configuration of Hybrid Grinding Center

## 6. Conclusion

The authors have reported that the effective utilization of various capabilities of machining centers for grinding use enables hard and brittle materials, like ceramics, to be ground efficiently and highly accurately. The machining center used for grinding and the grinding center, both developed based on our ideas, were unveiled at the international machine tools fair, gathering great attention. Since then, the manufacturers of machine tools, with few exceptions, have entered the market with their own grinding centers. Several dozen GCs have already found their way into various fields, proving their high effectiveness.

## References

1. Suzuki, K., Uematsu, T. and Nakagawa, T., "On MC Grinding of Hard and Brittle Materials, Reports Nos 1 through 22," Proceedings of the Precision Engineering Society Meeting, March 1985 through October 1988.
2. Uematsu, T., Suzuki, K. and Nakagawa, T., "Research on Ultrasonic Electrodischarge Grinding," Proceedings of the Spring Meeting of the Precision Engineering Society, 1988, p 655.
3. Nakagawa, T., Suzuki, K. and Uematsu, T., "Highly Efficient Grinding of Ceramics and Hard Metals on Grinding Centers," ANNALS OF CIRP., Vol 35 No 1, 1986, p 205.
4. Suzuki, K., Uematsu, T. and Nakagawa, T., "On-Machine Truing/Dressing of Metal Bond Grinding Wheels by Electrodischarge Machining," Ibid., Vol 36 No 1, 1987, p 115.
5. Uematsu, T., Suzuki, K., Yanase, T. and Nakagawa, T., "A New Complex Grinding Method for Ceramic Materials Combined With Ultrasonic Vibration and Electrodischarge Machining," Proc. of ASME (WAM) Symp. on MACMC, 1988, p 135.

## **Solid Phase Welding Technology, Its Applications**

43067178F Tokyo THE 91ST WORKSHOP ON PLASTIC WORKING in Japanese 16 Jun 89  
pp 53-60

[Article by Shinichi Matsuoka, Faculty of Engineering, The University of Tokyo]

### **[Text] 1. Present Status of Technology for Joining Materials**

Many new materials having various characteristics have been developed and manufactured in recent years. Needless to say, these materials have been seeing much use individually in their own right, but they have also been widely used in the form of compounds or complexes. In today's highly diversified and sophisticated technology, the technology for joining materials is indispensable as the basic technology for use in the manufacturing and assembling required in various fields, such as those involving general-purpose machines, precision machines, and semiconductors. The technology for joining materials has advanced rapidly and has come to be widely used, and with it demands are being made for it to meet highly sophisticated and complex requirements.

Various kinds of joining technology, such as welding, joining by mechanical force, and bonding by using bonding agents, have been developed. Which of these technologies should be employed is determined after taking into consideration the performance or capability demanded of the product or part.

In other words, an agreement between the material qualities of the material in question and its joining method becomes important, in addition to its other characteristics, such as strength, rigidity, toughness, shock resistance, electric conductivity, heat resistance, and economics. Table 1 lists various methods of joining materials categorized by energy source.

Table 1 classifies welding technologies by their machining energy sources, and shows that a majority of the welding methods require thermal energy. Riding the wave of industrial technology innovation, the importance of these technologies is continually increasing. For example, in the case in which the work involves the joining of materials that fail to produce a healthy weld with fusion welding technology, or when the work involves the welding of

Table 1. Ordinary Types of Joining Methods and Energy Sources

	Electric energy	Optical energy	Chemical energy	Thermal energy	Vibration (force) energy
Heat	Resistance welding Electron beam welding Plasma welding/thermal spraying Microwave welding	Laser welding Laser beam deposition		Thermal diffusion joining Brazing Thermal spraying Deposition	
Mechanics	Ion sputtering deposition Ion implantation Electromagnetic pressure welding		Explosive welding		Ultrasonic joining Friction pressure welding Powder forming
Others	Electroplating Electroforming		Chemical plating chemical vapor deposition (CVD) Thermal-hardening adhesion		

materials with different properties within a single structure, i.e., the welding of two different kinds of materials, the solid phase welding method is employed.

A large number of papers have been published on joining technologies, some of which have been put to practical use. However, even those technologies already put to commercial use have many problems awaiting solutions and, among the large variety of materials involved, some are seen that lead one to have second thoughts about the feasibility of welding them. As for important industrial materials, fabricating their complexes (composites) with metals or with each other is becoming inevitable and, as duly expected, the technology of welding or adhesion is becoming an important issue for these materials.

## 2. Kinds and Characteristics of Joining Methods

Table 1 lists welding technologies by energy source, but welding technologies are often classified by their welding mechanisms, i.e., vapor, liquid-phase, and solid-phase welding. In each of these technologies, the welding method and welding characteristics are greatly affected by the ceramic material being used.

Generally, it is preferable that welding be undertaken at low temperatures. One of the reasons for this is that low-temperature welding is least vulnerable to thermal deformation or heat-caused dimensional inaccuracy, thus enabling a good welded product to be obtained without changing any of the ceramic's characteristics. The following outlines the representative welding methods.

(1) Vapor deposition method: A ceramic substrate is heated in a vacuum (about  $4 \times 10^{-5}$  Torr) and a film of Al, Cu, Au or Ag, several microns thick, is vapor deposited on its surface according to the objective of use. The metallized ceramic is then used for welding (brazing) with a metal or other ceramic.

(2) Ion plating method: This is a deposition method conducted in a gas environment (ions). With this technique, a substrate can be coated with a layer of oxides such as  $\text{Al}_2\text{O}_3$ ,  $\text{SiO}_2$ , or  $\text{TiO}_2$ , with a layer of nitrides such as  $\text{TiN}$ ,  $\text{Si}_3\text{N}_4$ , or  $\text{AlN}$ , and with a layer of carbides such as  $\text{SiC}$  or  $\text{ZrN}$ .

(3) CVD (chemical vapor deposition) method: Since this technology is accompanied by chemical reactions, it is generally distinguished from physical (vacuum) deposition. When forming a thin film of  $\text{Al}_2\text{O}_3$ , for example, a substrate is heated in an oxygen ambient and a high-purity aluminum is blown onto the substrate, which enables a conductive thin film of  $\text{Al}_2\text{O}_3$  to be formed on the substrate.

(4) Bonding agent methods: These techniques, featuring relative ease of use, are being widely used in structural bonding due to advances in recent years in synthetic chemistry and conventional epoxy resins. As with welding methods using organic bonders, these techniques are applicable to all kinds of materials. They have the advantages of low bonding temperatures, good workability, and low cost, but have the disadvantages of low heat resistance, disparate bonding strengths, and unstable durability.

Inorganic bonding agents feature heat resistance up to  $1000^\circ\text{C}$ , with some able to withstand heat exceeding  $2000^\circ\text{C}$ .

(5) Thermal spraying: In this technology, a metal or ceramic powder is blown off into a high temperature flame to be sprayed onto the target for deposition. Of the various thermal spraying techniques, the plasma arc spraying method, employing a plasma jet, features extremely high temperatures and high flow velocities. Having a high welding strength and capable of forming a dense layer, this technique is applicable to materials with extremely high melting points.



(6) Thermal diffusion welding method: A kind of high-temperature heating process, in this method welding is obtained by forming diffused or reaction layers on solids by letting the solids come into contact with one another and heating them at high temperatures. This method requires extremely high-temperature heating, and the temperature must be equal to or above the sintering temperatures of the base materials, i.e., ceramics.

For this reason, the process has failed to find widespread use despite all the effort that has been spent in studying the technology.

(7) Powder forming: In this process, a raw material powder is charged into a mold and formed by applying high temperature heat and pressure simultaneously. It comes in the compression forming, hot pressing (HP), and hot isostatic pressing (HIP) forms, and these processes are being widely used.

A welding method involving the simultaneous application of heat and pressure, HP is generally used as a combination of an electric heating and hydraulic pressure process. In HIP, preparatory forming is first conducted at normal temperatures, and the twin effects of large isotropic pressures and high temperatures, using inert gases (such as AR) as the pressure medium, are employed for welding.

(8) Mechanical welding methods: These processes, which are quite different from the aforementioned welding mechanisms, include shrinkage fit, screw tightening, and bolt tightening. Characteristics of these processes include freedom from limitations on material combinations, low residual pressure, and high strength at high temperatures.

As described above, selecting the welding method best suited to its use objective and function enables its characteristics to be exploited to the highest extent. Needless to say, all the welding processes described above are greatly affected by such factors as the state of the material surface, the thermal expansion and wettability of the material, and interface reactions.

In the following the author describes the "ultrasonic welding method," which is considered to be the most ideal of all welding methods and has the potential to be adaptable to all kinds of materials, including its outline, an introduction of its characteristics, and evaluations based on two or three cases in which the technology has been employed.

### 3. Outline of Ultrasonic Welding Method

Figure 1 shows an ultrasonic welding machine for ceramic-metal bonding, and a schematic diagram of the sections to be welded. The method can be classified into two processes: 1) a process in which a ceramic and a metal are welded directly, and 2) a process in which a binder is used for welding. The latter again can be divided into two processes: one is a method in which an activation metal is used as an insert material, while in the other a metal is deposited in advance on the ceramic surface in a vacuum, the surface and the metal material are made to come into contact by applying pressure, and finally an ultrasonic vibration is added (input).

Ordinary ultrasonic welding machines use vertical vibrations, but in the welding of metallic materials and ceramics, the use of horizontal vibrations, as shown in Figure 1, is effective.

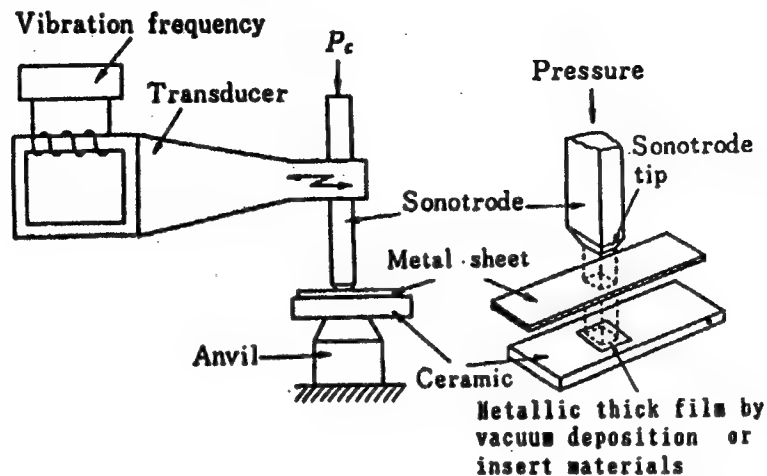


Figure 1. Ultrasonic Welding Machine and a Schematic Diagram of the Portions To Be Welded

### 3.1 Ultrasonic Welding Conditions and Methods

In each of the above cases, the output of the welding machine was 1200 w, the amplitude  $a$  of the ultrasonic vibration was in the 25~35  $\mu\text{m}$  (p-p) range, the input time  $T$  was 0.1~10 s, and the welding pressure  $P_c$  ranged from 5~50 MPa.

The ceramics used in the welding tests were sintered bodies, at normal temperatures, of oxides including factory automation,  $\text{SiO}_2$ , and  $\text{ZrO}_2$ , nitrides including  $\text{Si}_3\text{N}_4$  and  $\text{AlN}$ , and a carbide,  $\text{SiC}$ , and they had profiles of 3W x 5H x 30L ( $\text{mm}^3$ ) and surface roughness levels averaging 1  $\mu\text{m}$ . As for the metallic materials, Al (A1100, A1050) and Cu (C1020) plates, 0.5 mm thick, were used, and rolled copper foils (50  $\mu\text{m}$  thick) and indium (In) were used as insert materials.

For characteristics and evaluations of the welded products, welding strengths were compared by shearing strength (tensile strength) tests, and visual and structural examinations, such as SEM observations of the welds and structural analyses by EPMA, have been conducted.

### 3.2 Characteristics of Welding Materials and Evaluations

#### (1) Optimal welding conditions and the region where welding is available

Each ceramic-metal combination has optimal welding conditions, and when those conditions are sufficiently met, the welding strength is enhanced to a great extent. Figure 2 shows an example of this. In this figure, the regions where welding is available for combinations of various materials when the amplitude is 30  $\mu\text{m}$  are indicated. As a whole, with an increasing welding pressure, the required duration (input time) becomes shorter, and conversely, when the

pressure is low, slightly longer times are needed. Compared to Cu, Al can be welded in a shorter time. These are greatly affected by the deformabilities of the metallic materials and by the thermal conductivities and wettabilities of the ceramics.

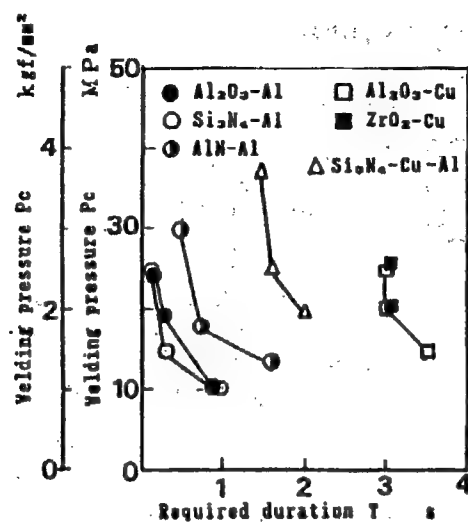


Figure 2. Combinations of Materials and Weldable Regions (Cu indicated by  $\Delta$  was used experimentally as a binder material)

## (2) SEM observation of welds

Figure 3 [not reproduced] shows SEM observations of SiO-Al (a) and Al<sub>2</sub>O<sub>3</sub>-Cu (b) welded joints. The microscopic SEM observations reveal that the weld surfaces are in a good state, with no spalling indicated at the weld interfaces, confirming that ultrasonic welding can be used for two different kinds of materials (ceramic-metal). Because of the difference in hardness between the two materials (Al is softer, as shown in Figure 3(a) [not reproduced]), the surface of the welded joint shows slightly different grade levels when the sample was subjected to grinding and polishing. A strip of bright and white spots appears on the weld because it is photographed as a secondary electron image. To keep this phenomenon to a minimum, the most important things are to prevent the generation of falling or sagging during grinding while the sample is being cut or polished, in addition to selecting the materials properly. Figure 3(b) [not reproduced] shows an example of grinding in which the grinding time was shortened to an extreme extent.

## (3) Strength of welded products

The SEM observations reveal that the welded joints are in a good state, but from a practical viewpoint, their welding strength is most important. Figure 4 shows the welding strengths of various welded products. All show slight elongation, and ruptures or shears are observed, as a whole, in the welded joints, with ruptures being confirmed in the aluminum base metals. The Al<sub>2</sub>O<sub>3</sub>-Al welded product has a welding strength close to that of its base metal, aluminum, indicating that it can be put to practical use readily.

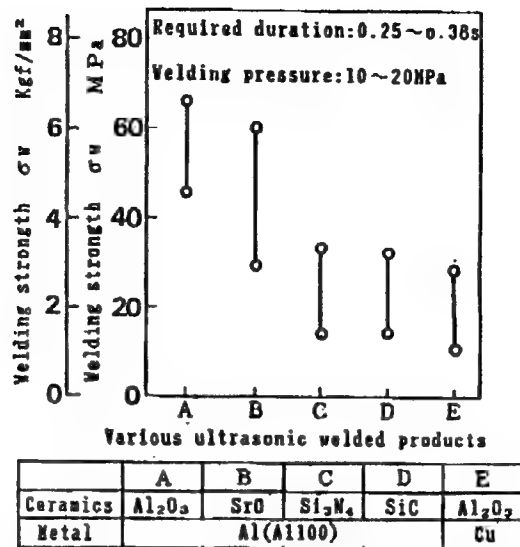


Figure 4. Welding (Shear) Strengths of Various Welded Products  
(Shearing speed: 3 mm/min)

The author made an attempt at generating a union between an annealed aluminum (heat treated at 550°C for 2 hours) and SiO<sub>2</sub> by welding, and Figure 5 shows the effects of the welding pressure and required duration on the welding strength. As for the relationship between  $T$  and  $\sigma_w$ , under a constant welding pressure of 20 MPa, and increasing the required duration to about 0.3 s, the welding strength increases steadily, but beyond that, extending the required duration has no effect on improving the welding strength. As for the  $P_c$ - $\sigma_w$  relationship, when the required duration is kept at a constant value of 0.5 s, the welding strengths are extremely low for welding pressures below about 20 MPa, while beyond the threshold value the welding strengths increase greatly and stabilize. However, care must be taken because when the welding pressures are larger than about 40 MPa, the ultrasonic vibration sometimes comes to a stop.

From the foregoing, one can see that altering the properties of aluminum gives rise to different welding strengths, but that the act does not affect the weldability of the metal at all. As seen above, all of the welded products display some level of welding strength, and this fact, the author believes, is a reflection not only of mechanical welding, but also of welding reactions.

#### (4) Influences of insert materials

In contrast to the direct welding mentioned above, this category of welding methods includes cases in which welding is obtained by using activation metals, such as Al, Cu, and In, as the insert materials, as well as cases in which the surface of a ceramic is metallized by the deposition of a metal film and welding is obtained by means of the metallized layer.

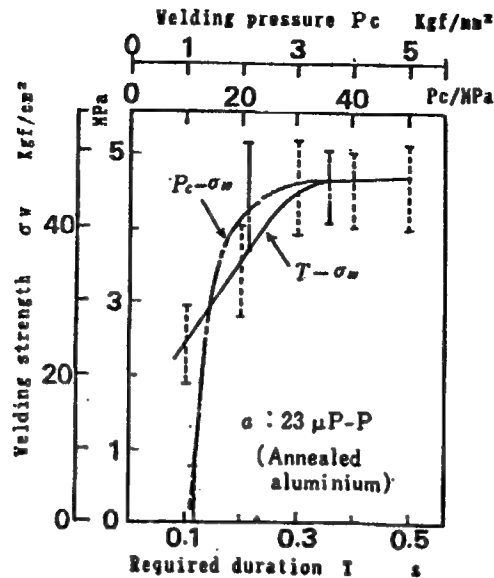


Figure 5. Relationship Between the Welding Strength  $\sigma_w$  of  $\text{SiO}_2\text{-Al}$  Welded Product and the Welding Pressure  $P_c$  and Required Duration  $T$

Figures 6(a) and (b) [not reproduced] show SEM photographs of the welded joints obtained by the two methods. Figure 6(a) [not reproduced] shows a case in which, using a rolled copper foil as a binder,  $\text{SiO}_2$  and aluminum have been welded at a welding pressure of 20 MPa for a required duration of 0.5 s. The effectiveness of the copper foil as a welding-assist material (binder) is apparent. In the case of Figure 6(b) [not reproduced], nickel was vapor deposited on the surface of  $\text{SiC}$ , and the surface and a thin plate of aluminum were welded by ultrasonic welding (welding pressure: 20 MPa, required duration: 0.5 s).

Electron microscope photographs of the welded joints in both cases reveal good welding interfaces, confirming that the ultrasonic welding of different materials is fully feasible. The insert material and the vapor deposition film, which were used as supplementary materials, have been proven to have the effects of promoting the welding process, but they exert no appreciable effect on the welding strength.

##### (5) Influences of roughness of the surfaces to be welded

In ultrasonic welding, materials are welded under a certain pressure by using a forcible vibrations so, as duly expected, the surface roughnesses of the materials pose problems. In other words, the surface roughness level is believed to affect the weldability and welding strength. Figure 7 shows an example of this.

The figure compares the welding strengths of ultrasonic welded products of  $\text{Al}_2\text{O}_3\text{-Al}$ , made by imparting random roughnesses to the surfaces of  $\text{Al}_2\text{O}_3$  materials by grinding and polishing and by joining the surfaces with aluminum

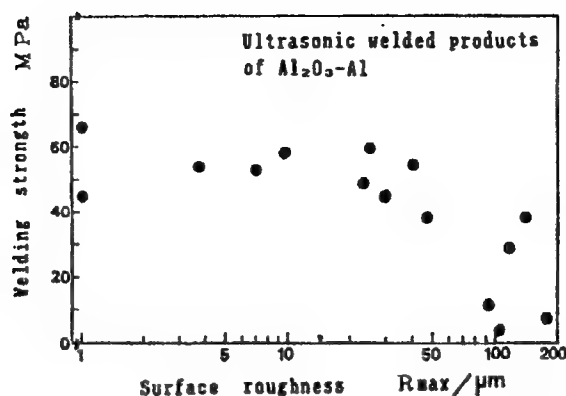


Figure 7. Influence of Surface Roughness on Welding Strength

by welding. Here, the roughness  $R$  shows the irregular cycle. The figure shows that the welding strengths of smooth surfaces with smaller roughness cycles are generally higher than those of coarser surfaces with larger roughness cycles.

Also, smaller surface roughnesses of  $Al_2O_3$  enable stable welded products with a smaller scatter of strengths to be obtained. This shows that when the surface roughness of the material onto which the ceramic is to be welded (base material) is about the same as or finer than the surface roughness of the ceramic, the vibration works more effectively, raising the welding strength. Therefore, when the surface roughness is small, reducing the amplitude of vibration is effective, and conversely, when the surface roughness is large, a large amplitude may be employed. However, one needs to pay attention to the fact that a large amplitude makes it impossible to obtain a stable strength and tends to destroy the surface of the material.

#### (6) Mechanisms of welding and interface properties

From the SEM observations and test results obtained so far, the mechanisms of ultrasonic welding are believed to involve the following procedures. Since the surfaces of the materials that come into contact have different roughness levels, they come into contact partially, that is, at several points, as shown in Figure 8(a). Thereafter, with the increasing welding pressure, the number of contact points, and thus the contact area, continually increases. When the pressure reaches a certain level, an ultrasonic vibration is applied immediately, which generates forced transverse vibrations at each of the contact surfaces or points (Figure 8(b)). Simultaneously, a friction heat is generated which reaches a high temperature zone in a short period of time and transforms the contact areas into welding status. The troublesome oxide films or organic membranes on the surfaces of the materials are destroyed by the vibration energies and are blown away, leaving the surfaces clean of impurities. This is analogous to forced friction under a certain pressure, and here the interface between the two contacting surfaces is in welding status and finally produces good welding, devoid of residual holes, as shown in Figure 8(c).

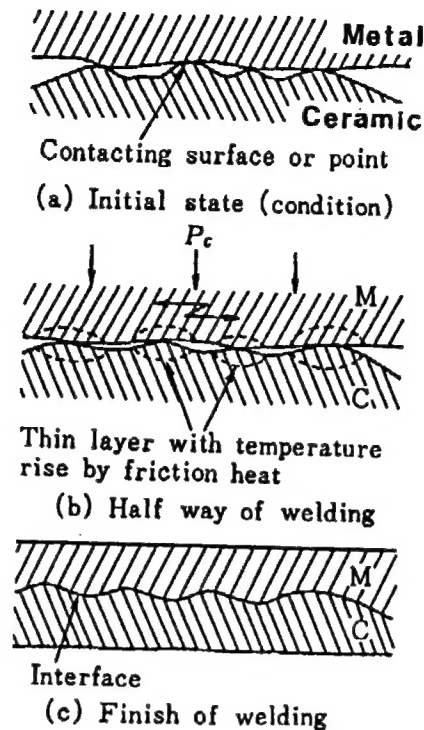


Figure 8. Deformation Behaviors of Material Surfaces in Ultrasonic Welding

As seen above, since the surface roughnesses of the contacting materials are different, the pressures acting on different contacting surfaces or points are not necessarily uniform, and hence the resulting deformations will not be the same across the entire contacting surface. The result is that microscopic slides will occur at these contacting surfaces or points, and these slides, coupled with the ultrasonic vibrations that are applied, will generate intense friction heat at the contacting surfaces or points, all of which will raise the temperature of the interface to an unexpected level, causing the entire area of the contacting surface to enter welding status.

For example, it has been confirmed that the heat generated by thermoelectric power during the ultrasonic welding of two metals (Al-Cu) ( $P_c$ : 8.6 MPa,  $T$ : 0.7 s) reaches as high as 520°C.

Figure 9 [not reproduced] shows SEM photographs of fractures generated during shearing tests of an  $Al_2O_3$ -Al welded product. The photographs show that the  $Al_2O_3$  surface has been torn off by the shearing and that part of it has moved onto the aluminum surface, depositing itself there, and thus increasing the welding strength. The same tendency was also observed in the cases of direct welding and in welding using insert materials.

As seen above, as soon as the clean surfaces come into contact with one another, the distances between the two materials that had been aggravated by plastic or elastic deformations get much smaller. Add to this the effect of temperature increases, brought about by vibrations, at the interface, and we

may be able to expect atom-to-atom welding or the formation of a reaction layer.

#### 4. Technology for Evaluating Welded Products

In order for welded products to be put to practical use, they must meet various conditions. These conditions range from general to specific, and contain the following: 1) welding strength; 2) airtightness; 3) heat resistance and low-temperature resistance; 4) heat and shock resistance; 5) water resistance/moisture resistance; 6) resistance to chemicals; 7) withstanding voltage (electrical resistivity); 8) resistance to weather; and 9) blocking properties.

How much emphasis will be placed on what items of the above conditions is determined by the objective and use of the welded product and the kinds of materials used. However, even one of the above items can have differing evaluations depending on the measuring methods employed. In the following, the author describes the basic and widely used welding strength measurement techniques.

##### 4.1 Measuring of Welding Strength

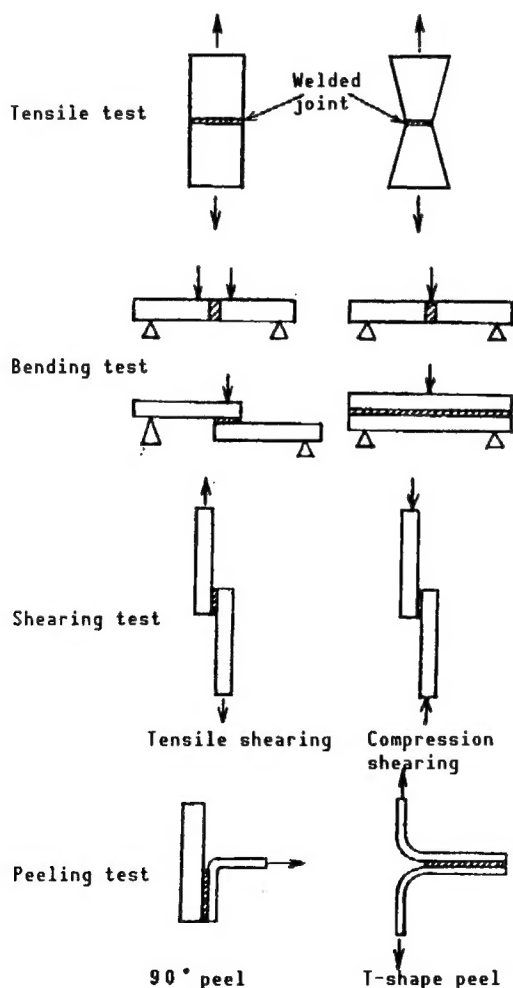


Figure 10 outlines the major methods for testing welding strength. The welding strength is greatly affected by such factors as the dimensions and profile of the testpiece, the combination of materials, the thickness of the welded layer, and the ambient temperature. Therefore, ordinarily, many samples with the same conditions are tested, and their average value is obtained for the welding strength evaluation. In addition, clearly recognizing the purpose of the welding strength test is important.

Figure 10. Major Methods for Testing Welding Strength



## 5. Conclusion

The author has outlined various welding technologies, the applications of which cover a broad area. The decision as to which technique should be employed for a specific application must be made after taking into account the purpose and use of welding, as well as the performance and function of the welded product. When these methods have been established as welding techniques in the field of production, it will become possible to select the optimal welding processes according to the materials and their combinations, thereby enabling welded products of a stable strength to be produced at low temperatures and yet in short spans of time.

- END -

16  
22161  
45

NTIS  
ATTN: PROCESS 103  
5285 PORT ROYAL RD  
SPRINGFIELD, VA

22161

This is a U.S. Government publication. Its contents in no way represent the policies, views, or attitudes of the U.S. Government. Users of this publication may cite FBIS or JPRS provided they do so in a manner clearly identifying them as the secondary source.

Foreign Broadcast Information Service (FBIS) and Joint Publications Research Service (JPRS) publications contain political, economic, military, and sociological news, commentary, and other information, as well as scientific and technical data and reports. All information has been obtained from foreign radio and television broadcasts, news agency transmissions, newspapers, books, and periodicals. Items generally are processed from the first or best available source; it should not be inferred that they have been disseminated only in the medium, in the language, or to the area indicated. Items from foreign language sources are translated; those from English-language sources are transcribed, with personal and place names rendered in accordance with FBIS transliteration style.

Headlines, editorial reports, and material enclosed in brackets [ ] are supplied by FBIS/JPRS. Processing indicators such as [Text] or [Excerpts] in the first line of each item indicate how the information was processed from the original. Unfamiliar names rendered phonetically are enclosed in parentheses. Words or names preceded by a question mark and enclosed in parentheses were not clear from the original source but have been supplied as appropriate to the context. Other unattributed parenthetical notes within the body of an item originate with the source. Times within items are as given by the source. Passages in boldface or italics are as published.

#### SUBSCRIPTION/PROCUREMENT INFORMATION

The FBIS DAILY REPORT contains current news and information and is published Monday through Friday in eight volumes: China, East Europe, Soviet Union, East Asia, Near East & South Asia, Sub-Saharan Africa, Latin America, and West Europe. Supplements to the DAILY REPORTs may also be available periodically and will be distributed to regular DAILY REPORT subscribers. JPRS publications, which include approximately 50 regional, worldwide, and topical reports, generally contain less time-sensitive information and are published periodically.

Current DAILY REPORTs and JPRS publications are listed in *Government Reports Announcements* issued semimonthly by the National Technical Information Service (NTIS), 5285 Port Royal Road, Springfield, Virginia 22161 and the *Monthly Catalog of U.S. Government Publications* issued by the Superintendent of Documents, U.S. Government Printing Office, Washington, D.C. 20402.

The public may subscribe to either hardcover or microfiche versions of the DAILY REPORTs and JPRS publications through NTIS at the above address or by calling (703) 487-4630. Subscription rates will be

provided by NTIS upon request. Subscriptions are available outside the United States from NTIS or appointed foreign dealers. New subscribers should expect a 30-day delay in receipt of the first issue.

U.S. Government offices may obtain subscriptions to the DAILY REPORTs or JPRS publications (hardcover or microfiche) at no charge through their sponsoring organizations. For additional information or assistance, call FBIS, (202) 338-6735, or write to P.O. Box 2604, Washington, D.C. 20013. Department of Defense consumers are required to submit requests through appropriate command validation channels to DIA, RTS-2C, Washington, D.C. 20301. (Telephone: (202) 373-3771, Autovon: 243-3771.)

Back issues or single copies of the DAILY REPORTs and JPRS publications are not available. Both the DAILY REPORTs and the JPRS publications are on file for public reference at the Library of Congress and at many Federal Depository Libraries. Reference copies may also be seen at many public and university libraries throughout the United States.